Performance of Distributed Fiber Raman Amplifiers with Incoherent Pumps

Ting Zhang

A Thesis

In

The Department of Electrical and Computer Engineering

Presented in Partial Fulfillment of the Requirements

for the Degree of Master of Applied Science at

Concordia University

Montreal, Quebec, Canada

Your file Votre référence
ISBN: 0-494-04406-3
Our file Notre référence
ISBN: 0-494-04406-3

ABSTRACT

Performance of Distributed Fiber Raman Amplifiers with Incoherent Pumps

Ting Zhang

In 2003, Ahura Company first introduced the high-power incoherent Raman pump, and illustrated the basic property of this pumping is to provide flat gain. After that, no paper relate to incoherent pumping has been published. In this thesis, distributed fiber Raman amplifiers (DFRAs) with incoherent pumping are investigated and the DFRAs performances are compared to those with the conventional coherent pumping for the first time. To achieve accurate modeling, a theoretical model, which includes effects of multiple-path interference (MPI), anti-Stokes, and Rayleigh scattering, is used, and a new Raman gain coefficient scaling method is employed in modeling. Theoretical modeling of incoherent pump is also given. First of all, these models are verified and proved to be accurate. Investigations are based on the above models for DFRAs with one or more incoherent pumps. By comparing the performance between the two types of DFRAs, we confirmed that DFRAs with incoherent pumping can have a much flatter gain than those with coherent pumping, and made the following contributions:

1. The gain ripple, the most important factor in the design of DFRAs, is reduced exponentially in dB with the increase of spectral width of incoherent pumps; while the average Raman gain, for the same pump power as coherent pumping, decreases linearly in dB and noise performance is degraded slightly due to the reduction of the Raman gain.
2. Keeping the spectral width un-changed and increasing the incoherent pump power improves the average Raman gain and noise performance, but noise is still slightly worse than coherent pumping for the same Raman gain level.
3. When multiple pumping is used, the number of pumping wavelengths is reduced significantly for the same gain ripple if incoherent pumping replaces coherent

pumping.

ACKNOWLEDGMENTS

Most of all, I would like to express my great gratitude to my research advisor Professor John X Zhang for his support and guidance over the past two years. His high expectation and enlightening advices have helped me stay improved, and made this thesis possible. I am also grateful to Guodong Zhang, AT&T USA, for his time and help. I also should give my great thanks to Idan Mandelbaum, the author of "Raman amplifier model in single-mode optical fiber", IEEE Photon. Tech. Lett., vol.15, pp. 1704-1706 , 2003, for his help in verification of DFRA model, and P. Gaarde, OFS Denmark, for providing the fiber parameters.

I would like to thank Natural Science of Engineering Research Council of Canada and Faulty of Electrical and Computer Science Engineering at Concordia University to support this project.

Learning together with other members in fiber optic communication system field has greatly enriched my education and life. I would like to thank all of them for their support and encouragement: Jinghong Fan, Bin Han, Lei Wang, and Zhenqian Qu. Their suggestions made the task of research enjoyable.

Finally, and most importantly, I would like to thank my husband Xuefei Jia, my parents, their love and encouragement made me overcome difficulties and complete this degree.

PUBLICATION RELATED TO THIS WORK

1. Ting Zhang, Xiupu Zhang, Guodong Zhang, "Performance of distributed fiber Raman amplifiers with incoherent pumping," *submitted to OFC 2005*
2. Ting Zhang, Xiupu Zhang, Guodong Zhang, "Distributed fiber Raman amplifiers with incoherent pumping," *submitted to IEEE Photon. Tech. Lett.*

TABLE OF CONTENTS

1 Introduction..... 1

1.1 Optical amplifier review..... 1

1.2 Aim of this thesis..... 3

1.3 Thesis structure..... 5

2 Fiber Raman amplifier principle..... 7

2.1 Raman amplification..... 7

2.2 Fiber Raman amplifiers 9

2.3 Scaling of Raman gain coefficients..... 11

3 Fiber Raman amplifier model..... 16

3.1 Basic definitions..... 16

3.2 General model..... 19

3.3 Equations for signal, pump, and ASE noise..... 22

4 Incoherent pumps..... 30

4.1 Incoherent pump theory..... 30

4.2 Incoherent pump modeling..... 31

5 Performance of DFRAs with one incoherent pump..... 34

5.1 Performance of C band DFRAs with one incoherent pump..... 34

5.2 Performance of L band DFRAs with one incoherent pump..... 41

5.3 FWHM effects on DFRAs performance with the same pump power..... 47

5.4 FWHM effects on ENF performance with the same average gain..... 49

6 Performance of DFRAs with two incoherent, or two, four and six coherent pumps 53

6.1 Performance of C- or L- band DFRAs with two incoherent, or two coherent, and four coherent pumps..... 53

6.2 Performance of C+L band DFRAs with two incoherent, or two, four and six coherent pumps 64

7 Conclusions..... 67

References..... 68

Appendix A..... 71

Appendix B..... 72

LIST OF FIGURES

Figure 1.1	Number of published papers and submitted U.S. patens each year since 1980 in the fields of EDFAs and FRAs.....	3
Figure 2.1	Energy diagram for the Raman scattering processes: Stokes scattering, anti-Stokes scattering and stimulated absorption.....	8
Figure 2.2	Schematic of a fiber-based Raman amplifier in the forward-pumping configuration.....	9
Figure 2.3	Raman-gain coefficients for SMF-28 and TW-Reach fiber. Both have pump wavelength of 1460 nm.....	12
Figure 2.4	Predicted and measured Raman gain spectra on a TrueWave-RS fiber from [3].....	15
Figure 2.5	Raman gain coefficient scaling for TW-Reach fiber from our model.....	15
Figure 3.1	General Raman amplifier.....	17
Figure 3.2	Transmission fiber separated in *m* segments to apply the integration in propagation equation.....	20
Figure 3.3	Wavelength distributions of signals, pumps and ASE noise.....	23
Figure 3.4	Power spectrum comparison: (a) from [4], (b) our work.....	27
Figure 3.5	On-off gain comparison: (a) from [4], (b) our work.....	28
Figure 3.6	Gain spectrum from our work, SRS between signals is gain, and	

MPI is considered..... 29

Figure 4.1 High-power broadband Raman pump module..... 30

Figure 4.2 Optical spectrum of an incoherent pump on sale [18]..... 31

Figure 4.3 Incoherent pump example..... 32

Figure 4.4 On-off gain comparison between one incoherent pump and one coherent pump. The power is both 230 mW..... 33

Figure 5.1.1 Gain comparison for Case 1 in Section 5.1..... 36

Figure 5.1.2 ENF comparison for Case 1 in Section 5.1..... 37

Figure 5.1.3 Gain comparison for Case 2 in Section 5.1..... 38

Figure 5.1.4 ENF comparison for Case 2 in Section 5.1..... 39

Figure 5.1.5 Gain comparison for Case 3 in Section 5.1..... 40

Figure 5.1.6 Gain comparison for Case 4 in Section 5.1..... 40

Figure 5.2.1 Gain comparison for Case 1 in Section 5.2..... 42

Figure 5.2.2 ENF comparison for Case 1 in Section 5.2..... 43

Figure 5.2.3 Gain comparison for Case 2 in Section 5.2..... 44

Figure 5.2.4 ENF comparison for Case 2 in Section 5.2..... 45

Figure 5.2.5 Gain comparison for Case 3 in Section 5.2..... 46

Figure 5.2.6 Gain comparison for Case 4 in Section 5.2..... 46

Figure 5.3.1 Gain comparison with FWHM of from 0 to 40 nm..... 47

Figure 5.3.2 FWHM effects on DFRA performance. Pump power is 300 mW..... 48

Figure 5.3.3 FWHM effects on DFRA performance. Pump power is 500 mW..... 49

Figure 5.4.1 Gain performance of power increased incoherent pump..... 50

Figure 5.4.2 ENF performance of power increased incoherent pump..... 51

Figure 5.4.3 FWHM effects on ENF and pump power with the same average gain..... 52

Figure 6.1.1 Gain comparison for Case 1 in Section 6.1..... 56

Figure 6.1.2 ENF comparison for Case 1 in Section 6.1..... 56

Figure 6.1.3 Gain comparison for Case 2 in Section 6.1..... 58

Figure 6.1.4 ENF comparison for Case 2 in Section 6.1..... 58

Figure 6.1.5 Gain comparison for Case 3 in Section 6.1..... 60

Figure 6.1.6 ENF comparison for Case 3 in Section 6.1..... 60

Figure 6.1.7 Gain comparison for Case 4 in Section 6.1..... 62

Figure 6.1.8 ENF comparison for Case 4 in Section 6.1..... 62

Figure 6.2.1 Gain comparison for Case in Section 6.2..... 65

Figure 6.2.2 ENF comparison for Case in Section 6.2..... 65

LIST OF TABLES

Table 5.1.1 Section 5.1 Summary for Case 1..... 36

Table 5.1.2 Section 5.1 Summary for Case 2..... 38

Table 5.1.3 Section 5.1 Gain ripple improvements..... 41

Table 5.2.1 Section 5.2 Summary for Case 1..... 42

Table 5.2.2 Section 5.2 Summary for Case 2..... 44

Table6.1.1 Section 6.1 List of the cases..... 54

Table 6.1.2 Section 6.1 Summary for Case 1..... 57

Table 6.1.3 Section 6.1 Summary for Case 2..... 59

Table 6.1.4 Section 6.1 Summary for Case 3..... 61

Table 6.1.5 Section 6.1 Summary for Case 4..... 63

Table 6.2.1 Summary for the Case in Section 6.2 66

Acronyms

ASE amplified spontaneous emission

DFRA distributed fiber Raman amplifier

EDFA erbium-doped fiber amplifier

FRA fiber Raman amplifier

FWHM full-width at half-maximum

FWM four wave mixing

MPI multiple-path interference

SOA semiconductor optical amplifier

SRS stimulated Raman scattering

WDM wavelength-division multiplexed

DWDM dense WDM

SBS stimulated Brillouin scattering

SPM self-phase modulation

GVD group-velocity dispersion

XPM cross-phase modulation

CHAPTER 1 Introduction

This chapter will provide a clear picture of background, origin, and targets of this thesis. In Section 1.1, three types of optical amplifiers are introduced, including their brief histories, functions, and developments. The aim of this project is given in Section 1.2, in which you can also find the basic idea of this work. The thesis structure is described in Section 1.3 to help understanding this work.

1.1 Optical amplifier review

Fiber-optic communication systems are also called light-wave systems because they employ optical fibers to transmit information. In 1980 [1], the first generation of light-wave systems became commercially available. Since then, fiber-optic communication systems have been deployed worldwide.

The advantages of fiber-optical communication systems are significantly increased capacity and transmission distance. However, the transmission distance of any optical transmission system is eventually limited by fiber losses that are caused by material absorption, Rayleigh scattering, and wave-guide imperfections. For long-haul systems, optoelectronic repeaters were used to solve the problem originated from the fiber loss. Since optoelectronic repeaters need convert the optical signal into electric signal at first, and then the optical signal is regenerated before re-transmitting, they become inevitably complex and expensive for wavelength-division multiplexed (WDM) light-wave systems. On the contrary, optical amplifiers are able to work without converting information to electric domain. Therefore, they have become a good alternative solution to overcome the loss limitation and have been deployed significantly since 1990s [2]. In the beginning, several kinds of optical amplifiers have been developed including semiconductor optical amplifiers (SOAs), erbium-doped fiber amplifiers (EDFAs), and fiber Raman amplifiers

(FRAs) [2].

SOAs were investigated in 1980 [3], devices were presented in 1987 [4], and they are the first really useful optical amplifiers. SOAs can be used as preamplifiers to enhance the signals before reaching the receivers, or boosters to inject desired signal power into the transmission fibers. Nowadays, SOAs are still the only optical amplifiers that can work at 1300 nm [5]. However, they can not be used for inline optical amplifiers in multi-channel long-haul systems due to chirp and inter-channel crosstalk.

EDFAs are named of the transmission fibers, which are doped with Erbium during the manufacturing process. The principle of EDFAs is the energy levels of Erbium ions in silica fiber, which makes Erbium work as a gain medium. As an important kind of fiber amplifiers, EDFAs have gained much attention because they can not only amplify signals in the wavelength region near 1.55um – C band, but also offer high-gain of up to 54 dB with quantum limited noise figure [6]. Today, most of the WDM system used EDFAs as inline amplifiers, which can increase the transmission distance almost unlimitedly under careful design.

FRAs were first studied in the early 1970s [7]. However, since FRAs need high pump power, it was only until the mid-1990s, with the development of suitable high-power pumps, FRAs regained interest. Figure 1.1 shows the number of published papers and submitted U.S. patents in EDFAs and FRAs every year since 1980 [2].

Compared to SOAs and EDFAs, FRAs can work at any wavelength region. That is because the amplification factor is decided by the frequency difference between the pump and the signal only, not by the energy level difference of a rare earth ion, which is the case for EDFAs. FRAs also have good noise performance and can be used as distributed amplifiers.

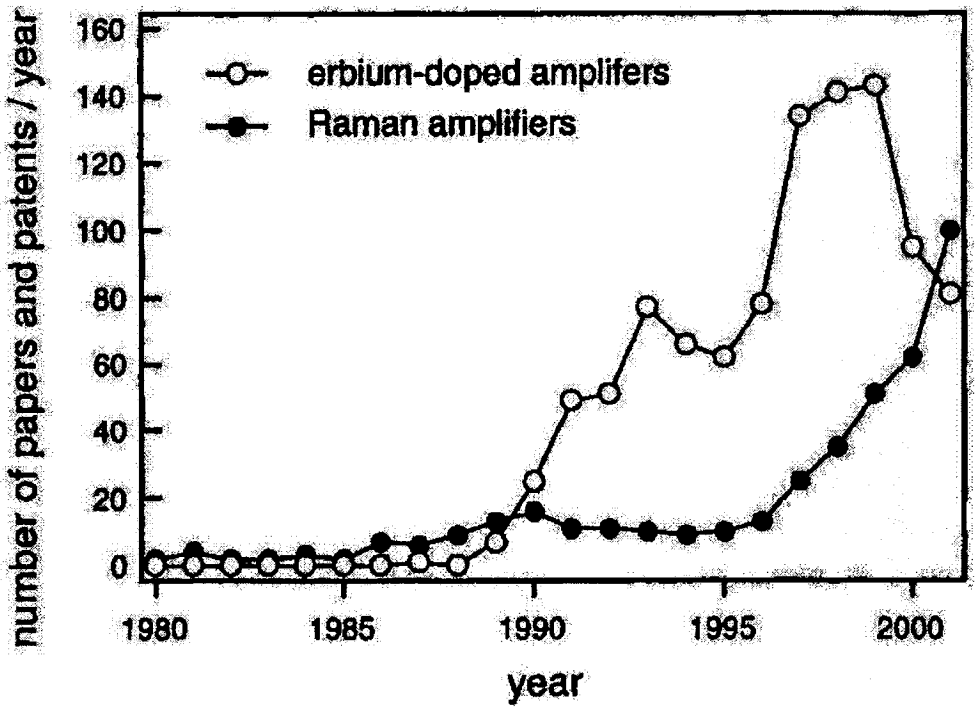

Figure 1.1 Number of published papers (conferences and journals of the OSA and IEEE) and submitted U.S. patents each year since 1980 in the fields of EDFAs and FRAs.

1.2 Aim of this thesis

The work presented in this thesis was inspired by the successful demonstration of high-power incoherent Raman pump sources. The basic idea is to study the performances of Distributed Fiber Raman Amplifiers (DFRAs) with incoherent pumps.

DFRAs have attracted great attention for their application in high-capacity long-haul dense wavelength division multiplexing transmission systems due to the improved optical signal to noise ration (OSNR) and reduced fiber nonlinear impairments [2, 8-12]. One of the challenges for DFRAs application in DWDM is to achieve a flat gain over a broadband cost-effectively. In the past, all DFRAs employ coherent pumps in which the power is located within a narrow bandwidth around the pump central-frequency. Based on the principle of Raman amplification, the signal amplification efficiency is decided by

the Raman gain coefficient of the coherent pump, which is a curve with significant change in its amplitude. As a result, fiber Raman amplifiers have to use several coherent pumps to achieve a more flatten gain. For example, a 25-km-long dispersion shifted fiber with 12 pumps provides a gain ripple of less than 0.1 dB [13]. Although multiple pumping [2, 9-12] and high order pumping [14-15] have been extensively applied to flatten the Raman gain, it has another challenge for DFRAs application in DWDM, which is to suppress the Raman pumping induced impairments. For instance, four wave mixing (FWM) can be generated by the interaction of pump-pump, pump-amplified spontaneous emission (ASE), and pump-signal [16-21], and the stimulated Brillouin scattering (SBS) caused by each longitudinal mode of high power Raman pumping sources. Time-division multiplexed pumping [22-24] and inserting a spool of high-dispersion fiber at pump output [20] have been proposed and demonstrated to combat the FWM impairment, but with additional penalties. Broadening the spectrum of Raman source, i.e., reducing the power of each individual longitudinal mode, can suppress the SBS impairment.

Very recently DFRAs using incoherent pumping have been demonstrated to obtain a flat broadband gain [25]. In contrast to the conventional coherent pumping source, the pumping power of incoherent pumping source spreads over a wide wavelength range from several nanometers to tens of nanometers, the phase and polarization of incoherent pumping source are completely random. Thus, the SBS impairment can be completely suppressed from incoherent pumping. Due to the random phase of incoherent pumps, the FWM generation by pump-pump, pump-ASE noise and pump-signal is significantly reduced. Another advantage of using incoherent pumping is that the polarization multiplexer for pumping source can be eliminated due to the pumping source's random polarization. For DFRAs with incoherent pumping, the signal amplification by Raman gain is given by the summation effect from pump power at the whole pump wavelength range.

In this thesis, we first verify the effectiveness of incoherent pumping by theoretical

analysis. The performances of DFRAs with incoherent pumping are investigated with the comparison to the conventional coherent pumping.

For our theoretical modeling in this thesis we considers stimulated Raman gain from other signals as gain, and MPI effects as noise. No-linear effects, such as self-phase modulation (SPM), group-velocity dispersion (GVD), four wave mixing, cross-phase modulation (XPM), are not considered.

1.3 Thesis structure

This section shows the structure of this thesis, and contents of each chapter are described.

The aim of Chapter 2 is to introduce the principle of FRAs. In the first part, spontaneous Raman scattering is explained. We show that spontaneous Raman scattering can be changed to stimulated Raman scattering, which is used in DFRAs, if injected light power exceeds a threshold value. Three types of Raman scattering are defined. An example illustrates how a fiber is used as a DFRA, and properties to be noticed in Raman amplifier design are given. The second part of Chapter 2 describes the scaling of Raman gain coefficients. Raman gain coefficients for SMF-28 and TW-Reach fibers are shown in figures. The relationship between Raman gain coefficients, pump wavelength, and effective area is given in equation (2.1), followed by an example.

In Chapter 3, Basic definitions are given to describe a FRA model. Corresponding to this physical model, a theoretical model is constructed by the basic equation that is used to calculate the power of each channel. The propagation equation for each kind of channels (pump, signal, and ASE noise) is defined in forward and backward direction separately for better understanding, and verification is followed.

In Chapter 4, you will find the incoherent pump theory, followed by an introduction of theoretical model used in this thesis. An incoherent pump example and a same power

coherent pump are given, and the corresponding gain spectra are also provided. From the gain comparison, it is clearly shown that incoherent pump can give much flatter gain than the coherent pump with the same total pump power.

In Chapter 5, performance of DFRAs with one incoherent and one coherent pump are studied. Eight cases of investigations, which cover C band and/or L band, are conducted based on SMF-28 and TW-Reach DFRAs. With the same total pump power, full-width at half magnitude (FWHM) effects on gain and equivalent noise figure (ENF) are illustrated. By keeping the average Raman gain identical, FWHM effects on ENF and pump power are revealed, too.

In Chapter 6, investigations are conducted for C-, L- and C+L- band DFRAs with multiple incoherent pumps. When total pump power is un-changed, incoherent pumps provide a much flatter gain than coherent pumps, and the number of pumping wavelengths for broadband DFRAs can be significantly reduced for incoherent pumping compared to the conventional coherent pumping to achieve the same gain flatness.

Chapter 7 concludes this thesis and sums up all the results shown in previous chapters.

CHAPTER 2 Fiber Raman Amplifier Principle

In the beginning of this chapter, it is necessary to explain the principle of FRAs which is the foundation of this thesis. Stimulated Raman scattering (SRS), which is changed from spontaneous Raman scattering when the injected power exceeds a threshold value, is described in Section 2.1. Section 2.2 gives an example of how a fiber can be used as a FRA, and properties to be understood in FRA design. Raman gain coefficient scaling is the topic of Section 2.3, which includes explanation of Raman gain coefficients, relationship among these coefficients, pump wavelength, and effective area, and how to use this relation equation.

2.1 Raman amplification

Fiber Raman amplifiers employ SRS which can be obtained in transmission fibers to amplify signal power when a high power pump propagates through the fibers. SRS origins from spontaneous Raman scattering with pump power exceeding a threshold value.

Spontaneous Raman scattering was first discovered by Raman, who received the Nobel Prize in Physics in 1930 for this great contribution [26]. The physical process of spontaneous Raman scattering is: optical beam incident on a molecule makes the bound electrons of this molecule oscillate at the frequency of the optical beam. Hence, the oscillating dipole moment produces optical radiation at the same frequency with a phase shift. At the same time, the molecular structure itself is oscillating at the frequencies of various molecular vibrations. Therefore, the induced oscillating dipole moment contains the sum and difference frequency terms between the optical and vibrational frequencies. These terms give rise to Raman scattered light in the re-radiated field. Spontaneous Raman scattering is an isotropic process and occurs in forward and backward directions.

There are three types of Raman scattering processes:

- Pump photons give up their energy to create other photons of reduced energy at a lower frequency. The remaining energy is absorbed by silica molecules, which end up in an excited vibrational state. This is called Stokes scattering. The vibrational energy levels of silica dictate the value of the frequency shift ($\Omega_r = \omega_p - \omega_s$).
- Pump photon is absorbed by a molecule that is already excited to emit a photon with energy equal to the sum of energies ($\Omega_r + \omega_p = \omega_{higher-frequency}$). This is called anti-Stokes scattering. It only takes place when a fiber temperature above the absolute zero.
- Signal photons absorbed by a molecule, which is in excited state, will generate a pump photon ($\Omega_r + \omega_s = \omega_p$). This is the inverse of the Stokes scattering.

Figure 2.1 describes the Raman scattering processes [14].

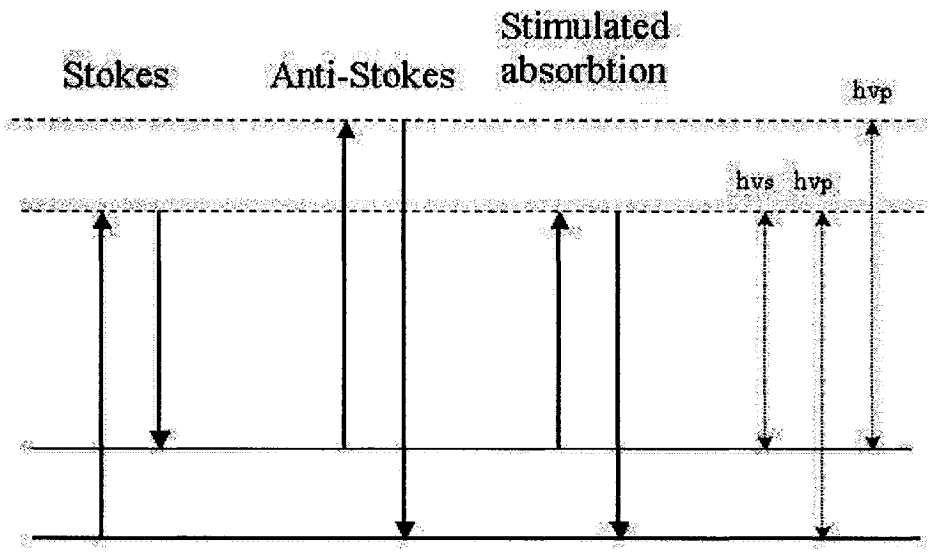

Figure 2.1: Energy diagram for the Raman scattering processes: Stokes scattering, anti-Stokes scattering and stimulated absorption. The energy differences between the levels are shown with dashed vertical lines on the right of the figure. The dashed horizontal lines show virtual levels.

Stokes and anti-Stokes processes can generate new signal waves. These new waves can also work as pumps and create other new waves through Stokes or anti-Stokes. This is called higher-order Raman scattering, and will go on indefinite times. However, each Stokes or anti-Stokes conversion costs power, especially for anti-Stokes. Consequently, high order Stokes is not significant.

Stokes scattering can be used to amplify the signals if the frequency difference between signal and pump are within the Raman Stokes line region. This is the basic principle of fiber Raman Amplifier. Moreover, Stolen found that Raman gain spectrum is temperature independent and anti-Stokes process occurs for amplifier with fiber temperature greater than 0 K [27]. For today's commercially used silica fiber, their energy level covers a continuum broad bandwidth, not discrete frequency separation points [28]. The energy converting efficiency is express by Raman gain coefficient. Further explanation about Raman gain coefficient can be found in Section 2.3.

2.2 Fiber Raman amplifiers

Figure 2.2 illustrates how a fiber works as a Raman amplifier [29]. Pumps and signals at frequencies ω_p and ω_s are coupled into one transmission fiber. SRS exists along the fiber and makes the energy transfer from pump to signal during the propagation. Therefore, the signals are amplified. At the output end, a filter is used to filter out the desired signal.

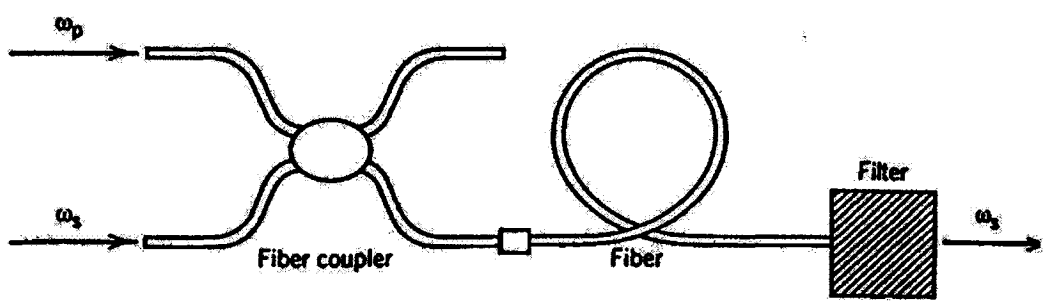

Figure 2.2 Schematic of a fiber-based Raman amplifier in the forward–pumping configuration.

Since Raman amplifiers obtain gain from stimulated Raman scattering, properties of SRS gain are critical in fiber Raman amplifier design. Following are the fundamental points to be noticed:

- Every kind of available fiber has its own Raman gain spectrum. This gain spectrum is a fiber property parameter, and depends primarily on the frequency separation between the pump and the signal, not on their absolute frequencies. That means, to amplify signal, or create new optical photon at the signal frequency, the frequency separation between the pump and the signal must equal to the frequency of the desired photon. It is found that gain factor is the maximum at frequency separation 13 - 14 THz or about 100 nm [30]. This fact implies how to design an effective Raman pump. For example, the best pump wavelength to amplify a signal at 1530nm is around 1430 nm.
- Raman gain does not depend on the relative propagation direction of pump and signal, which means signals will be amplified when they co-propagates or counter-propagates with pumps. This property provides Raman amplifiers with three kinds of pumping schemes: co-pumped (or forward pump), counter-pumped (or backward pump), and bi-directionally pumped. Each pumping scheme has its own advantages and suitable cases [31]: Roughly speaking, co-pumped amplifiers have the best noise performance; for short-length amplifiers (< 10 km), three pump schemes have no difference; counter-pumping performs better than both co-pumping and bi-directional pumping for a larger gain; bi-directional pumping is more suitable for very long distributed Raman amplifiers (> 100 km). In most of today's commercial optical communication systems, backward pumping is popular because when the fiber span is between 45 km and 100 km backward pumping works best considering gain and noise performance.
- Raman gain is polarization dependent [32]. The peak coupling strength between a pump and a signal is approximately an order of magnitude stronger if pump and

signal are co-polarized than orthogonally polarized. Therefore, almost no Raman amplification takes place when the signal and the pump are orthogonal in polarization states, and for un-polarized pumps, the Raman gain is reduced by a factor of two [27]. Considering the fact that signals transmit with any polarization states in fiber, pump beams need to be polarized before injecting it into the fiber.

2.3 Scaling of Raman gain coefficient

Raman-gain coefficients (denoted by g_R , normalized gain coefficients $g_R = Raman\ gain\ cross\text{-}section / A_{eff}$) is an efficiency factor related to the gain, which determines the strength of the coupling between a pump beam and a signal beam due to stimulated Raman scattering.

Figure 2.3 shows the measurements of g_R for two types of fibers, which are used in this thesis: SMF-28 fiber with effective area (denoted by A_{eff}) around $80\,\mu m^2$, and TW-Reach fiber with A_{eff} around $50\,\mu m^2$, with pump wavelength of 1460 nm. The Raman gain efficiency spectra are roughly triangular in shape, peaking at approximate 13 to 14 THz [30]. However, the peak values of these two g_R spectra are clearly different. That is because of the distinct compositions of SMF-28 and TW-Reach fibers fixed during the manufacturing processes. The refraction index of TW-Reach fiber is increased by doping the fiber core with more Germania (GeO_2). This leads to the decrease of the effective area, which inversely affects the g_R accordingly. Therefore, TW-Reach fiber has a bigger g_R value.

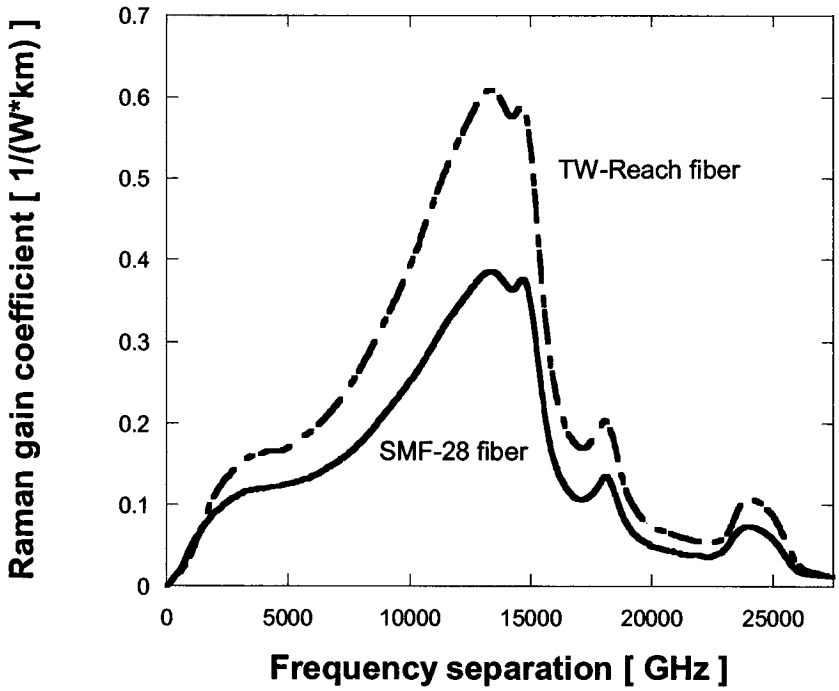

Figure 2.3 Raman-gain coefficients for SMF-28 fiber and TW-Reach fiber. Both have pump wavelength of 1460 nm.

For a given fiber, Raman gain spectra are fixed for a certain pump wavelength. However, the coefficients of g_R are not the same for different pump wavelengths, and in fact, it increases with the reduction of the pump wavelength. In [33], the relations between g_R, A_{eff}, and pump wavelength are clearly illustrated in Equation (2.1).

$$g_R(\Delta\nu, \Lambda_p) = g_R(\Delta\nu, \lambda_p) \times \frac{\lambda_s}{\Lambda_s} \times \left[\frac{A_{eff-ps}(\Delta\nu, \lambda_p)}{A_{eff-ps}(\Delta\nu, \Lambda_p)} \right] \tag{2.1}$$

Where

$$A_{eff-ps}(\Delta\nu, \lambda_p) = \frac{1}{2} \times \left[A_{eff}(\lambda_p) + A_{eff}(\lambda_s) \right]$$

Where Δv is the frequency separation between pump and signal; Λ_p, Λ_s, λ_p, and λ_s represent new pump, signal wavelength, and reference pump, signal wavelength respectively; and relative effective fiber area between a pump and a signal is represented by $A_{eff-ps}(\Delta v, \lambda_p)$.

Next, an example is given for application of this equation.

- How to find the g_R value of one signal (wavelength = 1555 nm) pumped by one pump located at 1425 nm. Fiber type is TW-Reach fiber.
- Known information: Reference g_R spectrum given by the reference wavelength of 1460 nm (see Figure 2.4), and TW-Reach fiber A_{eff} data at any wavelengths.
- Solution:

  Step 1.

  Calculate the frequency separation between the signal (1555 nm) and the new pump (1425 nm) with equation of $\Delta v = \frac{C}{\lambda_p} - \frac{C}{\lambda_s}$. Here, $\lambda_p = 1425nm$, and $\lambda_s = 1555nm$. C is light speed ($C = 2.99792458 \times 10^8 m/s$). Then, we obtain $\Delta v = 16977.9GHz$.

  Step 2.

  Find out g_R value based on $\Delta v = 16977.9GHz$ in the referenced Raman gain coefficient spectra ($g_R(\Delta v, \lambda_p) = 0.17219(W \cdot km)^{-1}$), and the reference signal wavelength λ_s with $\lambda_s = \frac{C}{\frac{C}{\lambda_p} - \Delta v}$, where, λ_p is the reference pump wavelength ($\lambda_p = 1460nm$). Therefore, we obtain $\lambda_s = 1591nm$.

Step 3.

Finding A_{eff} values in A_{eff} data file at wavelengths: $\lambda_p = 1460nm$, $\lambda_s = 1591nm$, and new pump and signal wavelengths: $\Lambda_p = 1425nm$, $\Lambda_s = 1555nm$, then we calculated $A_{eff-ps}(\Delta v, \lambda_p)$ and $A_{eff-ps}(\Delta v, \Lambda_p)$ with equation of $A_{eff-ps}(\Delta v, \lambda_p) = \frac{1}{2} \times [A_{eff}(\lambda_p) + A_{eff}(\lambda_s)]$. From A_{eff} data file, we know the following:

$$A_{eff}(\lambda_p = 1460\,nm) = 47.50461397\,\mu m^2$$
$$A_{eff}(\lambda_s = 1591\,nm) = 57.74642775\,\mu m^2$$
$$A_{eff}(\Lambda_p = 1425\,nm) = 46.22804304\,\mu m^2$$
$$A_{eff}(\Lambda_s = 1555\,nm) = 54.73575389\,\mu m^2$$

Calculated results are:

$$A_{eff-ps}(\Delta v, \lambda_p) = 52.62552086\,\mu m^2$$
$$A_{eff-ps}(\Delta v, \Lambda_p) = 50.48189797\,\mu m$$

Step 4.

Finally, using Equation (2.1) to get g_R expected and $g_R = 0.183657(W \cdot km)^{-1}$.

Figure 2.4 shows comparison for TW-RS fiber in [33] between calculations by (2.1) and measurements. To confirm the correctness of g_R scaling in this thesis, our calculations for TW-Reach fiber are shown in Figure 2.5. The g_R of TW-Reach fiber is close to, but slightly lower than the g_R of TW-RS fiber. Since we don't have parameters of TW-RS fiber, TW-Reach fiber is used in this thesis. The Raman gain spectra comparisons between TW-Reach and TW-RS fibers are illustrated in Appendix A. It is clearly shown that the g_R scaling trends in Figure 2.4 and Figure 2.5 are the same, which proves that our calculations are correct.

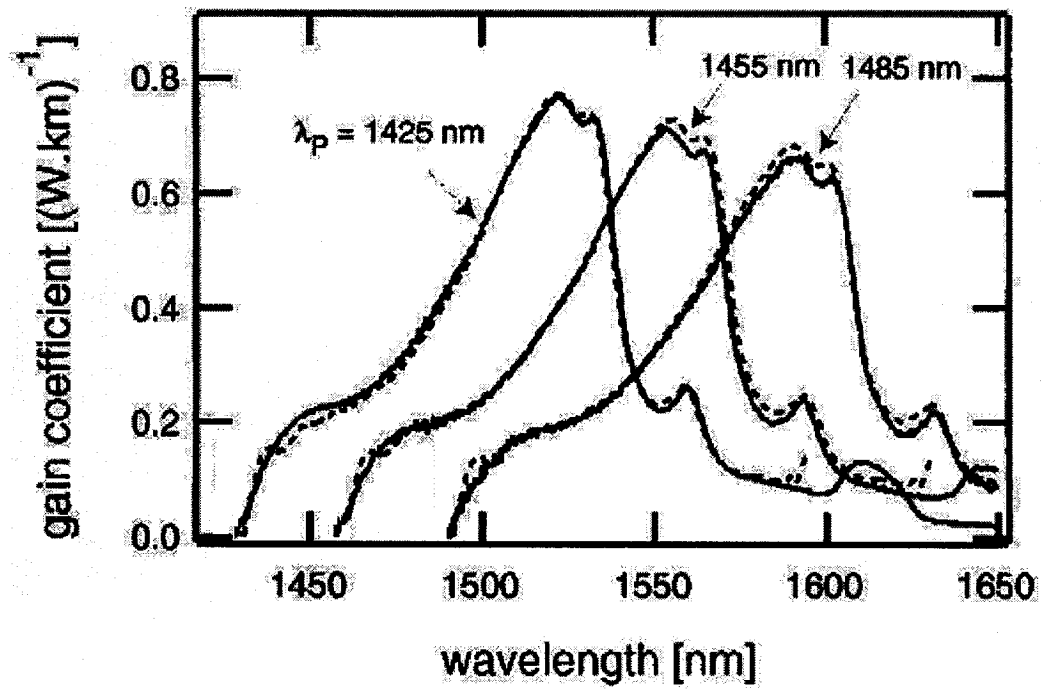

Figure 2.4 Predicted (dashed curves) and measured (solid curves) Raman gain spectra on a TrueWave RS fiber from [33].

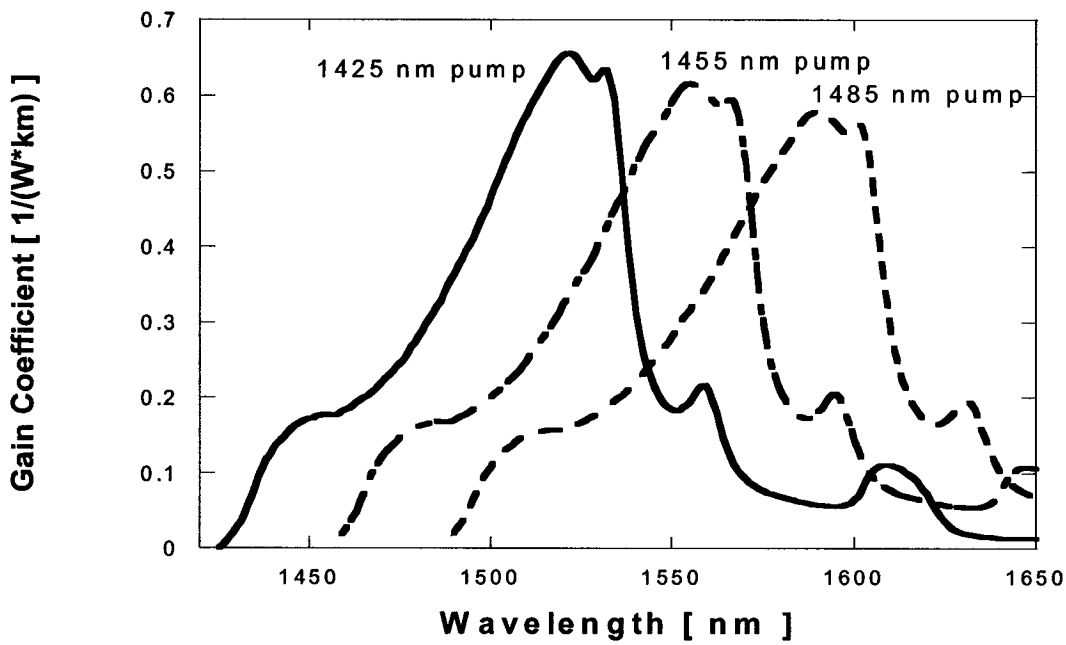

Figure 2.5 Raman gain coefficient scaling for TW-Reach fiber. Solid curve is for 1425 nm pump. Dot-dash curve is for 1455 nm pump. Dot curve is for 1485 nm pump.

CHAPTER 3 Fiber Raman Amplifier Model

The property of Raman gain based on the frequency separation between pump and signal makes fiber Raman amplification everywhere in the communication spectrum. Therefore, fiber Raman amplifiers have been considered as a flexible and simple way to amplify signal in both C and L band. Accordingly, the accuracy of fiber Raman amplifier modeling becomes extremely important, and many scientists have made their contributions in establishing and improving it. Stolen et al. [34] described modeling of Stokes amplified spontaneous emission (ASE) and multiple Stokes shifts in single-mode fiber. Kidorf et al. [35] gave detailed equations for a Raman amplifier model applied to single-mode optical fiber. Achtenhagen et al. [36] verified the gain predicted by this model, added Rayleigh backscattering and wavelength scaling approximation to account for effective fiber core area. Perlin et al. [11] added anti-Stokes spontaneous emissions. Berntson et al. [37] corrected the equation given by Kidorf in [35] for spontaneous absorption of signal photons. In this thesis, we use the Raman amplifier model for single-model optical fiber given in [38], which is the first explicit Raman propagation equations which include effects due to group velocity, MPI, as well as Stokes and anti-Stokes spontaneous emission.

In this chapter, basic definitions are given to describe a Raman amplifier model. Fundamental equation, which is used to calculate the powers of all channels during their propagation, is explained explicitly. Propagation equations for all kinds of channels (pump, signal, and ASE noise) are listed before comparing our modeling with in [38].

3.1 Basic definitions

Figure 3.1 illustrates a general fiber Raman amplifier. Parameters used to characterize the optical fiber are: length L; frequency dependent fiber attenuation $\alpha(\nu)$;

Raman gain coefficient $g_R(\Delta v, \lambda_p)$, which depends on the frequency separation between beams, and the shorter wavelength between two channels; frequency dependent Rayleigh scattering coefficient $\gamma(v)$ and effective area of the fiber $A_{eff}(v)$; and absolute temperature T of the optical fiber. For the position reference, z is used, which is set to zero at the input end, and L at the output end. Signal and pump beams having photon numbers of n_i traveling in the forward and backward direction are written as n_i^+, n_i^-, respectively. Therefore, $n_i(0+)$ is the input, and $n_i(L+)$ is the output. If the pump beam is injected backwardly, it is denoted as $n_i(L-)$. Otherwise, it is included in the input side.

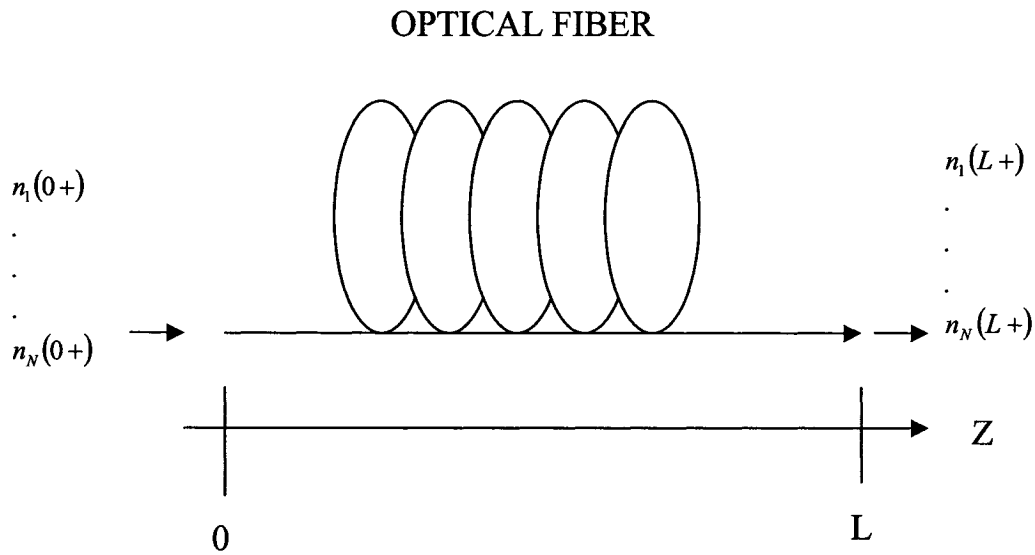

Figure 3.1 General Raman amplifier. $n_1(0+)..n_N(0+)$ are the number of photons in the forward traveling signal and pump beams at the input. Correspondingly, $n_1(L+)..n_N(L+)$ are the numbers of photons in the forward traveling ones at the output. L is the length of the optical fiber and z is the position in the fiber.

We use P_i to express the beam power for channel i in a limited bandwidth. This channel i can be signal or pump, and P_i is defined in Equation (3.1), where v_i is the frequency of the i-th channel. ASE noise power is calculated in a bandwidth of Δv. To indicate the difference, ASE noise power is denoted by P_i^{ASE}, and the definition is in Equation (3.2). Equation (3.3) is the relationship between Raman gain and Raman gain coefficient g_R.

$$P_i = h v_i n_i \tag{3.1}$$

$$P_i^{ASE} = \int_{\Delta v_i} n(v) h v dv \tag{3.2}$$

$$G(v_{signal}, v_{pump}) = g_R(v_{signal}, v_{pump}) \times P_{pump} \tag{3.3}$$

Raman gain is to indicate the amplification degree. The absolute gain from position z_1 to z_2 is defined in Equation (3.4), as P_s is the signal power at the two positions.

$$G_{absolute}(z_1 \rightarrow z_2) = \frac{P_s(z_2)}{P_s(z_1)} \tag{3.4}$$

The on-off Raman gain from position z_1 to z_2 is defined in Equation (3.5), which is the absolute gain minus fiber loss. Here α is in dB/km, and $L = z_1 - z_2$ is in km.

$$G_{on-off}(z_1 \rightarrow z_2)[dB] = G_{absolute}(z_1 \rightarrow z_2)[dB] - \alpha L \tag{3.5}$$

The noise figure of a Raman amplifier describes the noise performance, and it is defined by Equation (3.6) [39]. If the G is the on-off gain, the resulting noise figure is called equivalent noise figure (ENF).

$$F = \frac{1}{G}\left[\frac{P^{ASE+}(L)}{h v \Delta v} + 1\right] \tag{3.6}$$

Where $P^{ASE+}(L)$ is the forward ASE noise power in bandwidth of Δv at the output end.

3.2 General model

In Chapter 2, three kinds of Raman scattering are defined, Stokes scattering, anti-Stokes scattering, and inverse of Stokes scattering. In fact, inverse Stokes scattering is also an anti-Stokes process, which is different from anti-Stokes scattering only by the wavelength of absorbed photon. In last chapter, pump photon is absorbed during anti-Stokes scattering process, while signal photon is absorbed during inverse Stokes scattering process. However, when considering the Raman interaction between two arbitrary bands, each of which is within a narrow bandwidth Δv and has single-mode polarized light, only two processes are included: Stokes scattering and anti-Stokes scattering. Between this two, Stokes scattering is responsible for Raman gain as well as pump depletion. Equation (3.7) is our base of Raman amplifier model given in [38] by Stokes and anti-Stokes analysis.

$$
\begin{aligned}
\pm\frac{dP_i^{\pm}}{dz} = & -\alpha(v_i,T)P_i^{\pm} && ① \\
& +\gamma(v_i)P_i^{\mu} && ② \\
& +P_i^{\pm}\sum_{j}^{v_j>v_i} g_R(v_j,v_i)\left[P_j^{+}+P_j^{-}\right] && ③ \\
& +2\sum_{j}^{v_j>v_i}\left[P_j^{+}+P_j^{-}\right]hv_i\Delta v g_R(v_j,v_i)\times\left(1+\frac{1}{e^{\frac{h(v_j-v_i)}{kT}}-1}\right) && ④ \\
& -P_i^{\pm}\sum_{j}^{v_j<v_i}\frac{V_j}{V_i}\frac{v_j}{v_i}g_R(v_i,v_j)\left[P_j^{+}+P_j^{-}\right] && ⑤ \\
& +2\sum_{j}^{v_j<v_i}\left[P_j^{+}+P_j^{-}\right]hv_i\Delta v\frac{v_j}{v_i}\frac{V_j}{V_i}\times g_R(v_i,v_j)\frac{1}{e^{\frac{h(v_i-v_j)}{kT}}-1} && ⑥
\end{aligned}
\tag{3.7}
$$

Where h is Planck's constant, k is the Boltzmann constant, T is the temperature, v_j and v_i are the frequencies, V_i or V_j is group velocity denoted by subscript for different frequencies, and P_i^+ and P_i^- are the power at the i-th frequency in forward and backward, respectively. In the equation, ① and ② the present fiber loss and Rayleigh scattering; ③ is the gain from higher frequencies while ⑤is the depletion to lower frequencies; ④ and ⑥ are noise due to stimulated spontaneous emission, and anti-Stokes, respectively.

To apply this differential format equation to a fiber Raman amplifier with length L, the fiber can be separated into m segments, each of that has a length of $\Delta z = \frac{L}{m}$. Figure 3.2 gives the illustration.

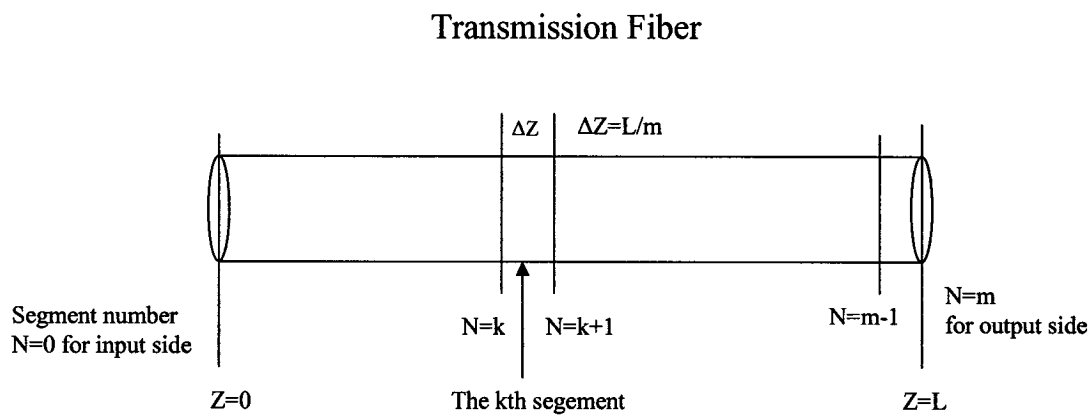

Figure 3.2 Transmission-fiber is separated into m segments to apply the integration in propagation equation.

Then, Equation (3.7) can be written as following in Equation (3.8)

$$\frac{dP_i^+(z_{k+1})}{dz} = -\alpha(v_i)P_i^+(z_k) + \gamma(v_i)P_i^-(z_k)$$

$$+ P_i^+(z_k)\sum_j^{v_j>v_i} g_R(v_j, v_i)\left[P_j^+(z_k) + P_j^-(z_k)\right]$$

$$+ 2\sum_j^{v_j>v_i}\left[P_j^+(z_k) + P_j^-(z_k)\right]hv_i\Delta v g_R(v_j, v_i)\times\left(1 + \frac{1}{\exp\left(\frac{h(v_j - v_i)}{kT}\right) - 1}\right)$$

$$- P_i^+(z_k)\sum_j^{v_j<v_i}\frac{V_j}{V_i}\frac{v_j}{v_i}g_R(v_i, v_j)\left[P_j^+(z_k) + P_j^-(z_k)\right]$$

$$+ 2\sum_j^{v_j<v_i}\left[P_j^+(z_k) + P_j^-(z_k)\right]hv_i\Delta v\frac{v_j}{v_i}\frac{V_j}{V_i}\times g_R(v_i, v_j)\left(\frac{1}{\exp\left(\frac{h(v_i - v_j)}{kT}\right) - 1}\right)$$

(3.8a)

$$\frac{dP_i^-(z_k)}{dz} = -\alpha(v_i)P_i^-(z_{k+1}) + \gamma(v_i)P_i^-(z_{k+1})$$

$$+ P_i^-(z_{k+1})\sum_j^{v_j>v_i} g_R(v_j, v_i)\left[P_j^+(z_{k+1}) + P_j^-(z_{k+1})\right]$$

$$+ 2\sum_j^{v_j>v_i}\left[P_j^+(z_{k+1}) + P_j^-(z_{k+1})\right]hv_i\Delta v g_R(v_j, v_i)\times\left(1 + \frac{1}{\exp\left(\frac{h(v_j - v_i)}{kT}\right) - 1}\right)$$

$$- P_i^-(z_{k+1})\sum_j^{v_j<v_i}\frac{V_j}{V_i}\frac{v_j}{v_i}g_R(v_i, v_j)\left[P_j^+(z_{k+1}) + P_j^-(z_{k+1})\right]$$

$$+ 2\sum_j^{v_j<v_i}\left[P_j^+(z_{k+1}) + P_j^-(z_{k+1})\right]hv_i\Delta v\frac{v_j}{v_i}\frac{V_j}{V_i}\times g_R(v_i, v_j)\left(\frac{1}{\exp\left(\frac{h(v_i - v_j)}{kT}\right) - 1}\right)$$

(3.8b)

Here, z_k is the k-th segment ($0 \le k \le m$). So, $P_i^+(z_0)$ is input signal and forward pump power, and $P_i^+(z_m)$ is the output. If the Raman amplifier is backward pumped, using $P_i^-(z_m)$ to indicate the inputted pump power.

3.3 Equations for signals, pumps, and ASE noise

For Raman amplifiers, inputs are signals and pumps. ASE noise is generated during the propagation. Figure 3.3 illustrates the wavelength distributions of signals, pumps and ASE noise.

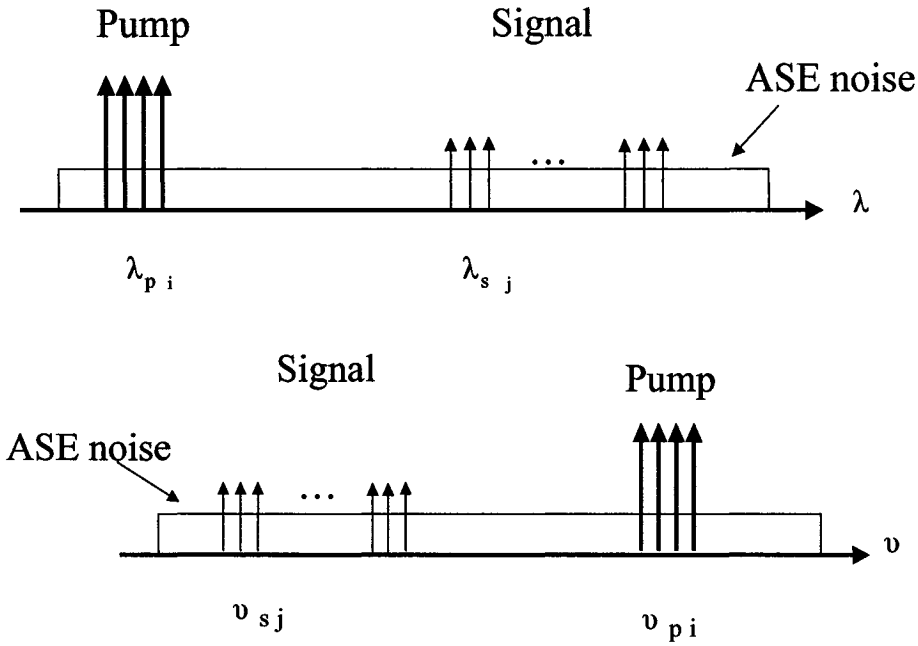

Figure 3.3 Wavelength distributions of signals, pumps, and ASE noises.

Signals obtain gains from pumps during the propagation. While they deplete their power by transferring energy to all the longer wavelength channels (signals and ASE noise). SRS crosstalk between signals can be considered as gain or noise depending on cases. In this thesis, they are considered as gain because for CW wave inputs, and also SRS between signals are commonly taken as gain. When the DFRA has more than one pump, the pumps located at shorter wavelengths deplete their power to pumps at all the longer wavelengths channels. Along with the propagation, signals can obtain power from generated ASE noise; however, the power is noise, and not gain; and also, the product from anti-Stokes process is noise. Based on the above considerations, we list signal, pump, and ASE noise propagation equations in Equation (3.9), Equation (3.10), Equation (3.11), respectively.

Signal equations:

Forward

$$\frac{dP_i^+(z_{k+1})}{dz} = -\alpha(v_i)P_i^+(z_k)$$

$$+P_i^+(z_k)\sum_j^{v_j(pumps+signals)>v_i} g_R(v_j,v_i)\left[P_j^+(z_k)+P_j^-(z_k)\right]$$

$$-P_i^+(z_k)\sum_j^{v_j(signals+noise)<v_i} \frac{V_j}{V_i}\frac{v_j}{v_i} g_R(v_i,v_j)\left[P_j^+(z_k)+P_j^-(z_k)\right]$$

(3.9)

Pump equations:

Forward

$$\frac{dP_i^+(z_{k+1})}{dz} = -\alpha(v_i)P_i^+(z_k)+\gamma(v_i)P_i^-(z_k)$$

$$+P_i^+(z_k)\sum_j^{v_j(pumps)>v_i} g_R(v_j,v_i)\left[P_j^+(z_k)+P_j^-(z_k)\right]$$

$$-P_i^+(z_k)\sum_j^{v_j(pumps+signals+noise)<v_i} \frac{V_j}{V_i}\frac{v_j}{v_i} g_R(v_j,v_i)\left[P_j^+(z_k)+P_j^-(z_k)\right]$$

(3.10a)

Pump equations:

Backward

$$\frac{dP_i^-(z_k)}{dz} = -\alpha(v_i)P_i^-(z_{k+1}) + \gamma(v_i)P_i^+(z_{k+1})$$

$$+ P_i^-(z_{k+1}) \sum_j^{v_j(pumps)>v_i} g_R(v_j, v_i)\left[P_j^+(z_{k+1}) + P_j^-(z_{k+1})\right]$$

$$- P_i^-(z_{k+1}) \sum_j^{v_j(pumps+noise)<v_i} \frac{V_j}{V_i}\frac{v_j}{v_i} g_R(v_j, v_i)\left[P_j^+(z_{k+1}) + P_j^-(z_{k+1})\right]$$

(3.10b)

ASE noise power:

Forward

$$\frac{dP_i^+(z_{k+1})}{dz} = -\alpha(v_i)P_i^+(z_k) + \gamma(v_i)P_i^-(z_k)$$

$$+ P_i^+(z_k) \sum_j^{v_j>v_i} g_R(v_j, v_i)\left[P_j^+(z_k) + P_j^-(z_k)\right]$$

$$+ 2hv_i\Delta v \sum_j^{v_j>v_i} g_R(v_j, v_i)\left[P_j^+(z_k) + P_j^-(z_k)\right]\left[1 + \frac{1}{\exp\left(\frac{h(v_j - v_i)}{kT}\right) - 1}\right]$$

$$- P_i^+(z_k) \sum_j^{v_j<v_i} \frac{V_j}{V_i}\frac{v_j}{v_i} g_R(v_j, v_i)\left[P_j^+(z_k) + P_j^-(z_k)\right]$$

$$+ 2hv_i\Delta v \sum_j^{v_j<v_i} \frac{V_j}{V_i}\frac{v_j}{v_i} g_R(v_j, v_i)\left[P_j^+(z_k) + P_j^-(z_k)\right]\left[\frac{1}{\exp\left(\frac{h(v_i - v_j)}{kT}\right) - 1}\right]$$

(3.11a)

ASE noise power:

Backward

$$\frac{dP_i^-(z_k)}{dz} = -\alpha(v_i)P_i^-(z_{k+1}) + \gamma(v_i)P_i^+(z_{k+1})$$

$$+ P_i^-(z_{k+1})\sum_j^{v_j>v_i} g_R(v_j, v_i)\left[P_j^+(z_{k+1}) + P_j^-(z_{k+1})\right]$$

$$+ 2hv_i\Delta v\sum_j^{v_j>v_i} g_R(v_j, v_i)\left[P_j^+(z_{k+1}) + P_j^-(z_{k+1})\right]\left[1 + \frac{1}{\exp\left(\frac{h(v_j - v_i)}{kT}\right) - 1}\right]$$

$$- P_i^-(z_{k+1})\sum_j^{v_j<v_i} \frac{V_j}{V_i}\frac{v_j}{v_i} g_R(v_j, v_i)\left[P_j^+(z_{k+1}) + P_j^-(z_{k+1})\right]$$

$$+ 2hv_i\Delta v\sum_j^{v_j<v_i} \frac{V_j}{V_i}\frac{v_j}{v_i} g_R(v_j, v_i)\left[P_j^+(z_{k+1}) + P_j^-(z_{k+1})\right]\left[\frac{1}{\exp\left(\frac{h(v_i - v_j)}{kT}\right) - 1}\right]$$

(3.11b)

To verify the correctness of our modeling, we repeat the same simulations as given in [38]. Verification 1 is based on a 13-km TW-Reach transmission fiber at 300 K temperature. Input is a 13mW signal at wavelength of 1560 nm. Figure 3.4 is the comparison of the results between [38] and our modeling. Since Figure 3.4 (a) is based on TW-RS fiber, while Figure 3.4 (b) is based on TW-Reach fiber, and it is nature that Figure 3.4 (a) and (b) have the same power density shape but with different absolute values due to different fibers.

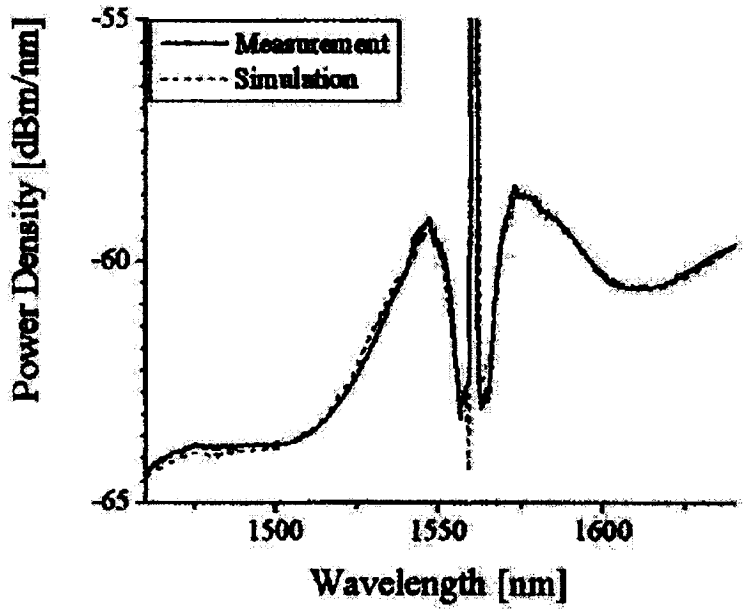

(a)

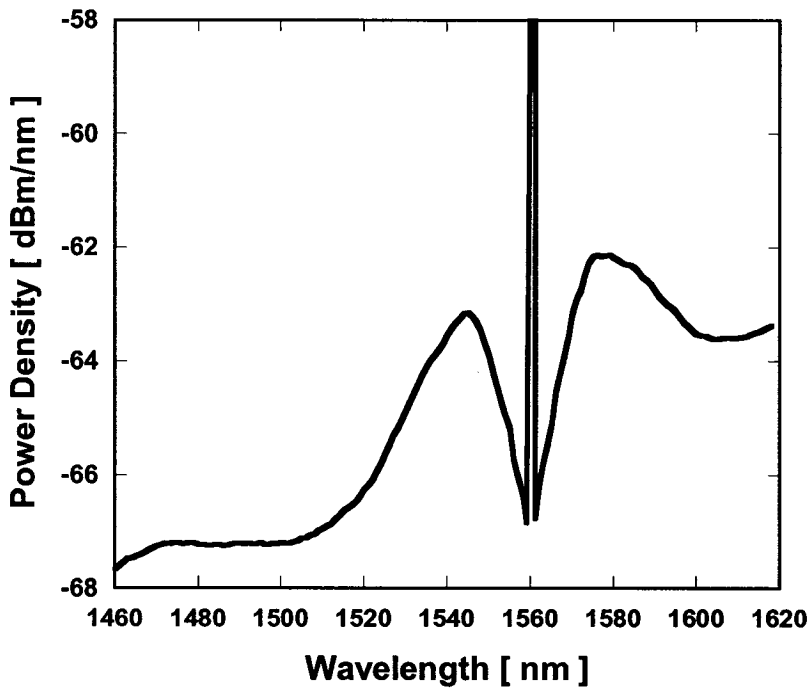

(b)

Figure 3.4 Power spectrum comparison: (a) from [38], (b) This work.

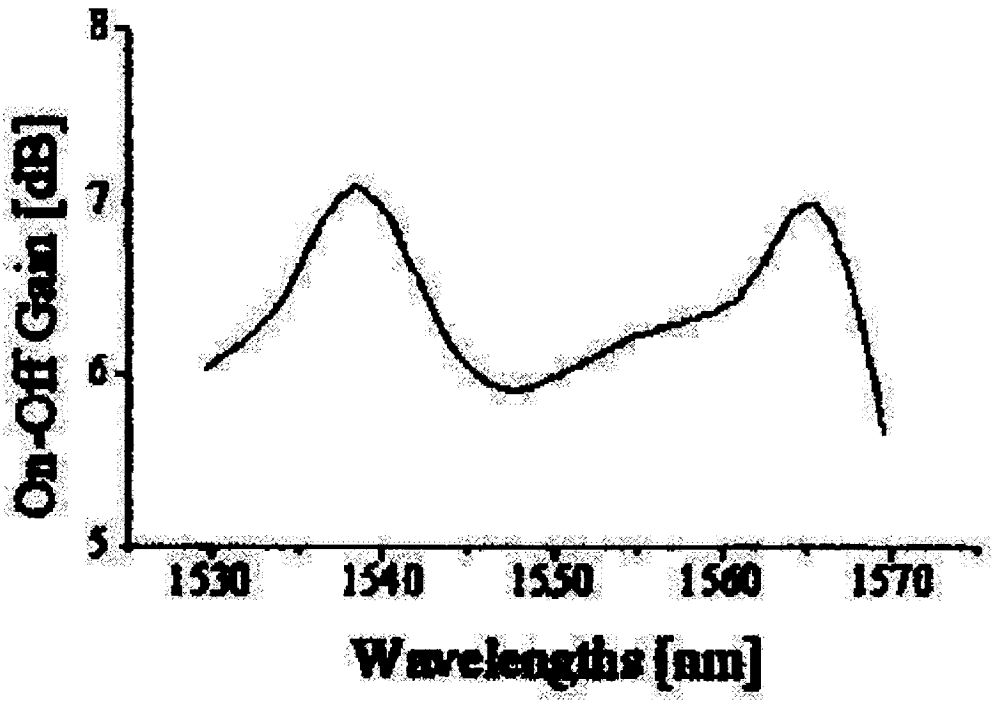

(a)

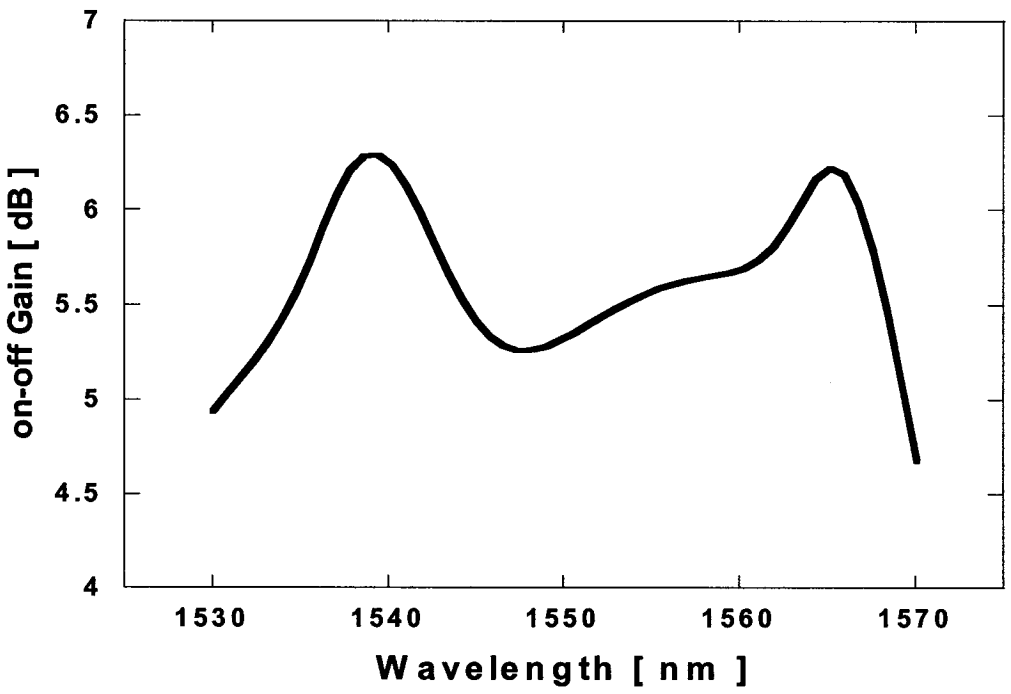

(b)

Figure 3.5 On-off gain comparison: (a) from [38], (b) our work. SRS between signals is noise, and MPI is not considered.

Verification 2 is to use a 100 km Corning SMF-28 fiber, with input of 51 channels in C band, each of which has a power of 1.96 mW. The channel spacing is 100 GHz. Two pumps are co-injected with 300 mW at 1430 nm and 262.5 mW at 1454 nm. Moreover, SRS between signals is considered as noise and MPI is not considered according to [38]. Figure 3.5 shows the comparison of on-off gain between [38] and our work. Gain spectrums in Figure 3.5 (a) and (b) are completely the same except that the gain in (b) is about 1 dB smaller than the gain in (a). The difference in absolute gain values may be due to the different g_R values (we do not have the same g_R as in [38]). Therefore, we confirmed the correctness of our modeling. As we declared in the beginning of Section 3.3, SRS between signals is considered as gain and MPI is considered as noise, the assumptions of this thesis. So we repeat the simulation of verification 2 with taking SRS between signals as gain and MPI as noise, and the gain spectrum is illustrated in Figure 3.6. From the spectrum in Figure 3.6, we see that SRS between signals has a significant impact on gain spectrum.

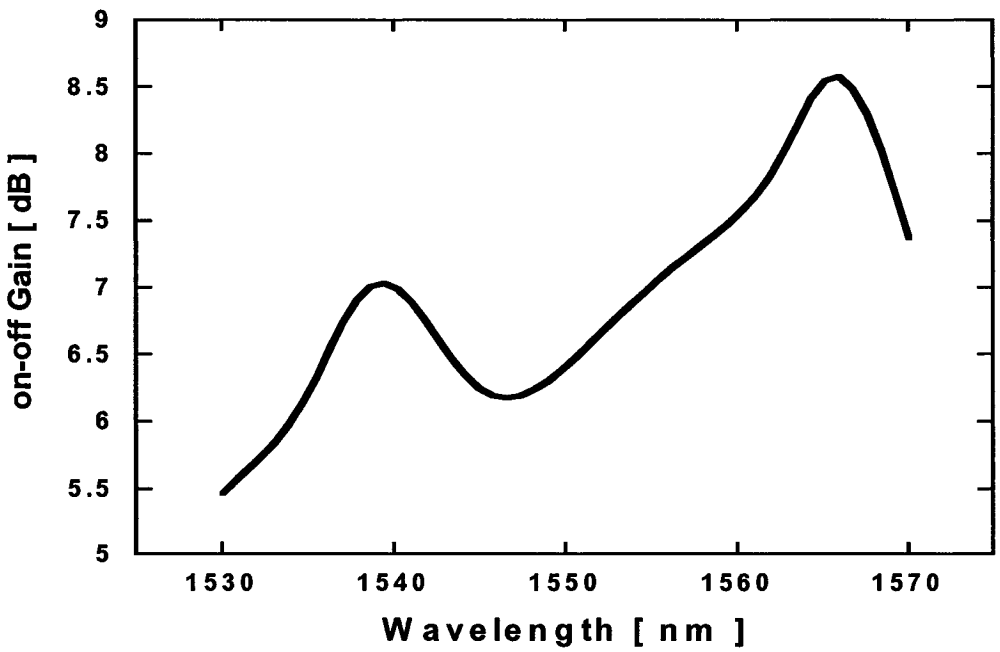

Figure 3.6 Gain spectrum from our work, SRS between signals is gain, and MPI is considered.

CHAPTER 4 Incoherent Pump Modeling

Incoherent pump is a kind of new fabricated Raman amplifier pump source provided by Ahura Corporation last year. This chapter is to explain its theory and modeling method used in this thesis. An incoherent pump example is given, and the corresponding gain spectrum is shown also.

4.1 Incoherent pump theory

Incoherent pump beam is a pump that spread its power within a broad bandwidth, not within a narrow bandwidth as a coherent pump beam does. This broadband pump is achieved by coupling low-power seed optical signal into a long-cavity semiconductor amplifier waveguide. This method is called seeded power optical amplifier (SPOA) concept. Semiconductor optical amplifier is designed and fabricated to have saturated output power of > 250 mW currently [25], and could be further increased. Figure 4.1 is a photograph of high-power broad bandwidth Raman pump module [41]. Within the butterfly package, seeded source input, optical amplifier devices, isolators, detectors, and thin-film signal/pump WDM optics are integrated. Figure 4.2, is an optical spectrum of an on sale incoherent pump.

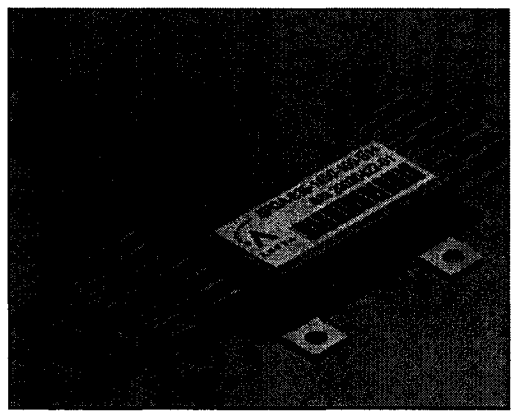

Figure 4.1 High-power broadband Raman pump module

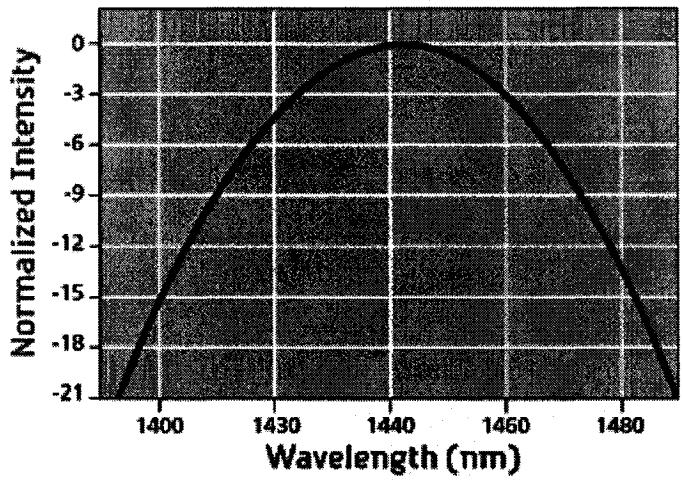

Figure 4.2 Optical-spectrum of an incoherent pump on sale [41].

From the introduction given by Ahura, we know that by adjusting the central wavelength, and input current of the pump model, required incoherent pump can be achieved easily. At this moment, Ahura Corporation provides incoherent pumps with central wavelength between 1440 nm and 1460 nm, with FWHM bandwidth of greater than or equal to 35 nm, and minimum output power of 125 mW.

In the thesis, incoherent pumps are not restricted to the current commercial products. Simply, we investigate DFRAs with incoherent pumps that provide good performance.

4.2 Incoherent pump modeling

Incoherent pump is modeled as follows. The Gaussian noise is generated in a broad bandwidth. After the noise passing through an approximate Gaussian filter, we obtain an approximate Gaussian-intensity spectrum. The incoherent pump is adjustable by changing the center wavelength, FWHM bandwidth of the filter and the power of Gaussian noise. Equation (4.1) is the referring approximate Gaussian filter equation.

$$H(\lambda)=\left[\frac{1}{1+\left[\frac{2(\lambda-\lambda_0)}{B_0}\right]^{2*N}}\right]^{\frac{1}{2}} \tag{4.1}$$

Where λ_0 is the central wavelength, and $B_0 = B_{3-dB}\left(2^{\frac{1}{N}}-1\right)^{-\frac{1}{2}}$. N is a value parameter between 2 and 5. In this thesis, N=2 is used always.

Figure 4.3 is an example of simulated incoherent pump. The filter is centered at 1453 nm, with FWHM bandwidth of equal to 35 nm. The Gaussian noise power is around 3.31 mW within 1 nm bandwidth. Let the Gaussian noise passes through the above filter, we obtain the incoherent pump shown in Figure 4.3. Its total power is 230 mW and spreads from 1404 nm to 1499 nm. Figure 4.4 shows the on-off Raman gain after a 50 km TW-Reach fiber, which is counter-pumped by the above incoherent pump and same power coherent pump located at 1453 nm.

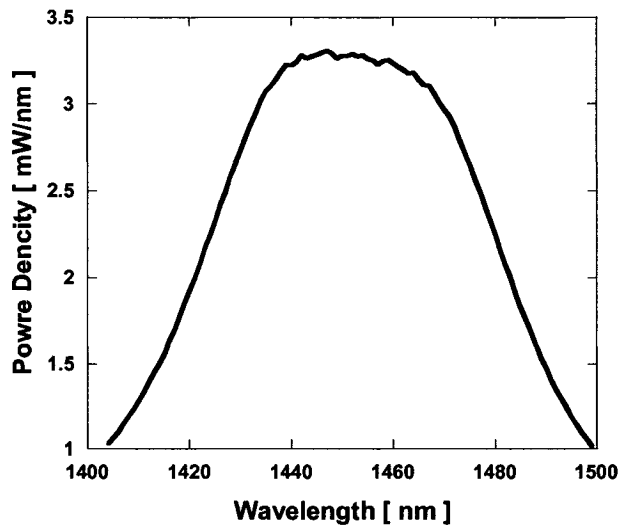

Figure 4.3 incoherent pump example: central wavelength 1453 nm, FWHM bandwidth 35 nm, N =2, total power 230 mW.

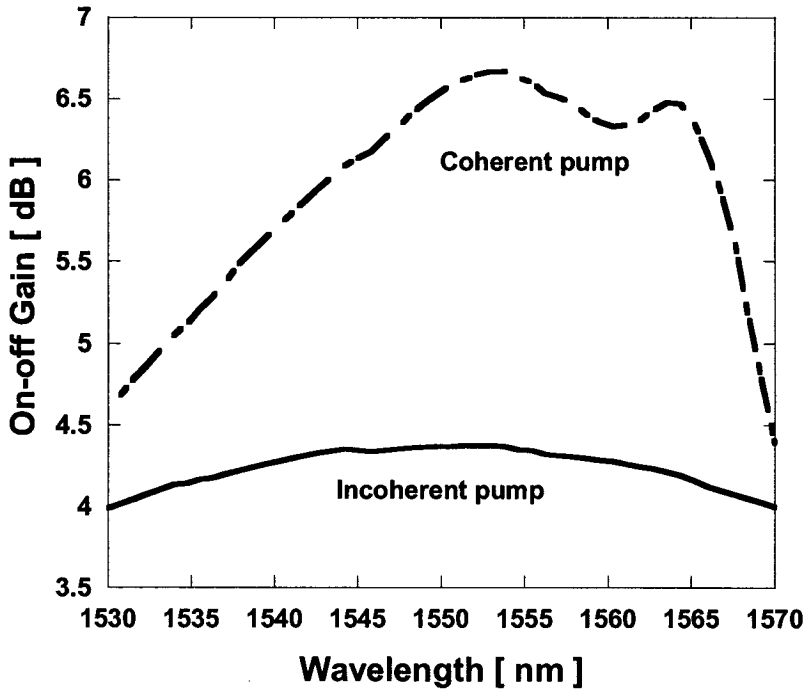

Figure 4.4 On-off gain comparison: The pump power is 230 mW. Incoherent pump is solid curve. Dot-dash curve is coherent pump located at 1453 nm.

Figure 4.4 shows that incoherent pump provides a more flat gain than coherent pump with the same pump power. The example shows that gain ripple by incoherent pump is 0.4 dB, while the smallest gain ripple is 2.3 dB from a coherent pump with 230 mW. However, gain values resulting from incoherent pump are much smaller than the values from coherent pump. The reason for this phenomenon is that incoherent pump spreads its power in a broadband range and amplifies signals in a broader wavelength range. Consequently, gain becomes smaller.

CHAPTER 5 Performance of DFRAs with One Incoherent Pump

The gain comparison in Chapter 4 shows that incoherent pump works better than coherent pump in gain flatness. Consequently, investigations are completed in this chapter to find out the gain and noise performance difference in detailed between one incoherent pump and one coherent pump. Comparisons of distributed fiber Raman amplifiers in C band are given in Section 5.1, while Section 5.2 is the analysis for L band. In each section, there are four cases, which present commonly used designs. SMF-28 and TW-Reach fibers, which are the popular single mode fibers used in transmission, are taken into account in this thesis. Raman amplifier fibers with span length of 50 km and 100 km are considered since they are common in system design. All DFRAs are backward pumped for fiber length of 50 km or 100 km, as counter-pump is more suitable [42]. In Section 5.3, we analyze the effects of FWHM on DFRAs performance when the total pump power is the same. While in Section 5.4, FWHM effects on ENF performance is studied when the average gain is the same. Trends of gain and noise with the changing of FWHM are clearly illustrated.

5.1 Performance of C-band DFRAs with one incoherent and one coherent pump

The C band is the most commonly used wavelength range in current fiber optical transmission systems, which covers from 1530 nm to 1570 nm. According to the Raman pump principle illustrated in Chapter 2, pumps, located between wavelengths 1430 nm and 1470 nm, have high gain coefficient for signals in C band. Therefore, when looking for the pumps that provide the high and flat gain in C band, we search them in the range between 1430 nm and 1470 nm. Four cases are considered in this section to show the gain and noise performance difference in detailed.

The first case is a TW-Reach DFRA with span length of 50 km. Input signals are 51

channels, each has a power of 0.1 mW, and channel spacing is 100 GHz. Therefore, signals start at 1530 nm, and end up at 1570 nm. The total pump power for each pumping scheme is set to be 265 mW. Incoherent pump with FWHM of 35 nm is used to compare to coherent pump. Their central wavelengths are optimized to have the best gain performances. As a result, we found that incoherent pump with central wavelength of 1452 nm provides an average gain of 4.8 dB with a ripple of 0.43 dB; while coherent pump located at 1454 nm provides an average gain of 6.8 dB with a ripple of 2.5 dB.

Shown in Figure 5.1.1, it is clear that the incoherent pump improves the gain ripple significantly, which is 2 dB. However, the average gain value is decreased by 2 dB for incoherent pump. The reason is that incoherent pump spreading its power to a wide wavelength range leads to providing smooth and smaller gain in a wider bandwidth, which means that the gain spectrum from the 265 mW/35 nm FWHM incoherent pump covers a bandwidth much wider than C band, and the gain in C band range has a small ripple. Therefore, incoherent pump efficiency is decreased. The degradation of average gain by using incoherent pump certainly makes its ENF become worse. As shown in Figure 5.1.2, the average ENF provided by coherent pump is –0.4 dB, while this value achieved by incoherent pump is –0.03 dB.

Considering that the FWHM affects the pump efficiency, we decrease the FWHM value of the incoherent pump to 25 nm. This time, the incoherent pump is optimized at center wavelength of 1453 nm. The dash lines in Figure 5.1.2 and Figure 5.1.3 are the corresponding gain and ENF. The comparisons show that after changing FWHM from 35 nm to 25 nm, the average noise figure is –0.116 dB improved by 0.09 dB, the average gain is 5.3 dB increased by 0.5 dB, and the gain ripple is 0.7 dB degraded by 0.3 dB. Detailed results are given in Table 5.1.1.

Table 5.1.1 Detailed results for Case 1.

Section 5.1, Summary for Case 1						
Fiber	TW-Reach, 50 km					
Signal	51 channel, 1530nm – 1570nm, 100GHz spacing, 0.1mW each channel.					
Pump	Incoherent pump 1		Coherent pump		Incoherent pump 2	
	Power [mW]	265	Power [mW]	265	Power [mW]	265
	Center wave-length [nm]	1452	Center wave-Length [nm]	1454	Center wave-Length [nm]	1453
	FWHM [nm]	35	FWHM [nm]	---	FWHM [nm]	25
Gain ripple [dB]	0.434		2.517		0.734	
Average on-off gain [dB]	4.820		6.810		5.309	
ENF ripple [dB]	0.490		1.085		0.521	
Average ENF [dB]	-0.025		-0.401		-0.116	

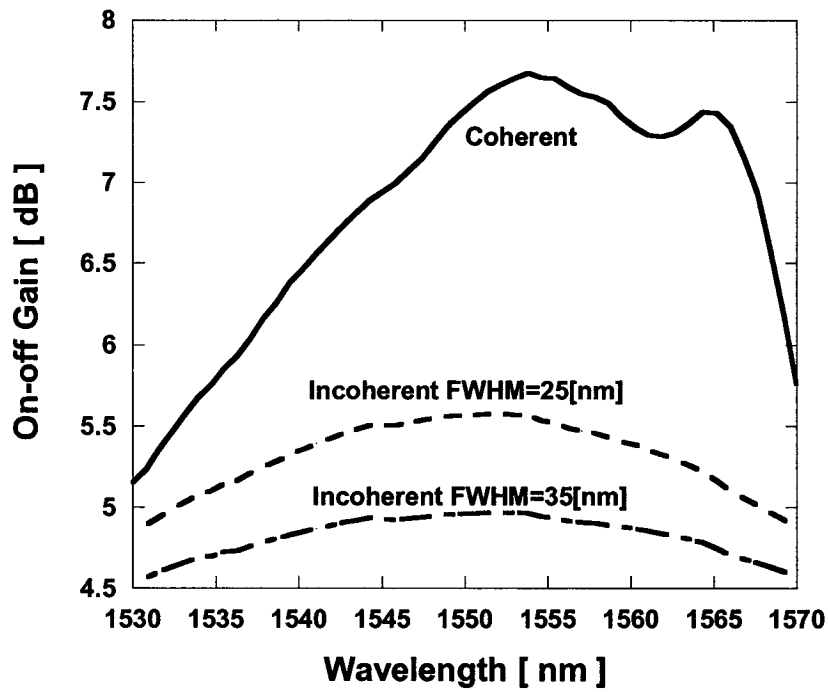

Figure 5.1.1 Gain comparison for Case 1. The pump power is 265 mW.

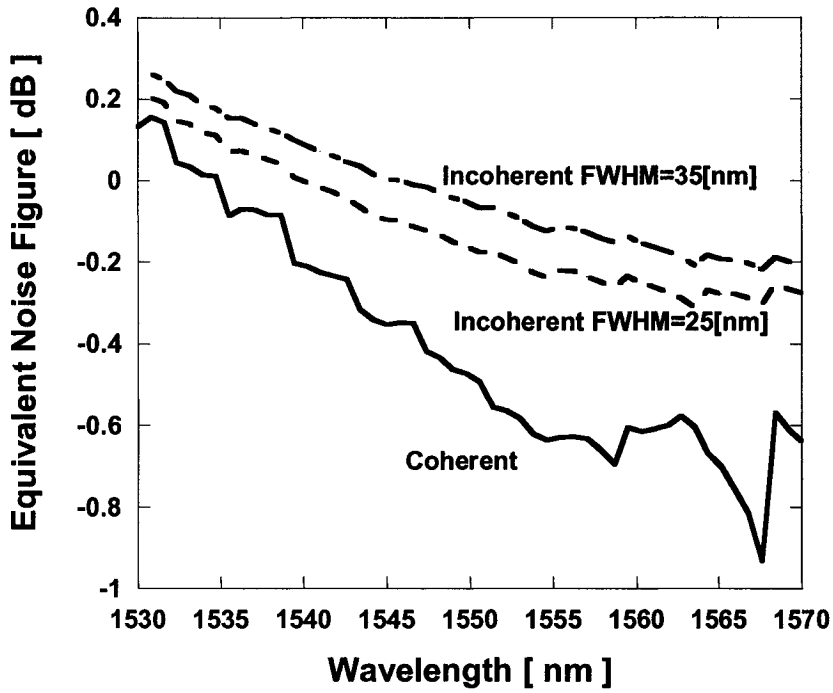

Figure 5.1.2 ENF comparison for Case 1. The pump power is 265 mW.

Now we consider the second case, which is based on a 100-km TW-Reach fiber. 51 input signal channels start at 1530 nm and end up at 1570 nm, with 100 GHZ spacing. In this case, input power of each channel is 1 mW, and total pump power is set to be 400 mW because of the increase in span length. Three pumping schemes are coherent pump, incoherent pumps with FWHM of 25 nm and 35 nm.

Under the above conditions, the incoherent and coherent pumps are optimized to find the best performance. As a result, the incoherent pump central wavelength is located at 1442 nm with FWHM of 35 nm; the coherent pump wavelength moves to 1453 nm; and the 25-nm FWHM incoherent pump gives flattest gain when centered at 1447 nm. Figure 5.1.3 shows the gain by applying the above three pumping schemes. The gain ripples are 4 dB, 1 dB, and 0.7 dB for coherent pump, incoherent pump with 25 nm and 35 nm FWHM, respectively. The improvement is significant by using the two incoherent pumps. However, it is accompanied with the decrease of average gain, which are 10.6 dB, 8 dB,

and 7.3 dB correspondingly. ENF values in turn become worse for the both 25- and 35-nm FWHM incoherent pumps, which are -0.75 dB, and –0.62 dB in Figure 5.1.4, compare to –1.3 dB by using the coherent pump. Table 5.1.2 has the detailed data.

Table 5.1.2 Detailed results for Case 2.

Section 5.1 Summary for Case 2						
Fiber	TW-Reach, 100 km					
Signal	51 channel, 1530nm – 1570nm, 100GHz spacing, 1mW each channel.					
Pump	Incoherent pump 1		Coherent pump		Incoherent pump 2	
	Power [mW]	400	Power [mW]	400	Power [mW]	400
	Center wave-length [nm]	1442	Center wave-Length [nm]	1454	Center wave-Length [nm]	1447
	FWHM [nm]	35	FWHM [nm]	----------	FWHM [nm]	25
Gain ripple [dB]	0.682		3.9985		1.03	
Average on-off gain [dB]	7.305		10.557		8.017	
ENF ripple [dB]	1.093		2.01		1.106	
Average ENF [dB]	-0.619		-1.305		-0.751	

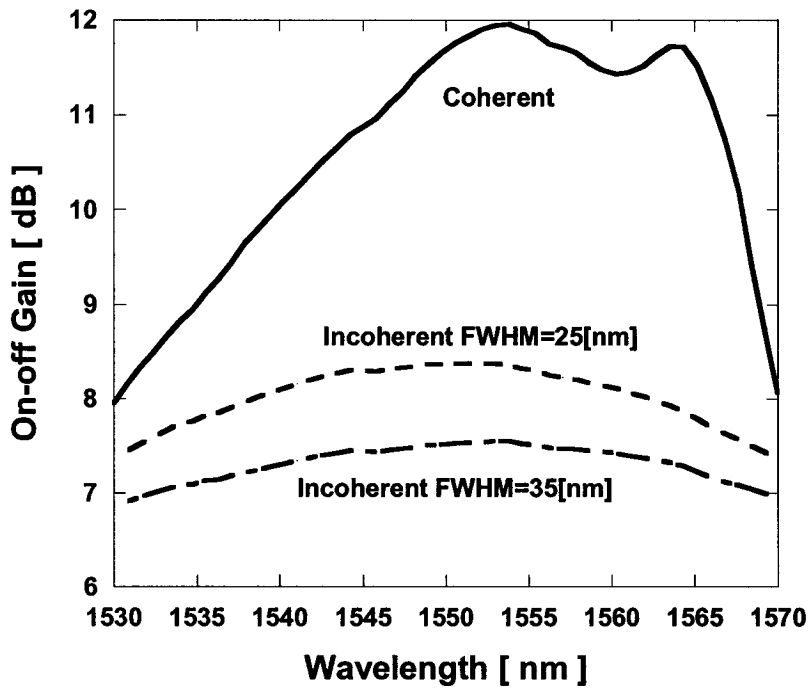

Figure 5.1.3 Gain comparison for Case 2. The pump power is 400 mW.

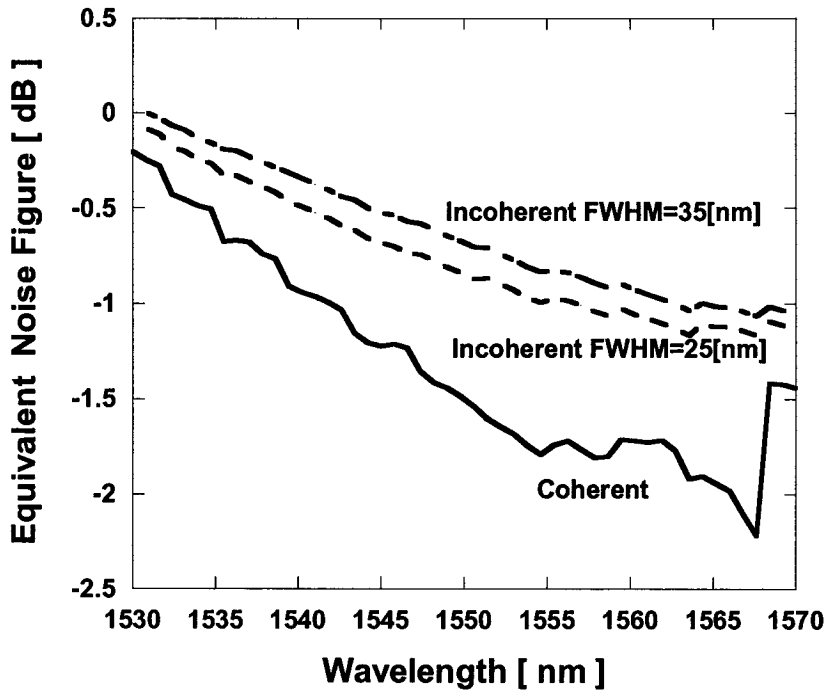

Figure 5.1.4 ENF comparison for Case 2. The pump power is 400 mW.

Investigations for Cases 1 and 2 reveal the same fact that with the same total pump power, incoherent pump provides more flat gain than coherent pump, but the average gain decreases. It has been shown that gain ripple improvement for 35-nm FWHM incoherent pump is nearly six times better, and for 25-nm FWHM incoherent pump is four times better comparing to the coherent pump. ENF values become worse for incoherent pumped DFRAs because of the degradation of gain.

Similar investigations have been conducted on SMF-28 fiber based DFRAs for both 50 km and 100 km span length, which are the Cases 3 and 4 in this section. Signal inputs are the same with those in 50 km and 100 km TW-Reach DFRAs correspondingly.

In Case 3, total pump power is 300 mW. Gain ripples after pump optimization are 2.2-, 0.6-, 0.35- dB for coherent pump, and incoherent pump with FWHM of 25 nm and 35 nm as shown in Figure 5.1.5. Corresponding average gain values are 6-, 4.6-, and 4 dB. In Case 4, total pump power is set to be 500 mW. The best gain performances found are

(average/ripple): 10.2-/4 dB for coherent pump, 7.22-/0.92 dB for 25-nm FWHM incoherent pump, and 6.26-/0.6 dB for 35-nm FWHM incoherent pump as shown in Figure 5.1.6. Detailed summary for Cases 3 and 4 are listed in Appendix B.

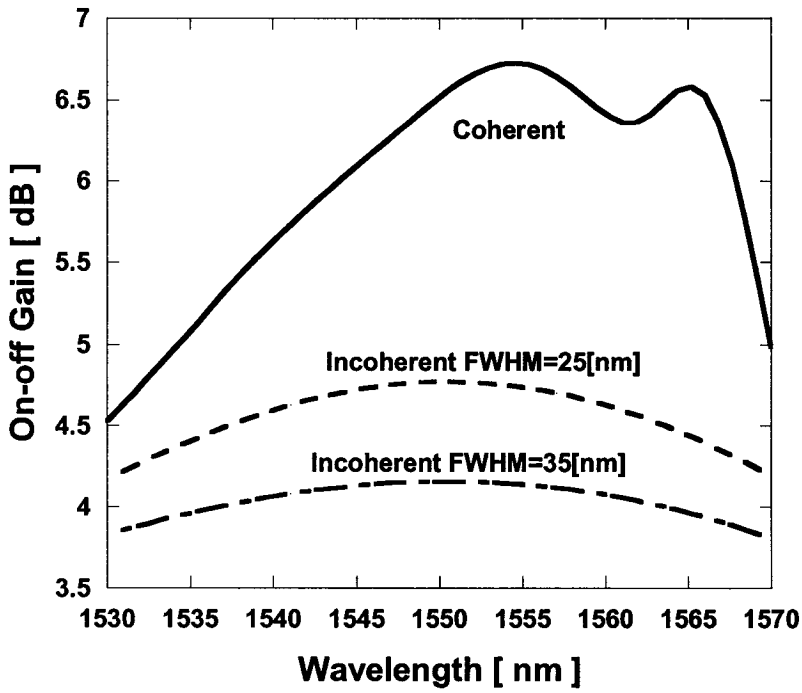

Figure 5.1.5 Gain comparison for Case 3. The pump power is 300 mW.

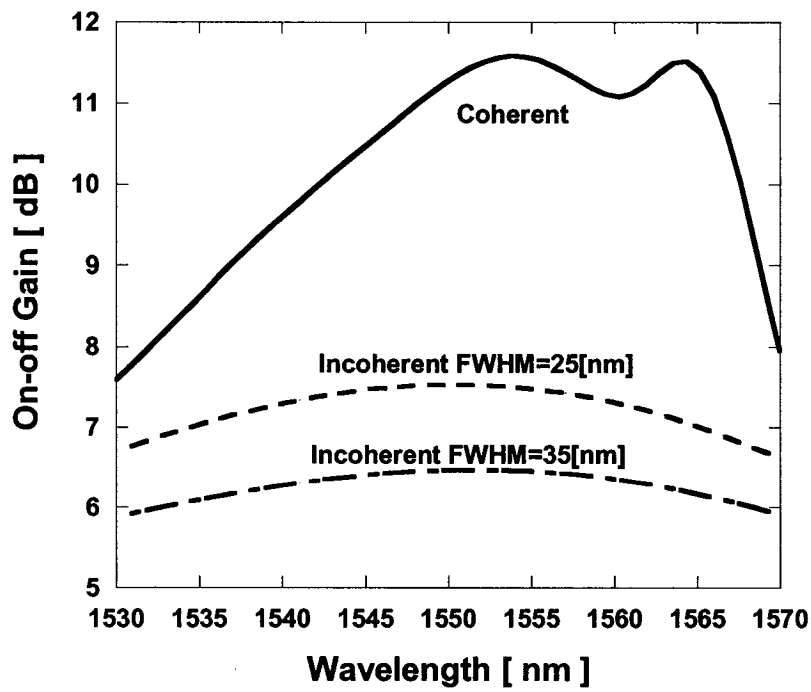

Figure 5.1.6 Gain comparison for Case 4. The pump power is 500 mW.

The results in Cases 3 and 4 show the same trend with Cases 1 and 2. Moreover, the gain ripple improvements are also around six times and four times better for incoherent pump 1 and 2. Table 5.1.3 lists the gain ripple improvements by times (gain ripple from coherent pump divided by gain ripple from incoherent pump), comparing to the corresponding coherent pumps for these four cases.

Table 5.1.3 Gain ripple improvements by times.

Section 5.1, Gain ripple improvements		
Case number	35-nm FWHM incoherent pump compares to coherent pump (times)	25-nm FWHM incoherent pump compares to coherent pump (times)
1	5.8	3.4
2	5.9	3.9
3	6.2	3.7
4	6.7	4.3

5.2 Performance of L-band DFRAs with one incoherent pump

One of DFRAs' advantages is that DFRA's can amplify signals in L band while EDFAs mainly work in C band, and SOAs are not good for in line amplification. L-band ranges from 1570 nm to 1610 nm. Signals in this band can be well amplified by Raman pumps located between 1470 and 1510 nm. Consequently, pump searching is limited in this area. Four cases are conducted in this section to find out the performance.

Case 1 is a 50 km long TW-Reach DFRA with 48 signal channels, from 1570 nm to 1610 nm. Channel spacing is 100 GHz, and each channel has power of 0.1 mW. Total input pump power is set to be 300 mW for this case, coherent and incoherent pump with FWHM of 35 and 15 nm are used to pump DFRA, respectively.

Figure 5.2.1 shows the gain comparison. Under the above configuration, pumps are optimized to have a good performance. The central wavelength is found to be 1485 nm for 35 nm FWHM incoherent pump. This incoherent pump provides a gain ripple of 0.4

dB, and average gain value of 5 dB. The coherent pump wavelength of 1488 nm gives a gain ripple of 2.3 dB, and average gain of 7.3 dB. For 15-nm FWHM incoherent pump, gain ripple is improved to be 1.25 dB, and average gain is reduced to 6.3 dB compared to the coherent pump. ENFs are smoother for incoherent pump as shown in Figure 5.2.2, and noises figures are also worse than the coherent pump. Table 5.2.1 shows the details.

Table 5.2.1 Detailed results for Case 1.

Section 5.2, Summary for Case 1						
Fiber	TW-Reach, 50 km					
Signal	48 channel, 1570nm – 1610nm, 100GHz spacing, 0.1mW each channel.					
Pump	Incoherent pump 1		Coherent pump		Incoherent pump 2	
	Power [mW]	300	Power [mW]	300	Power [mW]	300
	Center wave-length [nm]	1485	Center wave-Length [nm]	1488	Center wave-Length [nm]	1488
	FWHM [nm]	35	FWHM [nm]	----------	FWHM [nm]	15
Gain ripple [dB]	0.404		2.341		1.251	
Average on-off gain [dB]	5.143		7.255		6.290	
ENF ripple [dB]	0.474		0.925		0.603	
Average ENF [dB]	-0.090		-0.500		-0.298	

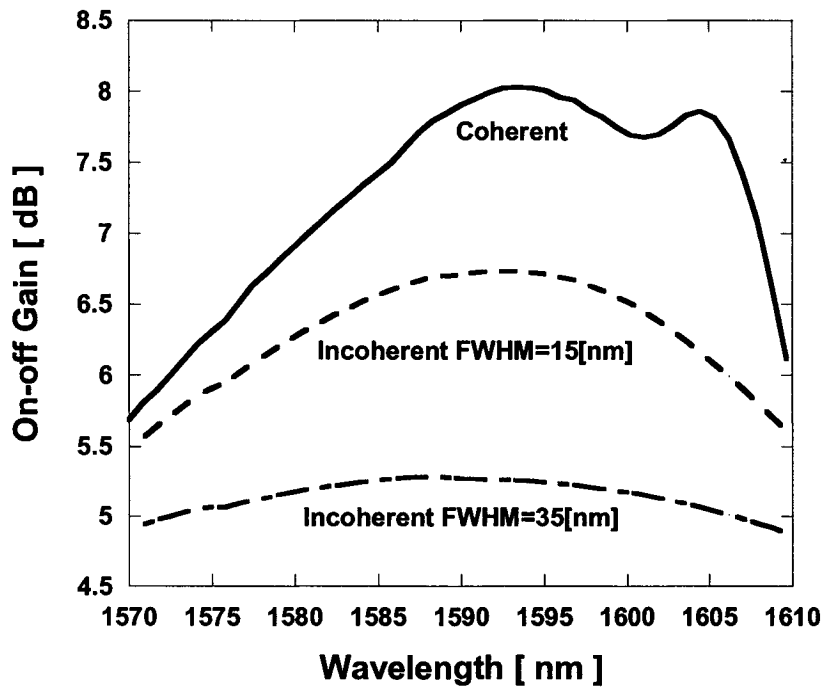

Figure 5.2.1 Gain comparison for Case 1, 300 mW total power for each pump.

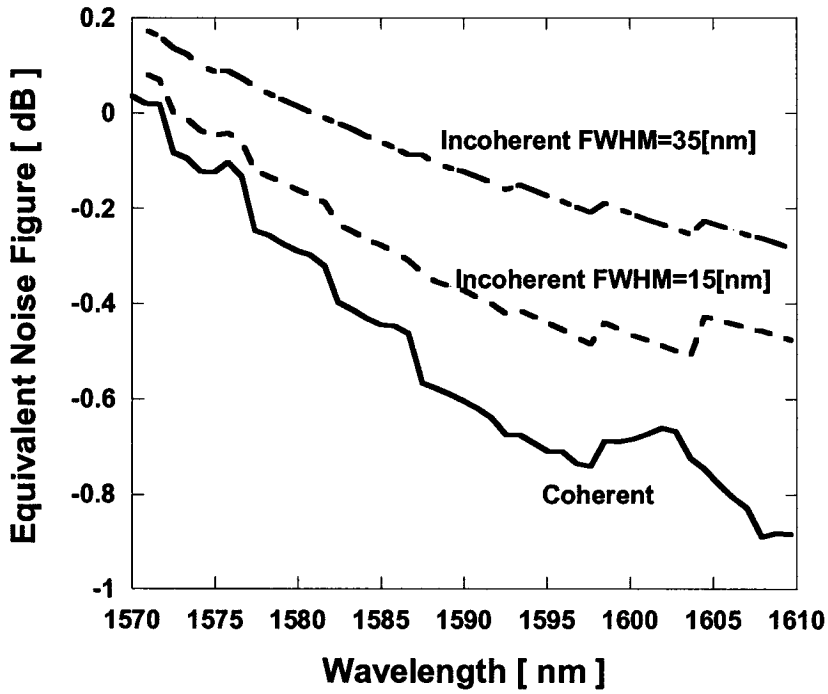

Figure 5.2.2 ENF comparison for Case 1, 300 mW total power for each pump.

Results in this case show the same fact as in C band, i.e. gain ripple nearly six times smaller for the incoherent pump 1. The relation is also held in the following three cases. However, the new brightness in Case 1 is that the gain ripple is reduced to nearly two times between incoherent pump 2 and coherent pump.

A 100 km length TW-Reach fiber is taken to complete for Case 2. Input power for each signal channel is 1 mW, and total pump power is set to be 500 mW. Other parameters are the same as those at Case 1 except that new pump central wavelengths have to be relocated for better performances. Shown in Figure 5.2.3, gain ripple is 0.66 dB for incoherent pump with 35-nm FWHM (incoherent pump 1), and 2.1 dB for incoherent pump with 15-nm FWHM (incoherent pump 2). Comparing the result of 4.24 dB from coherent pump, the six times and two times relations are held. Meanwhile, average gain values are 12.4-, 10.53-, and 8.56 dB for coherent pump, incoherent pumps with 15 nm and 35 nm FWHM, which shows a great drop for each pump compared to the previous one. ENF in Figure 5.2.4 is worse with the degradation of gain value. Table

5.2.2 provides the details.

Table 5.2.2 Detailed results for Case 2.

Section 5.2, Summary for Case 2						
Fiber	TW-Reach, 100 km					
Signal	48 channel, 1570nm – 1610nm, 100GHz spacing, 1mW each channel.					
Pump	Incoherent pump 1		Coherent pump		Incoherent pump 2	
	Power [mW]	500	Power [mW]	500	Power [mW]	500
	Center wave-length [nm]	1474	Center wave-Length [nm]	1488	Center wave-Length [nm]	1484
	FWHM [nm]	35	FWHM [nm]	----------	FWHM [nm]	15
Gain ripple [dB]	0.661		4.242		2.072	
Average on-off gain [dB]	8.562		12.400		10.527	
ENF ripple [dB]	1.098		1.856		1.196	
Average ENF [dB]	-0.876		-1.697		-1.286	

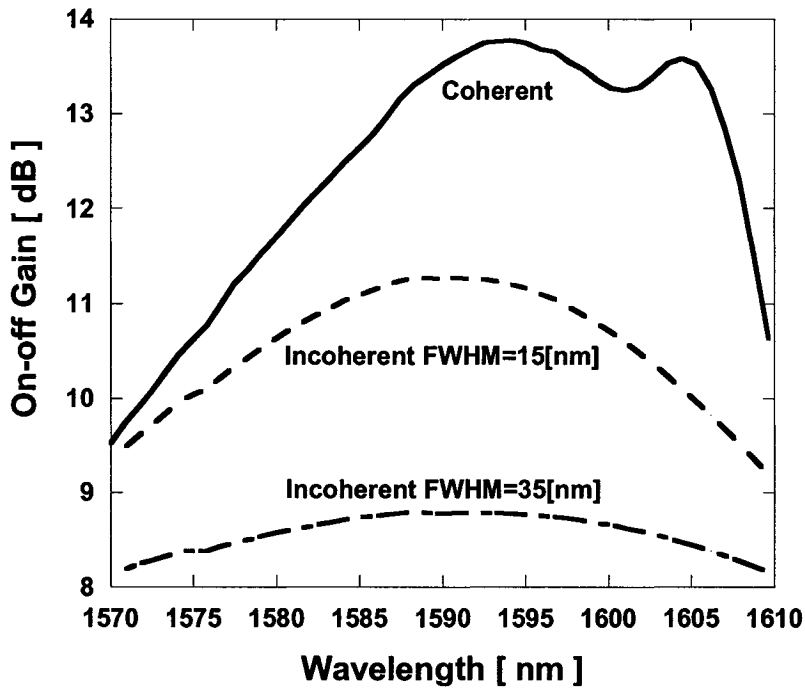

Figure 5.2.3 Gain comparison for Case 2, 500 mW total power for each pump.

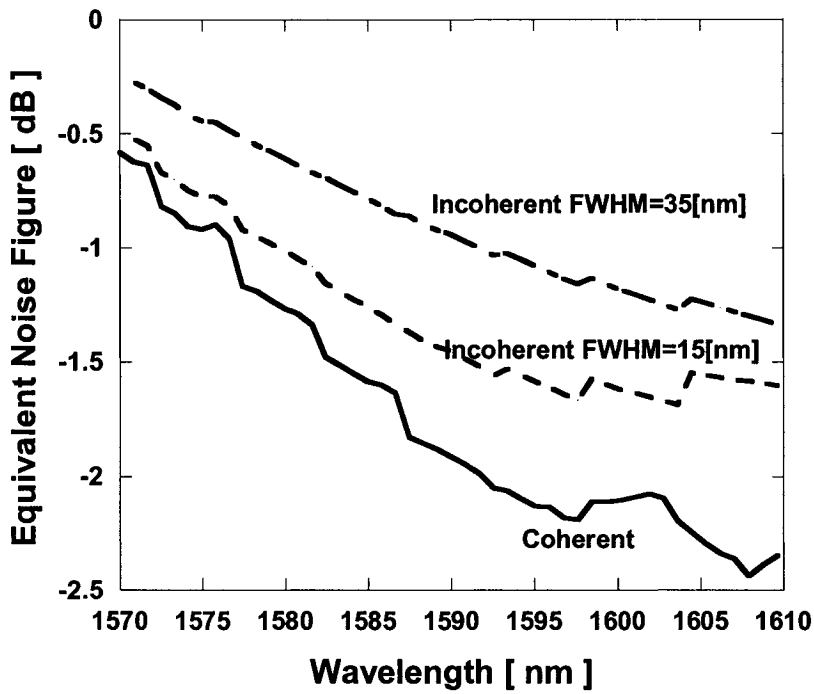

Figure 5.2.4 ENF comparison for Case 2, 500 mW total power for each pump.

We considered cases of SMF-28 50 km and 100 km as Cases 3 and 4. Signals settings and total pump powers for Case 3 and 4 are the same with those in Cases 1 and 2, respectively. In addition, central wavelength for each pump has been re-optimized. Find ENF and the detailed information in Appendix B.

Gain comparisons in Figure 5.2.5 and Figure 5.2.6 are for Cases 3 and 4. In Figure 5.2.5, gain ripples are 2.2-, 1.1-, and 0.4 dB for coherent pump, 15-nm and 35-nm FWHM incoherent pumps, respectively. In Figure 5.2.6, the ripples are 4.1-, 1.9-, and 0.65 dB for the same sequence as in Figure 5.2.5.

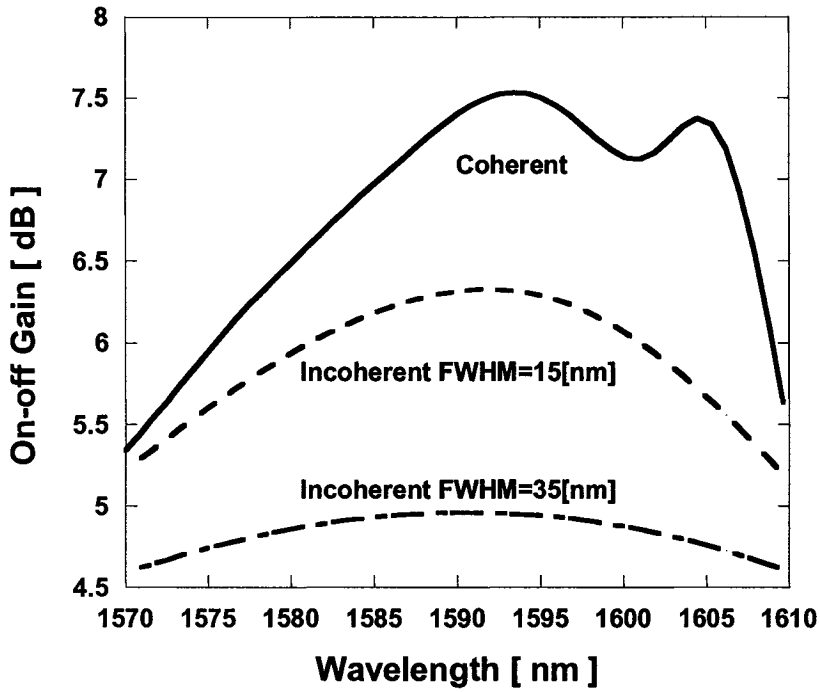

Figure 5.2.5 Gain comparison for Case 3, 300 mW total power for each pump.

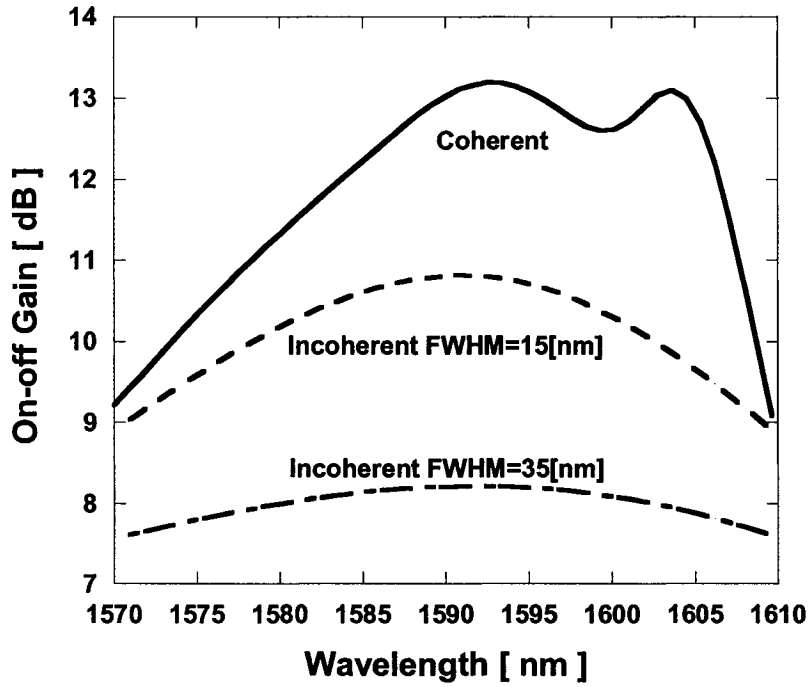

Figure 5.2.6 ENF comparison for Case 4, 500 mW total power for each pump.

5.3 FWHM effects on DFRA performance with the same pump power

After eight cases of investigations, which cover C band and L band, including different pump and signal input power, we found the same facts: with the same total pump power, gain ripple decreases dramatically with the increasing of the pump FWHM value, i.e. with the factor of 1/6, 1/4, and 1/2, an exponential relationship between FWHM and gain ripple. To explicitly know the relationship between FWHM and gain ripple, FWHM value is set to be 0 nm, 5 nm, 10 nm, 15 nm, 20nm, 25 nm, 30 nm, 35 nm, and 40 nm, respectively, to pump the DFRA from Case 1 in Section 5.2.

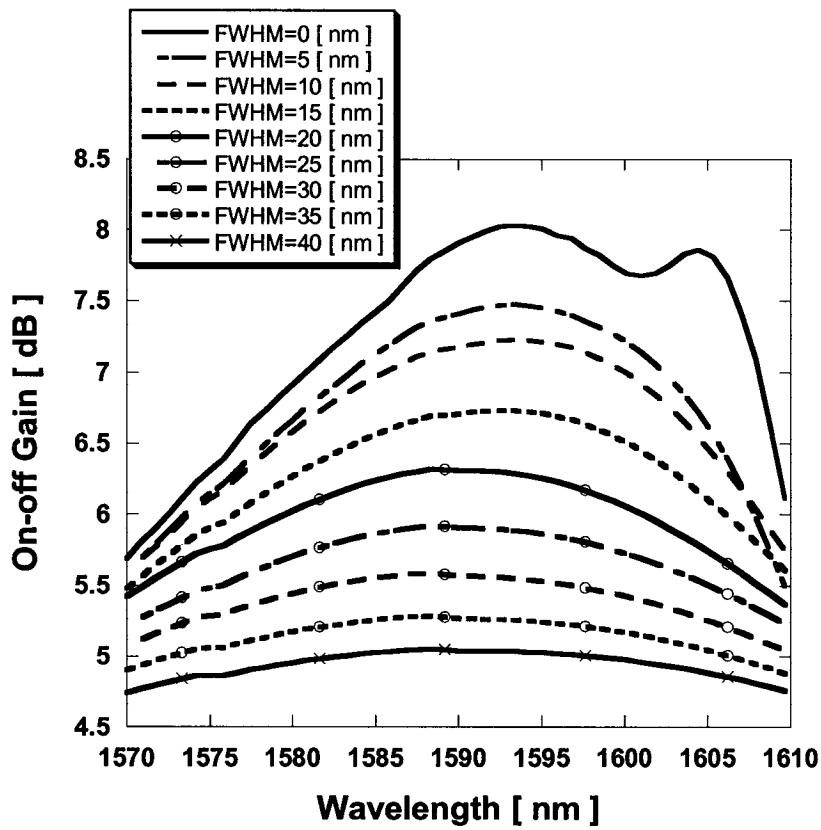

Figure 5.3.1 Gain comparison with FWHM value equal to 0 nm, 5 nm, 10 nm, 15 nm, 20 nm, 25 nm, 30 nm, 35 nm, 40 nm. Pump power is 300 mW. Others are the same with those in Section 5.2 Case 1.

Figure 5.3.1 shows the verification of gain with the increase of FWHM value. As you

can see, pumps with FWHM value between 20 nm and 40 nm give flatter gain. Gain shape starts to steeper when FWHM is less than 15 nm, and the hill become sharper quickly with the decrease of FWHM. However, the gain values go down while smooth gain is obtained. When FWHM is 40 nm, the average gain decreased to two-third of that value from the coherent pump. Considering both gain ripple and gain, FWHM value between 25 nm and 35 nm is preferred in DFRAs.

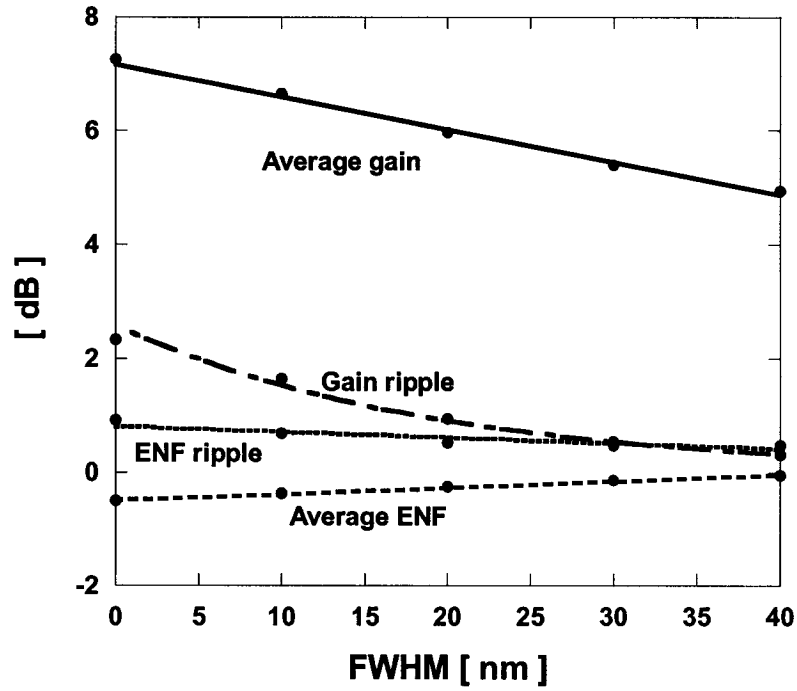

Figure 5.3.2 FWHM effects on DFRA performance. Pump power is 300 mW. FWHM = 0 nm, 5 nm, 10 nm, 15 nm, 20 nm, 25 nm, 30 nm, 35 nm, 40 nm. Others are the same with those in Section 5.2 Case 1.

Figure 5.3.2 shows the trend of gain ripple, average gain, ENF ripple, and average ENF when FWHM is increased. It is clearly shown that gain ripple decreases exponentially and the average gain decreases linearly with the FWHM increasing. On the other hand, the average ENF increases about 0.5 dB and the ENF ripple decrease about 0.5 dB when the FWHM of pumping source increases from 0 to 40 nm. In addition, there is a fact that the ripple of gain can't reach zero. So, instead of seeking flat gain blindly,

suitable FWHM value should be selected before the average gain drops to an unacceptable level.

We repeated the similar investigation on Case 2 in Section 5.2 and found the same relationship of average gain and gain ripple to FWHM. Figure 5.3.3 shows the results.

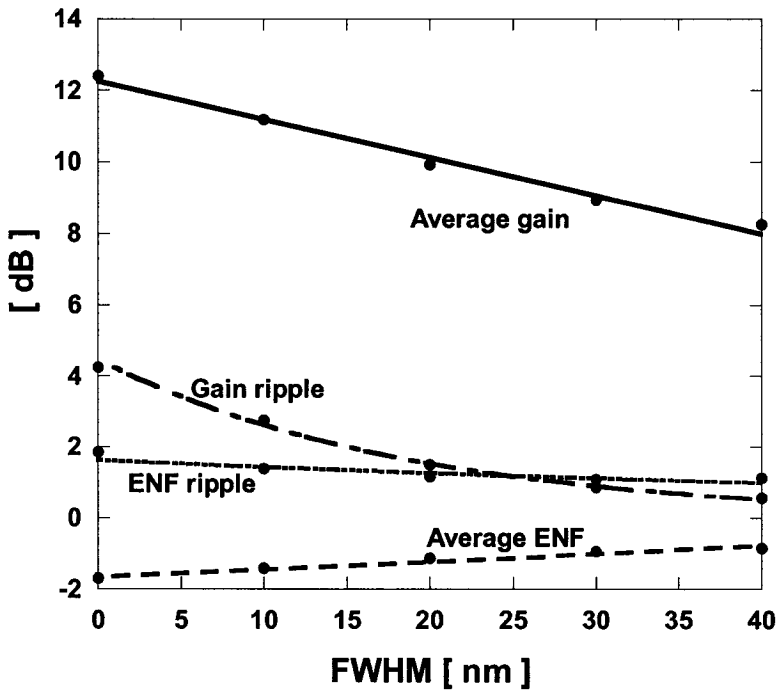

Figure 5.3.3 FWHM effects on DFRA performance. Pump power is 500 mW. FWHM = 0 nm, 5 nm, 10 nm, 15 nm, 20 nm, 25 nm, 30 nm, 35 nm, 40 nm. Signals are the same with those in Section 5.2 Case 2.

5.4 FWHM effects on ENF performance with the same average gain

All the simulations and analysis in the previous three sections are conducted under the condition of same total pump power. However, increasing the pump power to get a flat and high gain is a practical aim indeed. In this section, we first pumped a TW-Reach 50 km DFRA with a 383 mW incoherent pump with 35 nm FWHM. Input signals are the same with in Section 5.1 Case 1. This incoherent pump is optimized to have a central

wavelength at 1446 nm. The result obtained is a flat gain with a ripple of 0.56 dB and an average gain of 6.8 dB. Figure 5.4.1 shows the gain pumped by the 265 mW coherent, 383 mW incoherent, and 265 mW incoherent pumps. Among them, the 265 mW incoherent pump is the same one with a FWHM of 35 nm in Section 5.1 Case 1. It is obvious that by increasing the pump power from 265 mW to 383 mW, incoherent pump can provide the same flat gain as the 265-mW coherent pump, and the gain ripple is increased (from 0.43- to 0.56-dB) because of the increased pump power. Consequently, Figure 5.4.2 gives the ENF performance from 265-mW coherent, 383-mW incoherent, and 265-mW incoherent pumps. Average ENF values are –0.4-, 0.33-, and 0.025 dB correspondingly.

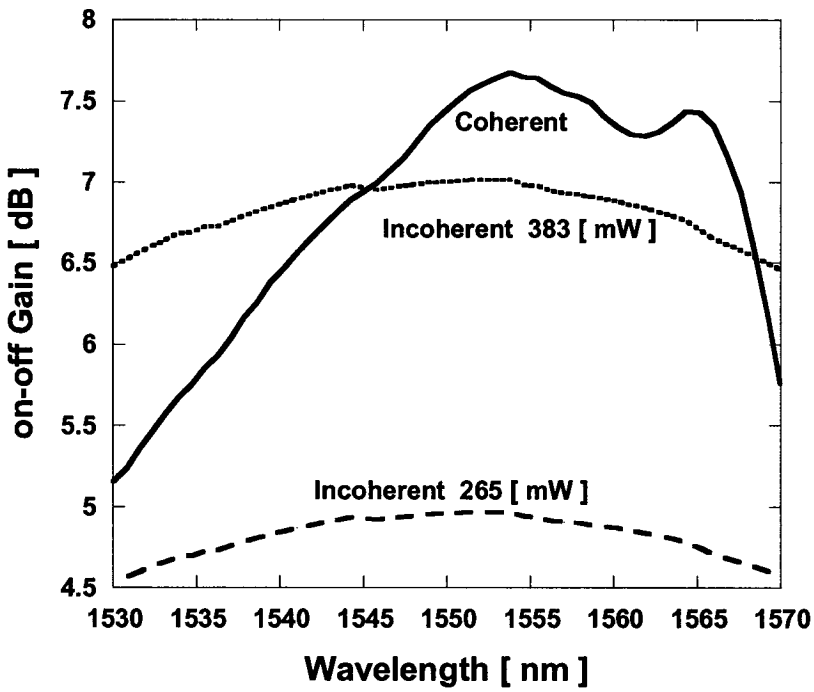

Figure 5.4.1 Gain performance from 265 mW coherent, 383 mW incoherent, and 265 mW incoherent pumps.

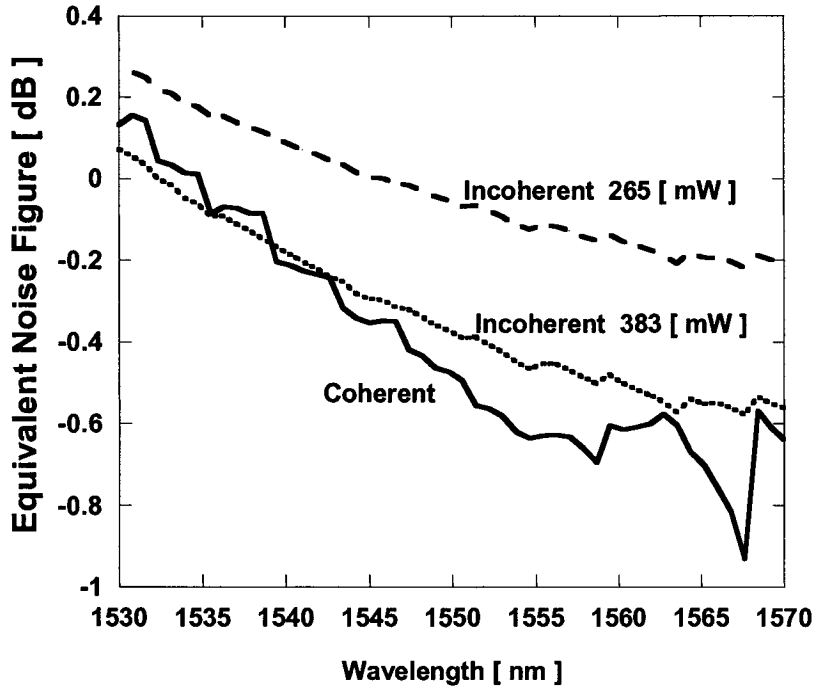

Figure 5.4.2 ENF performance from 265 mW coherent, 383 mW incoherent, and 265 mW incoherent pumps.

As shown in Figure 5.4.2, ENF by using incoherent pump is improved from –0.025 dB to –0.33 dB when increase the gain value from 4.8 dB to 6.8 dB. However, from the comparison between 265-mW coherent and 383-mW incoherent pumps, we found a slight degradation of ENF performance which is caused by the increased noise due to more pump power. This implies that with the same on-off gain, incoherent pump ENF performance is worse than coherent pump. Therefore, we complete simulations with FWHM value equal to 0-, 5-, 10-, 15-, 20-, 25-, 30-, 35-, 40- nm to find the effects of FWHM on ENF and pump power when the average gain is the same. The DFRA is a TW-Reach 50 km fiber. Signals are the same with Case 1 in Section 5.1. For all incoherent pumps with FWHM value from 0- to 40 nm, total pump power and central wavelengths are optimized to have a flat gain with average value of 6.8 dB. As shown in Figure 5.4.3, when keeping the gain un-changed, the average ENF and the total pump

power increase linearly with FWHM value. In addition, the degradation of average ENF is very slow, which is 0.08 dB, and the increase of pump power is fast, which is over 130 mW.

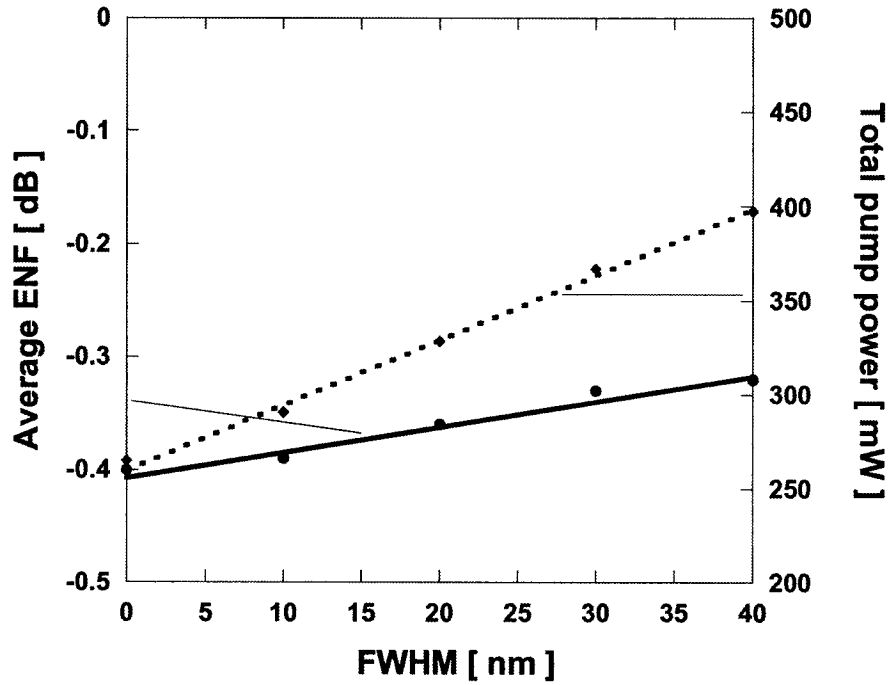

Figure 5.4.3 FWHM effects of ENF and pump power when the average gain is a constant equal to 6.8 dB.

CHAPTER 6 Performance of DFRAs with Two Incoherent, or Two, Four and Six Coherent Pumps

With the development of WDM, gain flatness became more and more important. During the past years, gain with small ripple was achieved by applying complex arithmetic, and all investigations were based on coherent pumps. In fact, it needs lots of coherent pumps to obtain a small ripple gain. For example, a gain ripple of less than 0.1 dB over 80 nm bandwidth of a 25-km-long dispersion-shifted fiber Raman amplifier needs 12 pumps [13]. Now, as Chapter 5 shows, incoherent pump can give flat gain and it obviously provides a better solution than coherent pump. However, our results in the Chapter 5 also indicate that one incoherent pump can't provide a gain ripple too small (i.e. 0.1 dB) with a reasonable gain value. For instance, the gain ripple of a C band 50 km TW-Reach DFRA, which is pumped by a 265 mW incoherent pump with FWHM equal to 35 nm, is 0.43 dB.

So, in this chapter, performances of DFRAs with two incoherent pumps are analyzed. Investigations are separated into C or L band, and C+L band, which are completed in Section 6.1 and 6.2, respectively. Section 6.1 consists of eight cases. Performances from two incoherent pumps are compared to those from two, and four coherent pumps in C- and L- band, respectively. Section 6.2 is the performance study over C+L band. Results from two incoherent pumps are compared to those from two, four, and six coherent pumps. Great gain improvement by incoherent pumps is confirmed after comparisons.

6.1 Performance of C- or L- band DFRA with two incoherent, or two coherent, and four coherent pumps

Before the comparison, we need to know how to set total pump power for two incoherent pumps. In Chapter 5, since only one incoherent pump with specified power is used for each pumping scheme, optimization is completed by adjusting the central wavelength. It does not take too much time to find the better incoherent pump setting, averagely, after six to eight simulations, we can get the result. However, for two incoherent pump case, the workload becomes much more than doubled since the two

incoherent pump power and the gain flatness are connected closely. The effect of wide bandwidth pumps on the gain is an accumulated result, which is much more complex than the effects of two coherent pumps. So when adjusting the module parameters, we have to consider both total power and gain ripple. These consume much time to find incoherent pumps, and increase the number of simulations to find flat gain. For example; when increasing one pump power to change gain value over partial wavelength, the other pump power has to be dropped down to keep the total power the same. Then the gain from the other pump will change again. Therefore, adjusting two incoherent pump power together may cause the gain over the whole studied bandwidth fluctuate like a wave, and make the process of looking for flat gain difficult.

To avoid the above problem, the simulations in this chapter do not fix the total pump power at the beginning. Instead, two incoherent pumps are adjusted one by one to decrease the gain ripple, and the total pump power will be fixed after flat gain is being achieved. Then, the total pump power will be used to limit coherent pumps.

Comparisons in this section are between two incoherent pumps, two coherent pumps, and four coherent pumps. DFRAs and signals are the same with those in Chapter 5 correspondingly. Eight cases (listed in Table 6.1.1) are conducted. Results for the first fourth cases are explained in this section. For figures and detailed dates of Cases 5 – 8, please find in Appendix B.

Table 6.1.1 Case list

Section 6.1 List of cases		
Group No	**DFRA**	**Wavelength**
1	SMF28 fiber, 50 km	C band
2	SMF28 fiber, 100 km	C band
3	TW-Reach fiber, 50 km	L band
4	TW-Reach fiber, 100 km	L band
5	TW-Reach fiber, 50 km	C band
6	TW-Reach fiber, 100 km	C band
7	SFM 28 fiber, 50 km	L band
8	SMF 28 fiber, 100 km	L band

Case 1 is a SMF-28 50 km DFRA. 51 input signal channels cover wavelength from 1530 nm to 1570 nm, which are separated by 100 GHz channel spacing. Uniform channel input power is 0.1 mW. For this DFRA and signals, total pump power is initially set to be around 450 mW. Based on the gain shape achieved, incoherent pumps are adjusted one by one to decrease the gain ripple. In this case, total pump power is ultimately fixed at 453 mW, that is the summation of one 279 mW incoherent pump and one 174 mW incoherent pump.

Figure 6.1.1 shows the gain performances for two incoherent, two coherent, and four coherent pumps. Optimized two coherent pumps are located at 1430 nm and 1458 nm with corresponding power of 213 mW and 240 mW. This configuration gives a big wave gain spectrum with a 0.77 dB ripple. Four coherent pumps reduce the gain ripple to 0.33 dB by locating them at 1425 nm with a power of 130 mW, 1436 nm with a power of 100 mW, 1455 nm with a power of 118 mW, and 1472 nm with a power of 105 mW. While for the result from two incoherent pumps (central wavelength/power/FWHM): 1425nm/278mW/12nm, and 1469nm/175mW/16nm, the gain spectrum looks like a comfortable calm lake surface with a 0.118 dB ripple. It is easily understood that four coherent pumps result in a flatter gain than two coherent pumps. The interesting note is that the average gain is reduced by the increase of the number of coherent pumps, similar behavior as the incoherent pump where the pump efficiency is reduced with the increase of FWHM. By comparing the cases of two incoherent pumps and four coherent pumps, we can easily find that the gain is much flatter by two incoherent pumps even compared to four coherent pumps. Corresponding to the gain profile, ENF is depicted in Figure 6.1.2. The worse noise performance by incoherent pump is directly induced by the gain reduction in Figure 6.1.1. If more pump power for incoherent pumps is used to obtain the same gain as for coherent pumps, the noise performance will be reduced to almost the same as those for coherent pumps, which has been proved in Section 5.4.

Note that FWHM values for the two incoherent pumps in this case are 12- and 16 nm. According to the Raman amplifier principle, one pump has its maximum pump effect over a certain wavelength. For example, in Figure 5.1.1, incoherent pumps have their over-average gain from 1440 nm to 1460 nm. So for two incoherent pumps, we want the gain curve consist of two waves over C-band. Therefore, FWHM values are reduced, and

after tries, we found that incoherent pumps with FWHM of 12 nm and 16 nm can provide better performance in C band.

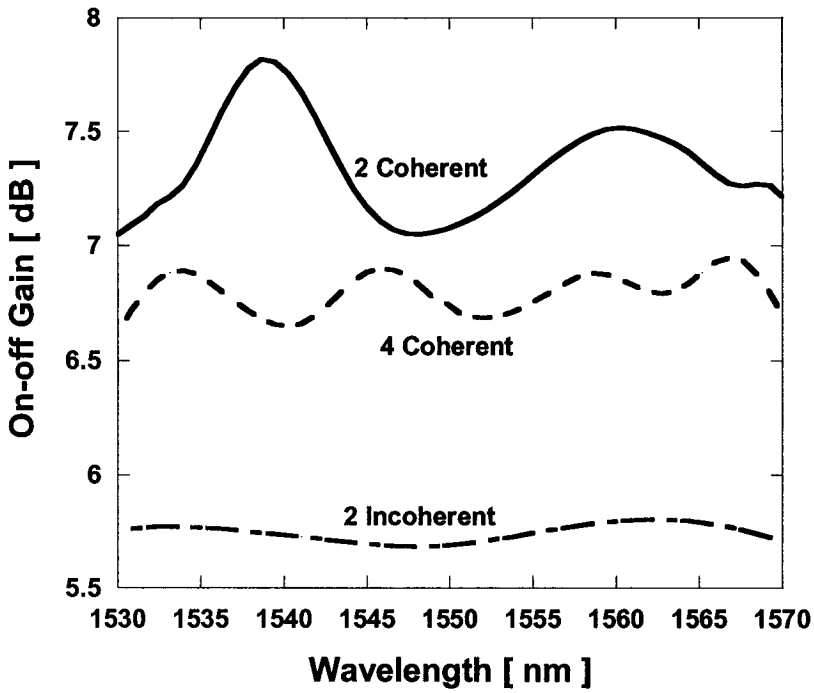

Figure 6.1.1 Gain comparison for Case 1. Total pump is 453 mW.

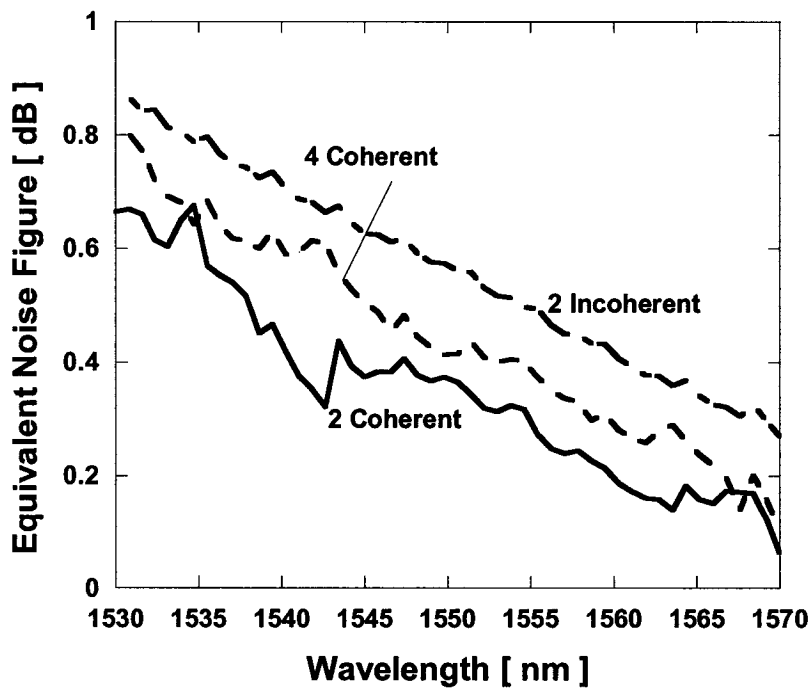

Figure 6.1.2 ENF comparison for Case 1. Total pump is 453 mW.

Table 6.1.2 Detail results for Case 1.

<table>
<tr><th colspan="12">Section 6.1, Summary for Case 1</th></tr>
<tr><td>Fiber</td><td colspan="11">SMF-28, 50km</td></tr>
<tr><td>Signal</td><td colspan="11">51 Channel, 1530nm – 1570nm, 100 GHz spacing, 0.1mW each channel</td></tr>
<tr><td rowspan="11">Pump</td><td colspan="3">2 Incoherent pump</td><td colspan="4">2 Coherent pump</td><td colspan="4">4 Coherent pump</td></tr>
<tr><td colspan="2">Total power [mW]</td><td>453</td><td colspan="2">Total power [mW]</td><td>453</td><td colspan="2">Total power [mW]</td><td>453</td></tr>
<tr><td rowspan="3">1</td><td>Power [mW]</td><td>278</td><td rowspan="3">1</td><td>Power [mW]</td><td>213</td><td rowspan="3">1</td><td>Power [mW]</td><td>130</td></tr>
<tr><td>Center wave-length [nm]</td><td>1425</td><td>Center wave-length [nm]</td><td>1430</td><td>Center wave-length [nm]</td><td>1425</td></tr>
<tr><td>FWHM [nm]</td><td>12</td><td rowspan="2">2</td><td>Power [mW]</td><td>240</td><td rowspan="2">2</td><td>Power [mW]</td><td>100</td></tr>
<tr><td rowspan="3">2</td><td>Power [mW]</td><td>175</td><td>Center wave-length [nm]</td><td>1458</td><td>Center wave-length [nm]</td><td>1436</td></tr>
<tr><td>Center wave-length [nm]</td><td>1469</td><td colspan="3" rowspan="2">----------</td><td rowspan="2">3</td><td>Power [mW]</td><td>118</td></tr>
<tr><td>FWHM [nm]</td><td>16</td><td>Center wave-length [nm]</td><td>1455</td></tr>
<tr><td colspan="3" rowspan="2">----------</td><td colspan="3" rowspan="2"></td><td>Power [mW]</td><td>105</td></tr>
<tr><td rowspan="2">4</td><td>Center wave-length [nm]</td><td>1472</td></tr>
<tr><td>Gain ripple [dB]</td><td colspan="3">0.118</td><td colspan="4">0.767</td><td colspan="4">0.333</td></tr>
<tr><td>Average on-off gain [dB]</td><td colspan="3">5.744</td><td colspan="4">7.344</td><td colspan="4">6.797</td></tr>
<tr><td>ENF ripple [dB]</td><td colspan="3">0.610</td><td colspan="4">0.624</td><td colspan="4">0.711</td></tr>
<tr><td>Average ENF [dB]</td><td colspan="3">0.569</td><td colspan="4">0.353</td><td colspan="4">0.450</td></tr>
</table>

For Case 2, SMF-28 fiber is used in the DFRA, but length is set to be 100 km. Consequently, uniform input power for 51 channels, which is separated by 100 GHz channel spacing, is 1 mW. Initial total pump power is about 600 mW, and fixed at 596 mW after optimization. Smooth gain spectrum consisting of two waves is found when FWHM values of the two incoherent pumps are 14 nm and 16 nm. With one 451 mW incoherent pump centered at 1426 nm, and one 145 mW incoherent pump centered at 1471 nm, the DRFA has a gain average at 7.6 dB, and a gain ripple of 0.101 dB. The gain wave is enhanced to a 0.46 dB ripple for four coherent pumps, and a 1.1 dB ripple for two coherent pumps. We noticed that the gain shown in Figure 6.1.3 decreases when the coherent pump number increases from two to four, and the ENF in Figure 6.1.4 gets worse too, which is agree with case 1. Table 6.1.3 gives the details.

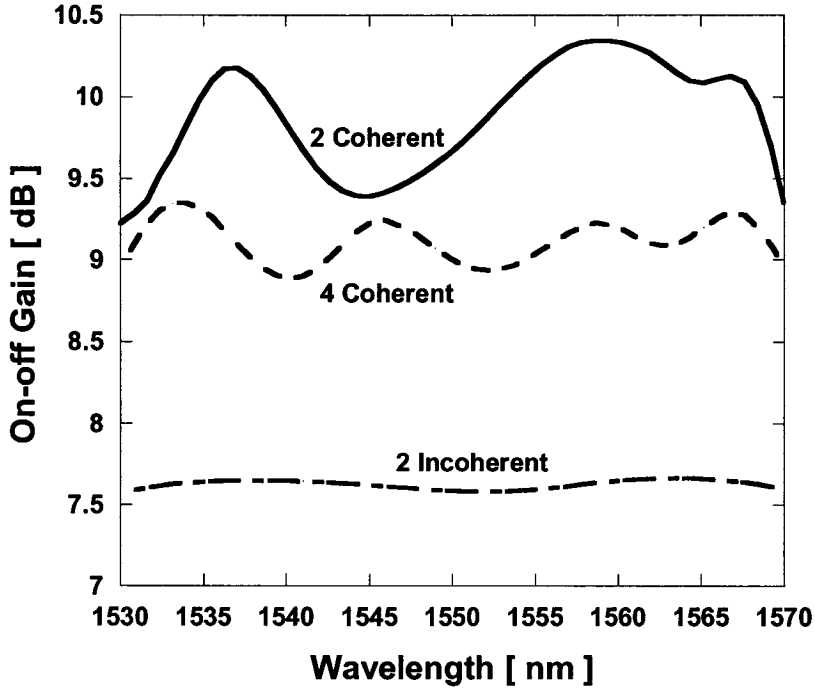

Figure 6.1.3 Gain comparisons of Case 2. Total pump is 596 mW.

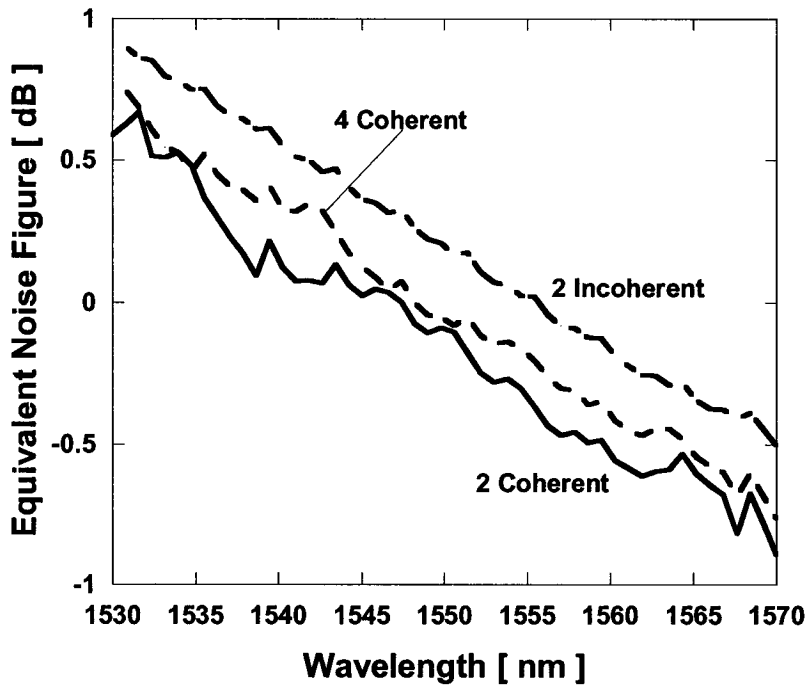

Figure 6.1.4 ENF comparison for Case 2. Total pump is 596 mW.

Table 6.1.3 Detailed results for Case 2.

Section 6.1, Summary for Case 2												
Fiber	SMF-28, 100km											
Signal	51 Channel, 1530nm – 1570nm, 100 GHz spacing, 1mW each channel											
Pump	2 Incoherent pump			2 Coherent pump			4 Coherent pump					
	Total power [mW]		596	Total power [mW]		596	Total power [mW]		596			
	1	Power [mW]	451	1	Power [mW]	300	1	Power [mW]	215			
		Center wave-length [nm]	1426		Center wave-length [nm]	1428		Center wave-length [nm]	1425			
		FWHM [nm]	14	2	Power [mW]	296	2	Power [mW]	145			
	2	Power [mW]	145		Center wave-length [nm]	1456		Center wave-length [nm]	1436			
		Center wave-length [nm]	1471	----------			3	Power [mW]	136			
		FWHM [nm]	16					Center wave-length [nm]	1455			
	----------						4	Power [mW]	100			
								Center wave-length [nm]	1470			
Gain ripple [dB]	0.101			1.122			0.461					
Average on-off gain [dB]	7.625			9.866			9.114					
ENF ripple [dB]	1.424			1.560			1.520					
Average ENF [dB]	0.208			-0.136			-0.015					

We considered the performance of two incoherent pumps in L band in Case 3. TW-Reach fiber is chosen to work as the DFRA, and the fiber length is set to be 50 km. Signals have 48 channels spread from 1570- to 1610-nm, with 0.1 mW uniform input power and 100 GHz channel spacing. Two incoherent pumps are optimized to get better performance. Two and four coherent pumps are also adjusted to achieve good gain results. The two incoherent pumps finalized at 1462 nm with 14 nm FWHM & 255 mW power, and 1507 nm with 16 nm FWHM & 185.4 mW power. Two coherent pumps work best at 1462 nm with power of 180 mW, and 1492 nm with power of 260.4 mW. The four coherent pumps are 1459 nm with power of 108.4 mW, 1471 nm with power of 87 mW, 1489 nm with power of 113 mW, and 1509 nm with power of 109 mW. Gain performances from the above three pumping cases are compared in Figure 6.1.5. Great flat gain with 0.08 dB ripple are achieved by using two incoherent pumps. Corresponding to 0.74 dB of two coherent pumps and 0.42 dB of four coherent pumps, the improvement

by applying two incoherent pumps is significant. Again, the gain ripple decreasing goes with the gain value degradation. Consequently, ENF by two incoherent pumps in Figure 6.1.6 becomes the worst among those three. Table 6.1.5 has the detailed data.

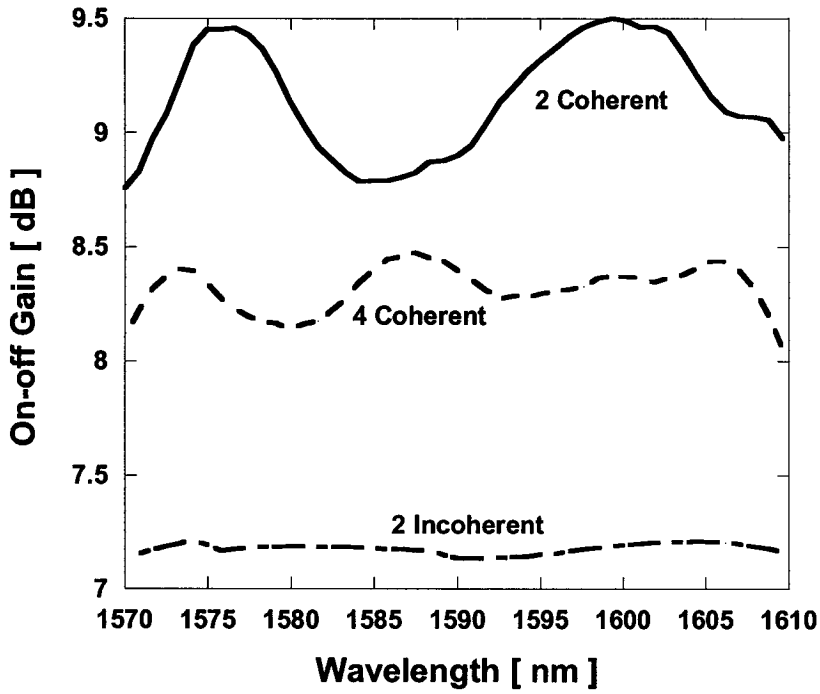

Figure 6.1.5 Gain comparisons of Case 3. Total pump is 440.4 mW.

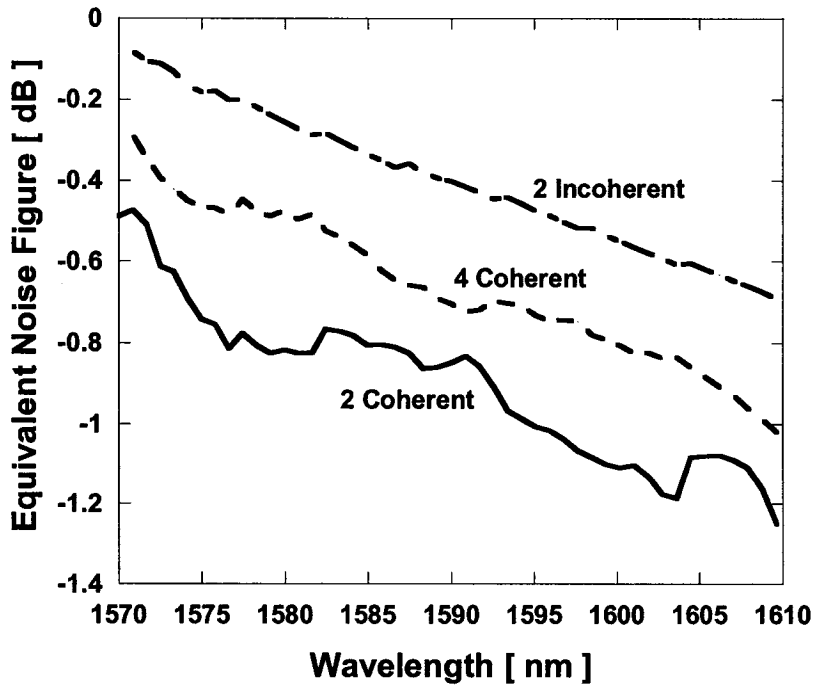

Figure 6.1.6 ENF comparisons of Case 3. Total pump is 440.4 mW.

Table 6.1.4 Detailed results for Case 3.

Section 6.1, Summary for Case 3												
Fiber	TW-Reach, 50km											
Signal	48 Channel, 1570nm – 1610nm, 100 GHz spacing, 0.1mW each channel											
Pump	2 Incoherent pump			2 Coherent pump				4 Coherent pump				
	Total power [mW]		440.4	Total power [mW]		440.4		Total power [mW]		440.4		
	1	Power [mW]	255	1	Power [mW]	180		1	Power [mW]	108.4		
		Center wave-length [nm]	1462		Center wave-length [nm]	1462			Center wave-length [nm]	1459		
		FWHM [nm]	14	2	Power [mW]	260.4		2	Power [mW]	87		
	2	Power [mW]	185.4		Center wave-length [nm]	1492			Center wave-length [nm]	1471		
		Center wave-length [nm]	1507	----------				3	Power [mW]	113		
		FWHM [nm]	16						Center wave-length [nm]	1489		
	----------							4	Power [mW]	109		
									Center wave-length [nm]	1509		
Gain ripple [dB]	0.082			0.743				0.422				
Average on-off gain [dB]	7.178			9.149				8.316				
ENF ripple [dB]	0.629			0.777				0.765				
Average ENF [dB]	-0.392			-0.898				-0.654				

When changed the fiber length to 100 km, and uniform input signal power to 1 mW, the Case 4 is completed. Other settings are un-changed except that we have to look for pumps for this case to get flat gain. The two incoherent pumps after optimization are 1462 nm with 14 nm FWHM and power of 359 mW, and 1507 nm with 16 nm FWHM and power of 180.8 mW. So the total pump power is 539.8 mW. This power is segmented by 1462 nm with 249.8 mW and 1491 nm with 290 mW for two coherent pumps case, and spreaded to 1459 nm with 155 mW, 1471 nm with 118.8 mW, 1489 nm with 155 mW, and 1514 nm with 111 mW for four coherent pumps case. By applying the above pumps schemes, we achieved 0.12-, 0.97-, and 0.46 dB gain ripple for two incoherent, two coherent, and four coherent pumps, respectively. Average gain values are 9-, 11.5- and 10- dB as shown in Figure 6.1.7 correspondingly. Table 6.1.5 gives the detailed information.

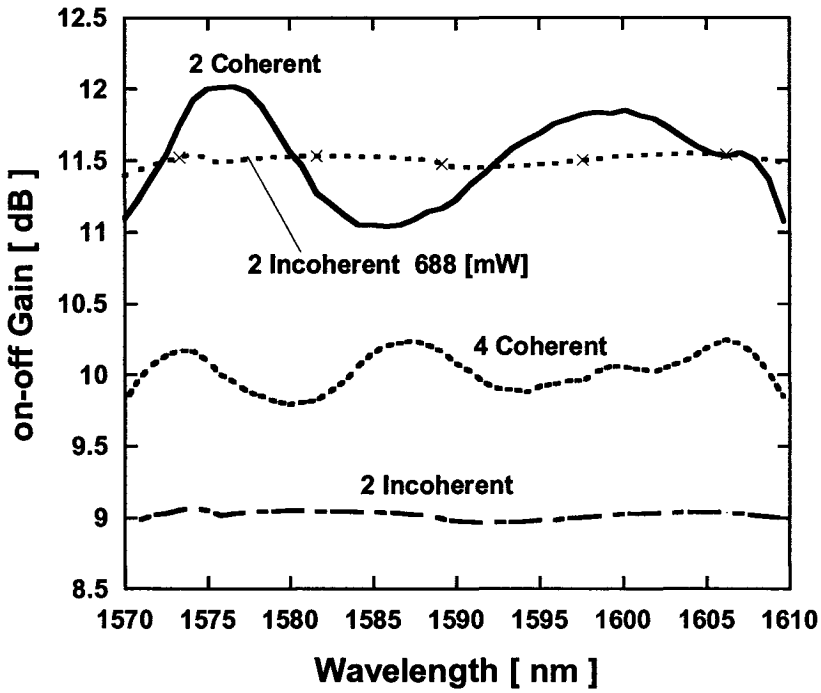

Figure 6.1.7 Gain comparisons of Case 4. Total pump is 539.8 mW.

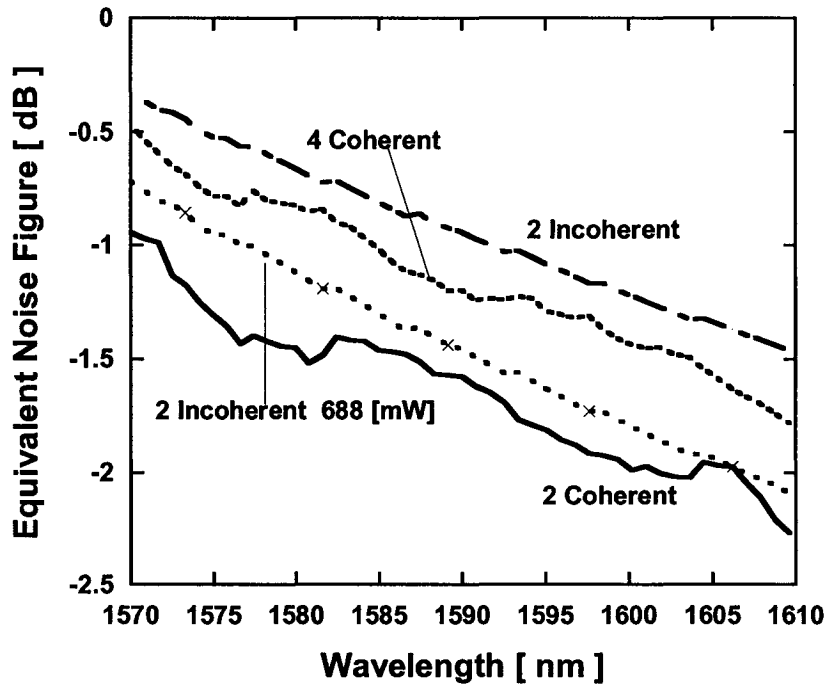

Figure 6.1.8 ENF comparisons of Case 4. Total pump is 539.8 mW.

For all the above cases, average gain values by using two incoherent pumps are degraded. Consequently, ENF by incoherent pumps are also got worse because of the low gain value. So total power of two incoherent pumps is increased to 688 mW to improve the gain value to the two coherent pump level. As shown in Figure 6.1.7, the two incoherent pumps with 688 mW power provide an average gain of 11.5 dB, consequently, the average ENF in Figure 6.1.8 is decreased from –0.92 dB to –1.44 dB. However, the ENF performance from 688 mW incoherent pumps is still a little worse than that from 539.8 mW two coherent pumps (-1.636 dB) which agrees with the conclusion in Section 5.4.

Table 6.1.5 Detailed results for Case 4.

Section 6.1, Summary for Case 4											
Fiber	TW-Reach, 100km										
Signal	48 Channel, 1570nm – 1610nm, 100 GHz spacing, 1mW each channel										
Pump	2 Incoherent pump			2 Coherent pump			4 Coherent pump				
	Total power [mW]		539.8	Total power [mW]		539.8	Total power [mW]		539.8		
	1	Power [mW]	359	1	Power [mW]	249.8	1	Power [mW]	155		
		Center wave-length [nm]	1462		Center wave-length [nm]	1462		Center wave-length [nm]	1459		
		FWHM [nm]	14	2	Power [mW]	290	2	Power [mW]	118.8		
	2	Power [mW]	180.8		Center wave-length [nm]	1491		Center wave-length [nm]	1471		
		Center wave-length [nm]	1507	----------			3	Power [mW]	155		
		FWHM [nm]	16					Center wave-length [nm]	1489		
	----------						4	Power [mW]	111		
								Center wave-length [nm]	1514		
Gain ripple [dB]	0.117			0.974			0.456				
Average on-off gain [dB]	9.019			11.526			10.023				
ENF ripple [dB]	1.135			1.323			1.313				
Average ENF [dB]	-0.924			-1.636			-1.141				

6.2 Performance of C+L band DFRAs with two incoherent, or two, four and six coherent pumps

The last case considered in the thesis is the performance comparison of DFRA with two incoherent, two coherent, four coherent, six coherent pumps over C + L band. Since Raman amplifier is widely used in DWDM systems, the input signal change spacing is chosen to be 50 GHz. So it needs 184 channels to cover the bandwidth from 1530- to 1605- nm. The uniform signal power is 0.5 mW. TW-Reach 100 km fiber is the DFRA. Total pump power is 668 mW for each pumping scheme. All the incoherent and coherent pumps are optimized to get higher and flatter gain, and the pumping data are as follow: the two incoherent pumps are 1429 nm with 20 nm FWHM and power of 571 mW, and 1491 nm with FWHM 20 nm and 97 mW; for the two coherent pumps, one is 1441 nm with power of 430 mW, and the other is 1484 nm with power of 238 mW; the four coherent pumps are 1429 nm with power of 320 mW, 1445 nm with power of 130 mW, 1462 nm with power of 85 mW, and 1491 nm with power of 133 mW; the six coherent pumps are located at 1425-, 1433-, 1444-, 1460-, 1480-, 1500-nm, and corresponding powers are 200-, 150-, 110-, 75-, 70-, 63-mW, respectively. Gain ripple is getting decreased as the number of coherent pumps increasing. As shown in Figure 6.2.1, gain ripples are 3.5-, 1-, 0.9- dB for two, four, and six coherent pumping cases. However, two incoherent pumps can provide a flat gain with 0.63 dB ripple. This result implies that to get the similar flat gain, the number of coherent pumps is at least three times greater than the number of incoherent pumps. Although incoherent pumps decrease the pumping efficiency, which leads to the degradation of gain, increasing the coherent pump number also decreases the average gain value. It is clear that the 13 dB average gain from two coherent pumps has big difference with the 10 dB from two incoherent pumps, but 10.8 dB from six coherent pumps is not an advantage. Therefore, for DWDM over C + L band, two incoherent pumps works well in both gain flatness and average gain. ENF performances shown in Figure 6.2.2 are close, especially between two incoherent and six coherent pumps, which agrees with the average gain. Table 6.2.1 gives the detailed data.

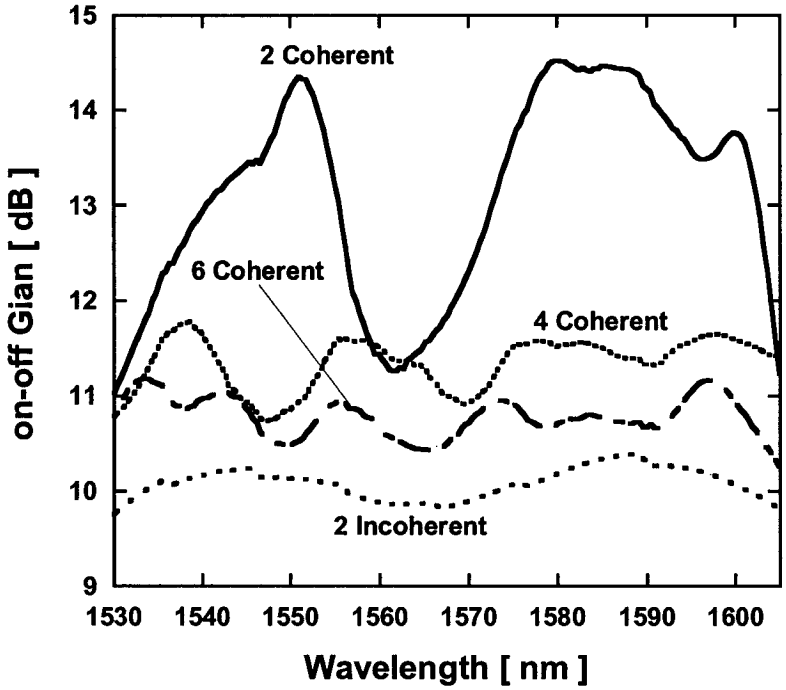

Figure 6.2.1 Gain comparisons. Total pump is 668 mW.

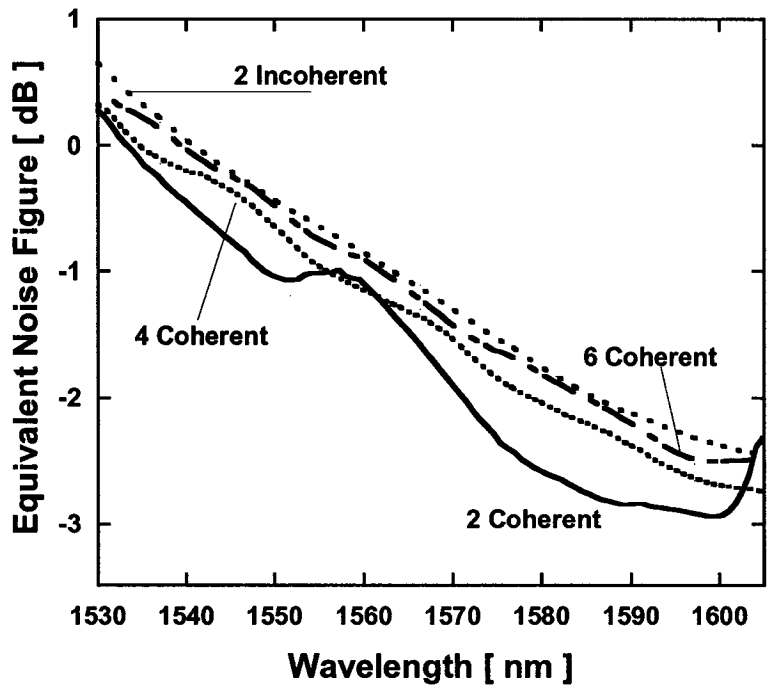

Figure 6.2.2 ENF comparisons. Total pump is 668 mW.

Table 6.2.1 Detailed results for the Case in Section 6.2.1 DFRA is TW-Reach 100 km. Backward pump power is 668 mW.
C. W. is Central Wavelength. A. G. is Average Gain. G. R. is Gain Ripple. A. ENF is Average ENF.

Section 6.2 Summary																
Fiber	TW-Reach 100 km															
Signal	184 channel, 1530 – 1605 nm, 50 GHz channel spacing, 0.5 mW per channel															
Pump	2 Incoherent			2 Coherent			4 Coherent			6 Coherent		
	Total Power [mW]		668	Total Power [mW]		668	Total Power [mW]		668	Total Power [mW]		668
	1	C W [nm]	1429	1	C W [nm]	1441	1	C W [nm]	1429	1	C W [nm]	1425
		Power [mW]	571		Power [mW]	430		Power [mW]	320		Power [mW]	200
		FWHM [nm]	20	2	C W [nm]	1484	2	C W [nm]	1445	2	C W [nm]	1433
	2	C W [nm]	1491		Power [mW]	238		Power [mW]	130		Power [mW]	150
		Power [mW]	97				3	C W [nm]	1462	3	C W [nm]	1444
		FWHM [nm]	20					Power [mW]	85		Power [mW]	110
							4	C W [nm]	1491	4	C W [nm]	1460
								Power [mW]	133		Power [mW]	75
	----------			----------			----------			5	C W [nm]	1480
											Power [mW]	70
										6	C W [nm]	1500
											Power [mW]	63
A. G. [dB]	10			13			11.3			10.8		
G. R. [dB]	0.63			3.5			1			0.9		
A. ENF [dB]	-1.11			-1.67			-1.38			-1.2		

CHAPTER 7 Conclusions

Based on the basic property introduction of high-power incoherent pumping by Ahura Company, a theoretical study of DFRAs with incoherent pumping is for the first time carried out in this thesis. After verifying our theoretical model with [38] and using the Raman gain coefficient scaling method from [33], investigations are conducted in several cases to analyze the performance of incoherent pumped DFRAs.

Performances of DFRAs with one or more incoherent pumps are studied. By comparing to coherent pump, we have confirmed that DFRAs with incoherent pumping can have a much flatter gain than that with coherent pumping. Moreover, we got the following conclusions:

1. With the same pumping power, the average Raman gain for incoherent pumping is smaller than for coherent pumping and the ENF for incoherent pumping is higher than for coherent pumping because of the decreased gain.
2. The gain ripple decreases exponentially and the average gain decreases linearly with the increase of FWHM value under the condition of same pump power. ENF degrades with the FWHM too because of the decreased gain.
3. With the same gain level, incoherent pumped DFRAs have a little worse noise performance than coherent pumped DFRA. That is because, incoherent pump needs more pump power to get the same average gain as the coherent pump, and the incoherent pump high power makes more noise.
4. By comparing the results from two, four, and six coherent pumps, we have found that when multiple pumping is used, the number of pumping wavelengths is reduced significantly for the same gain ripple if incoherent pumping replaces coherent pumping.

References

[1].G.Agrawal "Fiber-Optic Communication Systems: Evolution of Lightwave Systems," *Chapter 1, pp.5, The Institute of Optics University of Rochester, Rochester, NY, third edition, 2002.*

[2] M. Islam, "Raman amplifiers for telecommunications," *IEEE J. Selected Topics in Quantum Electron. vol.8, pp.548-559, 2002.*

[3]. Y. Yamamoto, "Characteristics of AlGaAs Fabry-Perot cavity type laser amplifiers," *IEEE Journal of Quantum Electronics, QE-16(10), pp.1047-1052, 1980.*

[4]. T. Saitoh and T. Mukai, "1.5-um GaInAs traveling-wave semiconductor laser amplifier," *IEEE Journal of Quantum Electronics, QE-23(6, pp.1010-1020, 1987.*

[5]. P. Kuindersma, G Cuijpers, J. Reid, G Hoven, and S. Walczyk, "An experimental analysis of the system performance of cascades of 1.3 um semiconductor optical amplifiers," *European Conference on Optical Communication in Edinbourgh, United Kingdom, September, 1997, pp. 79-82.*

[6]. R. Laming, M. Zervas, and D. Payne, "54 dB gain quantum-noise-limited Erbium-doped fiber amplifier," *European Conference on Optical Communication in Berlin, Germany, volume 1, pp. 89-92, 1992.*

[7]. R. Stolen and E. Ippen, "Raman gain in glass optical waveguides," *Appl. Phys. Lett., vol.22, page 276-278, 1973.*

[8] L. Mollenauer, J. Gordon, and M. Islam, "Soliton propagation in long fibers with periodically compensated loss," *IEEE J. Quantum Electron., vol.22, pp. 157-173, 1986.*

[9] Bromage, "Raman amplification for fiber communication systems", *J. Lightwave Tech., vol.22, pp. 79-93, 2004.*

[10] V. Perlin, G. Winful, "Optimal design of flat gain wide band fiber Raman amplifiers," *J. Lightwave Tech., vol.20, pp.250-254, 2002.*

[11] V. Perlin, G. Winful, "On distributed Raman amplification for ultrabroad-band long-haul WDM systems," *J. Lightwave Tech., vol.20, pp.409-416, 2002.*

[12] X. Liu, B. Lee, "Optimal design for ultra-broad band amplifiers," *J. Lightwave Tech., vol.21, pp.3446-3455, 2003.*

[13] G Agrawal, "Fiber-Optic Communication Systems: Amplifier Performance," *Section 6.3, pp. 249-250. The Institute of Optics University of Rochester, Rochester, NY, third edition, 2002.*

[14] J. Bouteiller, K. Brar, S. Radic, J. Bromage, Z. Wang, C. Headley, "Dual-order Raman pump providing improved noise figure and large gain bandwidth," *OFC 2002, PD FB3.*

[15] K. Rottwitt, A. Stentz, T. Nielsen, P. Hansen, K. Feder, K. Walker, "Transparent 80 km bi-directionally pumped distributed Raman amplifier with second-order pumping," *ECOC 1999, vol.2 pp144-145.*

[16] T. Kung, C. Chang, J. Dung, S. Chi, "Four-wave mixing between pump and signal in a

distributed Raman amplfier," *J. Lightwave Tech., vol.21, pp.1164-1170, 2003.*

[17] J. Bouteiller, L. Leng, C. Headley, "Pump–pump four-wave mixing in distributed Raman amplified systems," *J. Lightwave Tech., vol.22, pp.723-732, 2004*

[18] W. Wong, C. Chen, M. Ho, and H. Lee, "Phase-matched four-wave mixing between pumps and signals in a co-pumped Raman amplifier," *IEEE Photon. Tech. Lett., vol.15, pp.209-211, 2003.*

[19] X. Zhou, M. Birk, S. Woodward, "Pump-noise induced FWM effect and its reduction in a distributed Raman fiber amplifiers," *IEEE Photon. Tech. Lett., vol.14, pp.1686-1688, 2002.*

[20] F. Pasquale and F. Meli, "New Raman pump module for reducing pump–signal four-wave-mixing interaction in co-pumped distributed Raman amplifiers," *J. Lightwave Techn., vol.22, pp.1742-1748, 2003*

[21] S. Sugliani, G. Sacchi, G. Bolognini, S. Faralli, F. Pasquale, "Effective suppression of penalties induced by parametric nonlinear interaction in distributed Raman amplifiers based on NZ-DS fibers," *IEEE Photon. Tech. Lett., vol.16, pp.81-83, 2004.*

[22] G. Bolognini, S. Sugliani, F. Pasquale, "Double Rayleigh scattering noise in Raman amplifiers using pump time-division-multiplexing schemes," *IEEE Photon. Tech. Lett., vol.16, pp.1286-1288, 2004.*

[23] J. Bromage, P. Winzer, L. Nelson, M. Mermelstein, C. Headley, "Amplified spontaneous emission in pulse-pumped Raman amplifiers," *IEEE Photon. Tech. Lett., vol.15, pp.667-669, 2003.*

[24] J. Nicholson, J. Fini, J. Bouteiller, J. Bromage, K. Brar, "Stretched ultrashort pulses for high repetition rate swept wavelength Raman pumping," *J. Lightwave Tech., vol.22, pp.71-78, 2004.*

[25] D. Vakhshoori, M. Azimi, P. Chen, B. Han, M. Jiang, L. Knopp, C. Lu, Y. Shen, G. Rodes, S. Vote, P. Wang, X. Zhu, "Raman amplification using high-power incoherent semiconductor pump sources", *OFC 2003, PD47.*

[26] C. Raman and K. Krishnan, "A new type of secondary radiation," *Nature, vol.121 ,pp.501, 1928.*

[27] R. Stolen, "Nonlinear properties of optical fibers," *Optical fiber Telecommunications, chapter 5, pp.127-133. Academic Press, New York, 1979.*

[28] G. Agrawal, "Nonlinear Fiber Optics," *Chapter 8, pp.316-336. Optics and Photonics, Academic Press, San Diego, second edition, 1995.*

[29] G.Agrawal, "Fiber-Optic Communication Systems: Raman Amplifiers," *Chapter 6, pp.243. The Institute of Optics University of Rochester, Rochester, NY, third edition, 2002.*

[30] A. Chraplyvy, "Optical power limits in multi-channel wavelength-division multiplexed systems due to stimulated Raman scattering," *Electron. Letter, vol.20, pp. 58-59, 1984.*

[31] M. Nissov, "Long-Haul Optical Transmission Using Distributed Raman Amplification," *Chapter 3, pp.42-45, December, 1997.*

[32] R. Stolen, "Polarization effects in fiber Raman and Brillouin lasers," *IEEE, Journal Quantum Electron., vol.Qe-15, pp.1157-1160, 1979.*

[33] K. Rottwitt, A. Stentz, L. Leng, M. Lines, H. Smith, "Scaling of the Raman gain coefficient: applications to Germanosilicate fibers", *IEEE J. Lightwave Technol., vol.21, pp. 1652-1662, 2003.*

[34] R. Stolen, C. Lee, and R. Jain, "Development of the stimulated Raman spectrum in single-mode silica fibers," *J. Opt. Soc. Amer. B, vol.1, pp.652-657, 1984.*

[35] H. Kidorf, K. Rottwitt, M. Nissov, M. Ma, and E. Rabarijaona, "Pump interactions in a 100-nm bandwidth Raman amplifier," *IEEE Photon. Technol. Letter, vol.11, pp.530-532, May 1999.*

[36] M.Achtenhagen, T. Chang, B. Nyman, and A. Hardy, "Analysis of a multiple-pump Raman amplifier," *Appl. Phys. Lett., vol.78, pp.1322-1324, 2001.*

[37] A. Berntson, S. Popov, E. Vanin, G. Jacobsen, and J. Karlsson, "Polarization dependence and gain tilt of Raman amplifiers for WDM systems," *OFC 2001, Baltimore, MD, Paper MI2-1.*

[38] I. Mandelbaum, M. Bolshtyansky, "Raman amplifier model in single-mode optical fiber", *IEEE Photon. Tech. Lett., vol.15, pp. 1704-1706 , 2003.*

[39] B. Pedersen, A. Bjarklev, J. Povlsen, K. Dybdal, and C. Larsen, "The design of Erbium-doped fiber amplifers," *Journal of Lightwave Technology, vol.9 pp.1105-1112, September 1991.*

[40] *www.ofsoptics.com*.

[41] *www.ahuracorp.com*.

[42] M. Nissov, "Long-Haul Optical Transmission Using Distributed Raman Amplification," *Chapter 3, pp.41-48, December, 1997.*

Appendix A

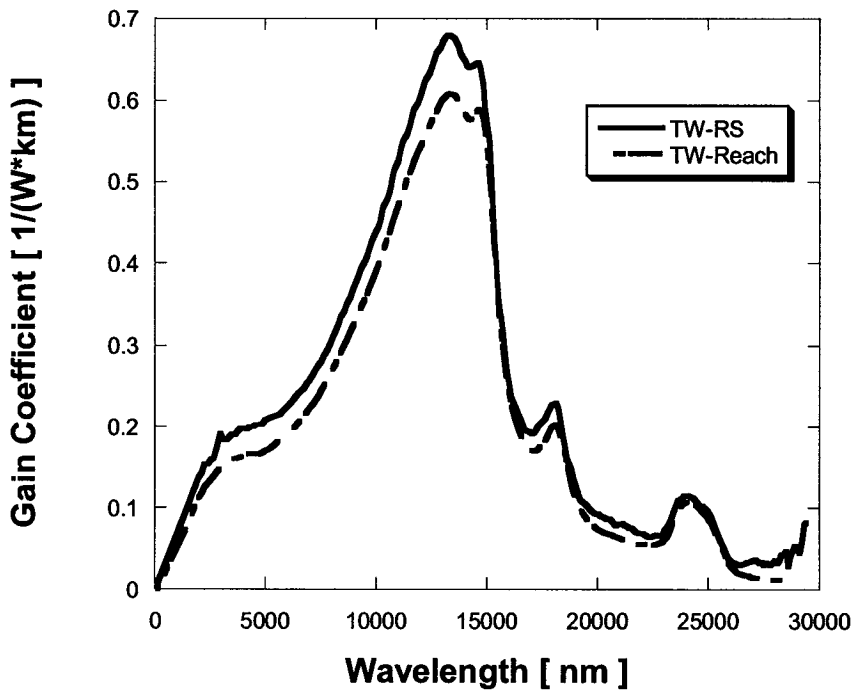

Figure a: Raman gain-coefficient lines of TW-RS fiber and TW-Reach fiber.

Appendix B

Table 5.1.4 Detailed results for Case 3 in Section 5.1.

Section 5.1, Summary for Case 3						
Fiber	SMF-28, 50 km					
Signal	51 channel, 1530nm – 1570nm, 100GHz spacing, 0.1mW each channel.					
Pump	Incoherent pump 1		Coherent pump		Incoherent pump 2	
	Power [mW]	300	Power [mW]	300	Power [mW]	300
	Center wave-length [nm]	1446	Center wave-Length [nm]	1454	Center wave-Length [nm]	1450
	FWHM [nm]	35	FWHM [nm]	----------	FWHM [nm]	25
Gain ripple [dB]	0.355		2.193		0.596	
Average on-off gain [dB]	4.04		5.972		4.559	
ENF ripple [dB]	0.478		0.865		0.495	
Average ENF [dB]	0.628		0.479		0.601	

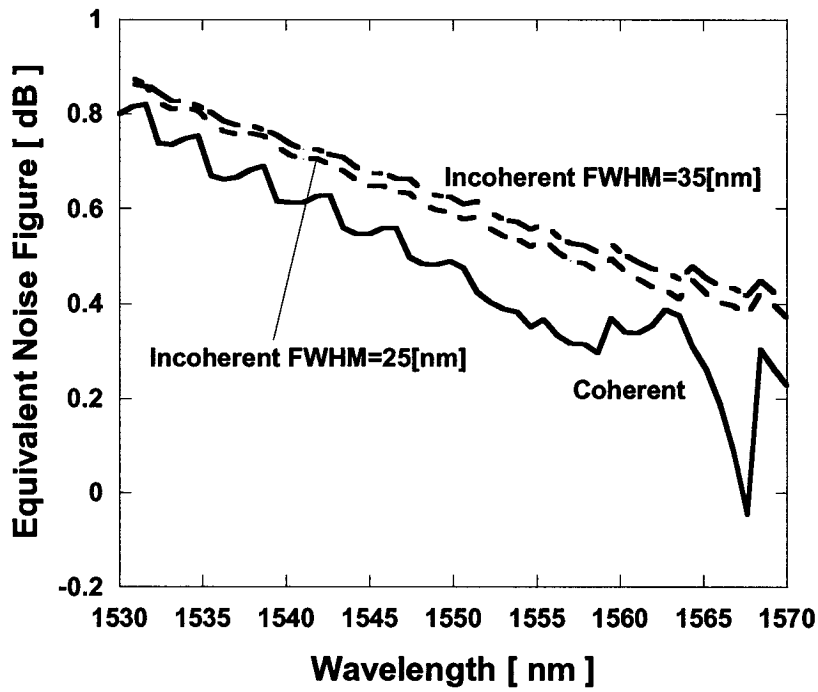

Figure 5.1.7 ENF performance for Case 3 in Section 5.1

Table 5.1.5 Detailed results for Case 4 in Section 5.1.

Section 5.1, Summary for Case 4						
Fiber	SMF-28, 100 km					
Signal	51 channel, 1530nm – 1570nm, 100GHz spacing, 1mW each channel.					
Pump	Incoherent pump 1		Coherent pump		Incoherent pump 2	
	Power [mW]	500	Power [mW]	500	Power [mW]	500
	Center wave-length [nm]	1433	Center wave-Length [nm]	1453	Center wave-Length [nm]	1441
	FWHM [nm]	35	FWHM [nm]	----------	FWHM [nm]	25
Gain ripple [dB]	0.596		3.987		0.92	
Average on-off gain [dB]	6.264		10.214		7.221	
ENF ripple [dB]	1.287		2.001		1.303	
Average ENF [dB]	0.338		-0.129		0.244	

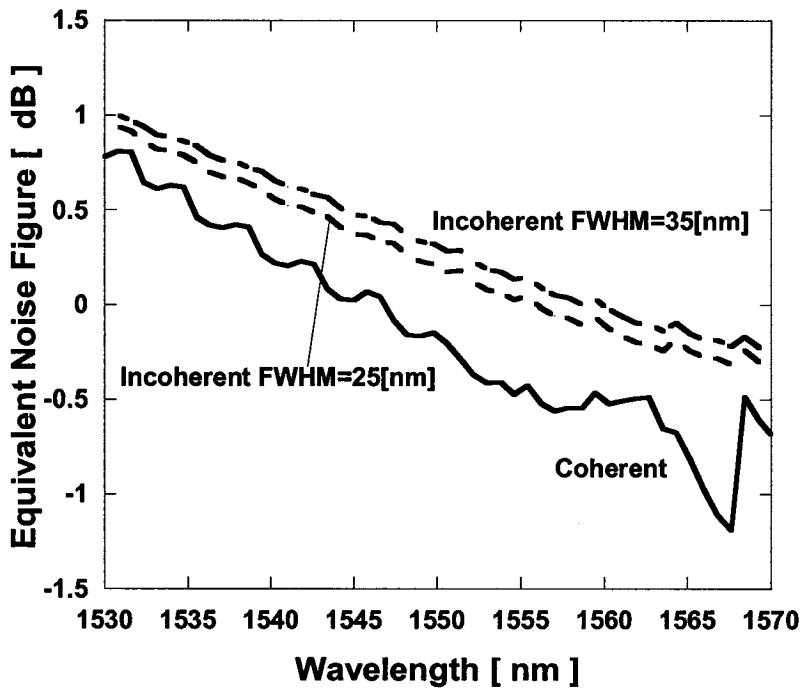

Figure 5.1.8 ENF performance for Case 4 in Section 5.1

Table 5.2.3 Detailed results for Case 3 in Section 5.2.

Section 5.2, Summary for Case 3						
Fiber	SFM-28, 50 km					
Signal	48 channel, 1570nm – 1610nm, 100GHz spacing, 0.1mW each channel.					
Pump	Incoherent pump 1		Coherent pump		Incoherent pump 2	
	Power [mW]	300	Power [mW]	300	Power [mW]	300
	Center wave-length [nm]	1484	Center wave-Length [nm]	1488	Center wave-Length [nm]	1487
	FWHM [nm]	35	FWHM [nm]	----------	FWHM [nm]	15
Gain ripple [dB]	0.370		2.186		1.127	
Average on-off gain [dB]	4.835		6.786		5.908	
ENF ripple [dB]	0.603		1.016		0.668	
Average ENF [dB]	0.454		0.212		0.327	

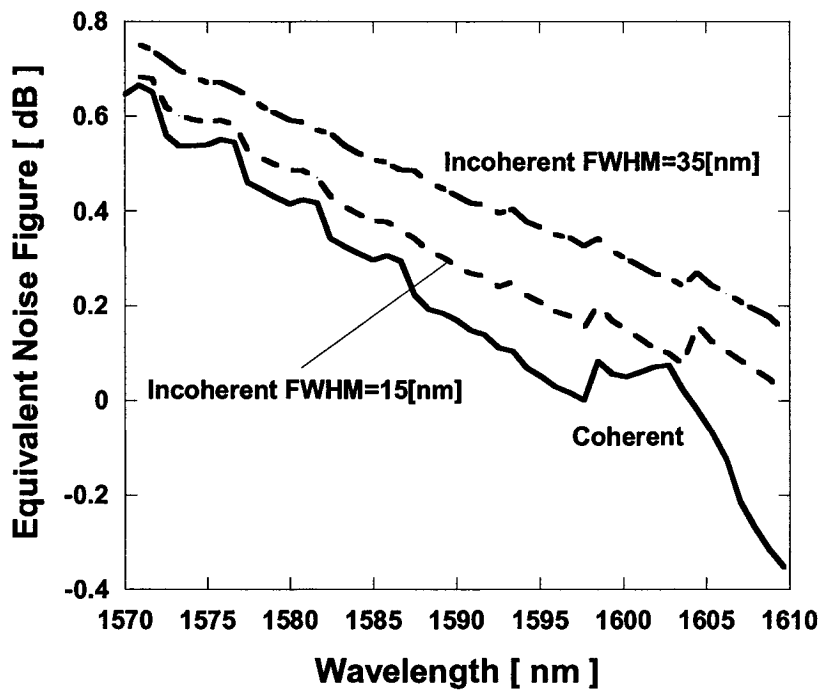

Figure 5.2.7 ENF performance for Case 3 in Section 5.2

Table 5.2.4 Detailed results for Case 4 in Section 5.2.

Section 5.2, Summary for Case 4						
Fiber	SMF-28, 100 km					
Signal	48 channel, 1570nm – 1610nm, 100GHz spacing, 1mW each channel.					
Pump	Incoherent pump 1		Coherent pump		Incoherent pump 2	
	Power [mW]	500	Power [mW]	500	Power [mW]	500
	Center wave-length [nm]	1471	Center wave-Length [nm]	1487	Center wave-Length [nm]	1483
	FWHM [nm]	35	FWHM [nm]	----------	FWHM [nm]	15
Gain ripple [dB]	0.646		4.107		1.911	
Average on-off gain [dB]	7.991		11.824		10.093	
ENF ripple [dB]	1.453		1.914		1.541	
Average ENF [dB]	-0.205		-0.766		-0.505	

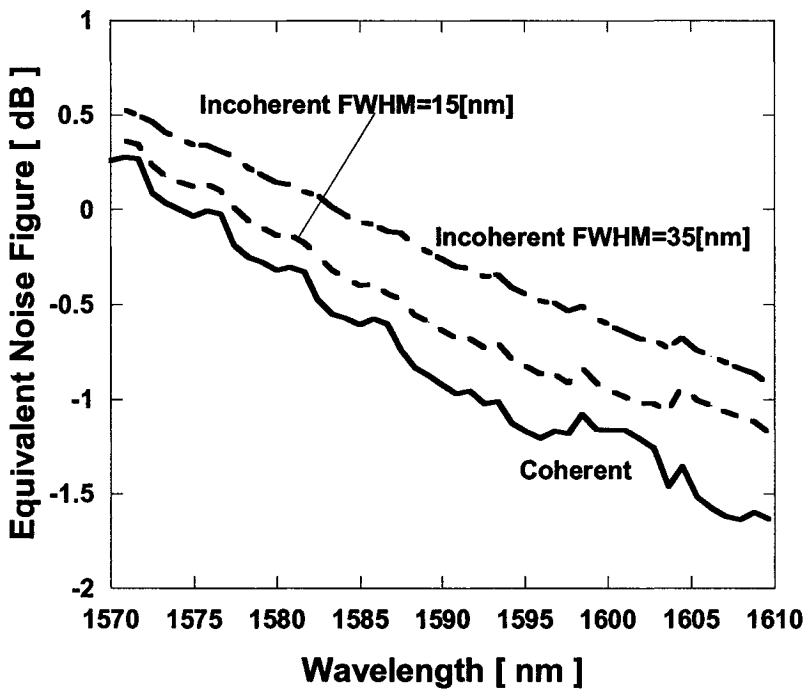

Figure 5.2.8 ENF performance for Case 4 in Section 5.2

Table 6.1.6 Detail results for Case 5 in Section 6.1.

Section 6.1, Summary for Case 5												
Fiber	TW-Reach, 50km											
Signal	51 Channel, 1530nm – 1570nm, 100 GHz spacing, 0.1mW each channel											
Pump	2 Incoherent pump			2 Coherent pump				4 Coherent pump				
	Total power [mW]		438.6	Total power [mW]		438.6		Total power [mW]		438.6		
	1	Power [mW]	250	1	Power [mW]	190		1	Power [mW]	105		
		Center wave-length [nm]	1428		Center wave-length [nm]	1429			Center wave-length [nm]	1425		
		FWHM [nm]	12	2	Power [mW]	248.6		2	Power [mW]	97		
	2	Power [mW]	188.6		Center wave-length [nm]	1459			Center wave-length [nm]	1436		
		Center wave-length [nm]	1471	----------				3	Power [mW]	132		
		FWHM [nm]	16						Center wave-length [nm]	1455		
	----------							4	Power [mW]	104.6		
									Center wave-length [nm]	1474		
Gain ripple [dB]	0.136			0.947				0.460				
Average on-off gain [dB]	7.639			9.531				8.784				
ENF ripple [dB]	0.693			0.825				0.815				
Average ENF [dB]	-0.452			-0.950				-0.716				

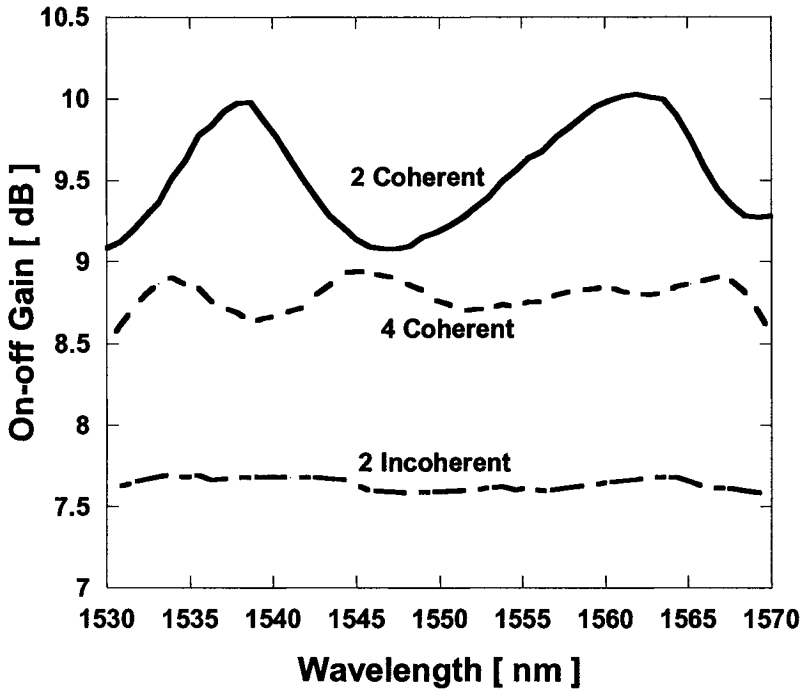

Figure 6.1.9 Gain performance for Case 5 in Section 6.1

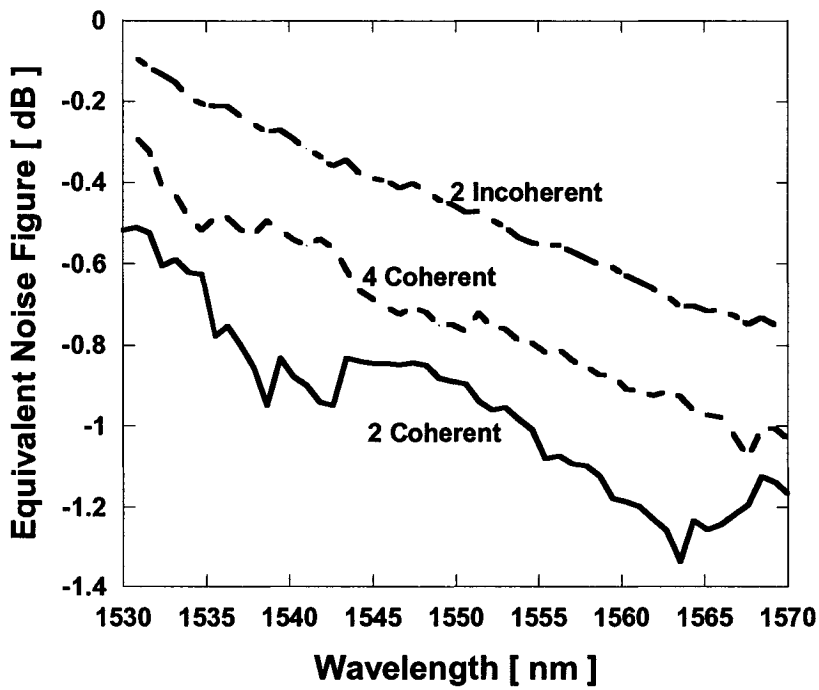

Figure 6.1.10 ENF performance for Case 5 in Section 6.1

Table 6.1.7 Detail results for Case 6 in Section 6.1.

<table>
<tr><th colspan="10">Section 6.1, Summary for Case 6</th></tr>
<tr><td>Fiber</td><td colspan="9">TW-Reach, 100km</td></tr>
<tr><td>Signal</td><td colspan="9">51 Channel, 1530nm – 1570nm, 100 GHz spacing, 1mW each channel</td></tr>
<tr><td rowspan="11">Pump</td><td colspan="3">2 Incoherent pump</td><td colspan="3">2 Coherent pump</td><td colspan="3">4 Coherent pump</td></tr>
<tr><td colspan="2">Total power [mW]</td><td>510</td><td colspan="2">Total power [mW]</td><td>510</td><td colspan="2">Total power [mW]</td><td>510</td></tr>
<tr><td rowspan="3">1</td><td>Power [mW]</td><td>347</td><td rowspan="3">1</td><td>Power [mW]</td><td>240</td><td rowspan="3">1</td><td>Power [mW]</td><td>144</td></tr>
<tr><td>Center wave-length [nm]</td><td>1426</td><td>Center wave-length [nm]</td><td>1429</td><td>Center wave-length [nm]</td><td>1425</td></tr>
<tr><td>FWHM [nm]</td><td>14</td><td rowspan="3">2</td><td>Power [mW]</td><td>270</td><td rowspan="3">2</td><td>Power [mW]</td><td>118</td></tr>
<tr><td rowspan="3">2</td><td>Power [mW]</td><td>163</td><td>Center wave-length [nm]</td><td>1457</td><td>Center wave-length [nm]</td><td>1436</td></tr>
<tr><td>Center wave-length [nm]</td><td>1471</td><td colspan="3" rowspan="3">----------</td><td rowspan="2">3</td><td>Power [mW]</td><td>140</td></tr>
<tr><td>FWHM [nm]</td><td>16</td><td>Center wave-length [nm]</td><td>1455</td></tr>
<tr><td colspan="3" rowspan="2">----------</td><td rowspan="2">4</td><td>Power [mW]</td><td>108</td></tr>
<tr><td>Center wave-length [nm]</td><td>1470</td></tr>
<tr><td>Gain ripple [dB]</td><td colspan="3">0.125</td><td colspan="3">1.193</td><td colspan="3">0.544</td></tr>
<tr><td>Average on-off gain [dB]</td><td colspan="3">8.937</td><td colspan="3">11.573</td><td colspan="3">10.746</td></tr>
<tr><td>ENF ripple [dB]</td><td colspan="3">1.221</td><td colspan="3">1.244</td><td colspan="3">1.360</td></tr>
<tr><td>Average ENF [dB]</td><td colspan="3">-0.920</td><td colspan="3">-1.623</td><td colspan="3">-1.362</td></tr>
</table>

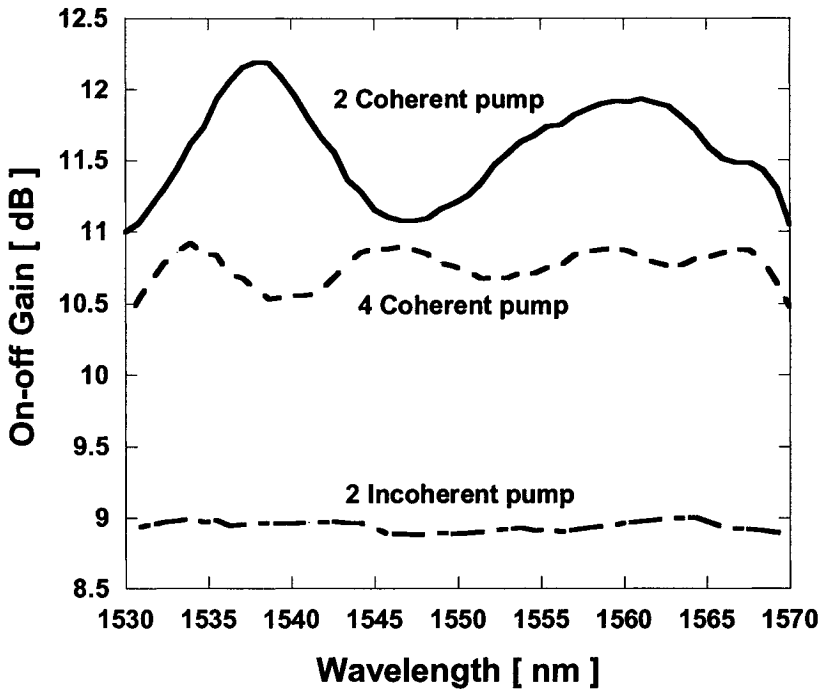

Figure 6.1.11 Gain performance for Case 6 in Section 6.1

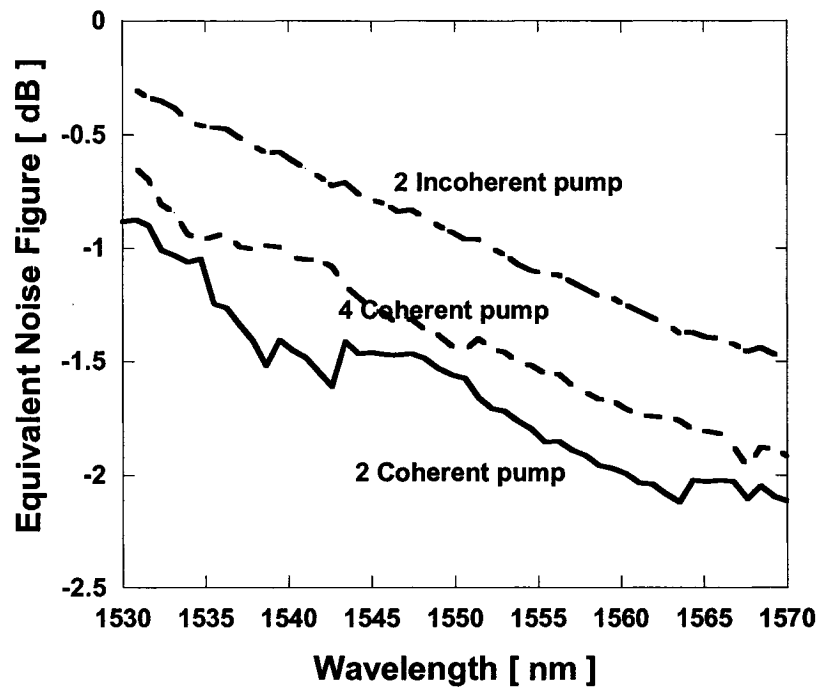

Figure 6.1.12 ENF performance for Case 6 in Section 6.1

Table 6.1.8 Detail results for Case 7 in Section 6.1.

Section 6.1, Summary for Case 7												
Fiber	SMF-28, 50km											
Signal	48 Channel, 1570nm – 1610nm, 100 GHz spacing, 0.1mW each channel											
Pump	2 Incoherent pump			2 Coherent pump				4 Coherent pump				
	Total power [mW]		481	Total power [mW]		481		Total power [mW]		481		
	1	Power [mW]	297	1	Power [mW]	221		1	Power [mW]	130		
		Center wave-length [nm]	1461		Center wave-length [nm]	1463			Center wave-length [nm]	1460		
		FWHM [nm]	14	2	Power [mW]	260		2	Power [mW]	105		
	2	Power [mW]	184		Center wave-length [nm]	1494			Center wave-length [nm]	1471		
		Center wave-length [nm]	1507	----------				3	Power [mW]	130		
		FWHM [nm]	16						Center wave-length [nm]	1489		
	----------							4	Power [mW]	116		
									Center wave-length [nm]	1510		
Gain ripple [dB]	0.0800			0.865				0.430				
Average on-off gain [dB]	7.243			8.947				8.340				
ENF ripple [dB]	0.800			0.773				0.986				
Average ENF [dB]	0.262			-0.046				0.101				

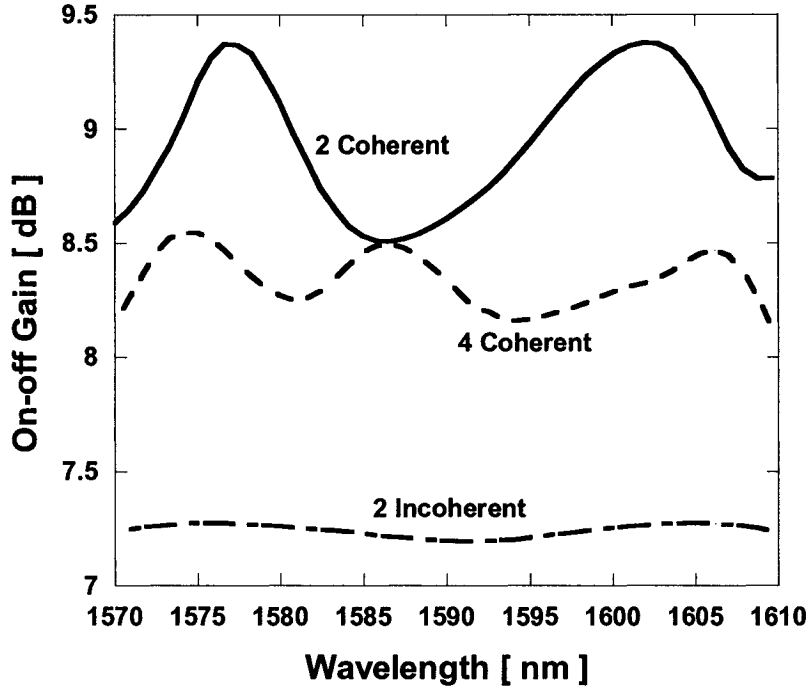

Figure 6.1.13 Gain performance for Case 7 in Section 6.1

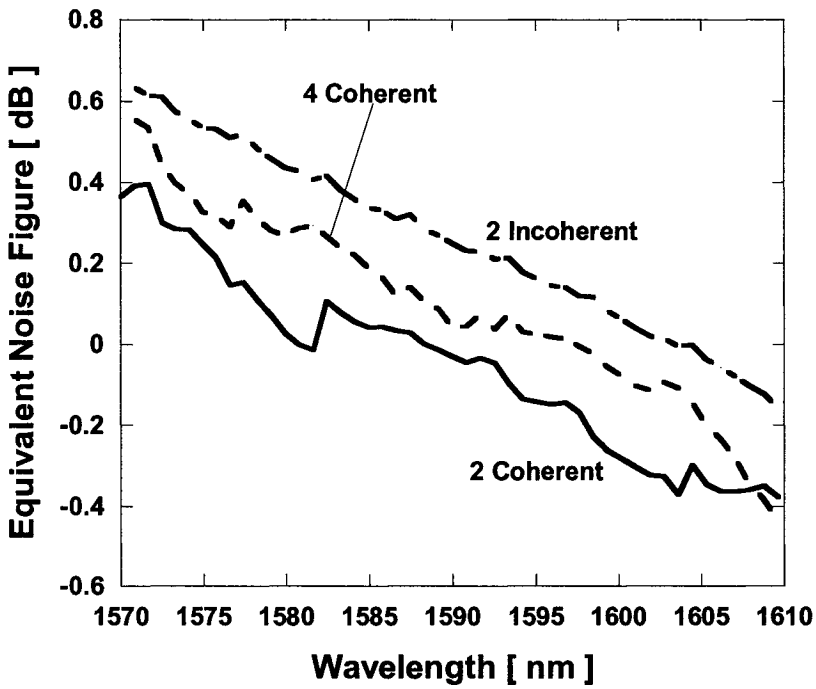

Figure 6.1.14 ENF performance for Case 7 in Section 6.1

Table 6.1.9 Detail results for Case 8 in Section 6.1.

Section 6.1, Summary for Case 8												
Fiber	SMF-28, 100km											
Signal	48 Channel, 1570nm – 1610nm, 100 GHz spacing, 1mW each channel											
Pump	2 Incoherent pump			2 Coherent pump				4 Coherent pump				
	Total power [mW]		583	Total power [mW]		583		Total power [mW]		583		
	1	Power [mW]	418	1	Power [mW]	275		1	Power [mW]	175		
		Center wave-length [nm]	1460		Center wave-length [nm]	1461			Center wave-length [nm]	1460		
		FWHM [nm]	14	2	Power [mW]	308		2	Power [mW]	142		
	2	Power [mW]	165		Center wave-length [nm]	1490			Center wave-length [nm]	1471		
		Center wave-length [nm]	1505	----------				3	Power [mW]	141		
		FWHM [nm]	16						Center wave-length [nm]	1488		
	----------							4	Power [mW]	125		
									Center wave-length [nm]	1520		
Gain ripple [dB]	0.088			1.205				0.535				
Average on-off gain [dB]	9.271			11.618				9.931				
ENF ripple [dB]	1.574			2.024				1.817				
Average ENF [dB]	-0.394			-0.837				-0.377				

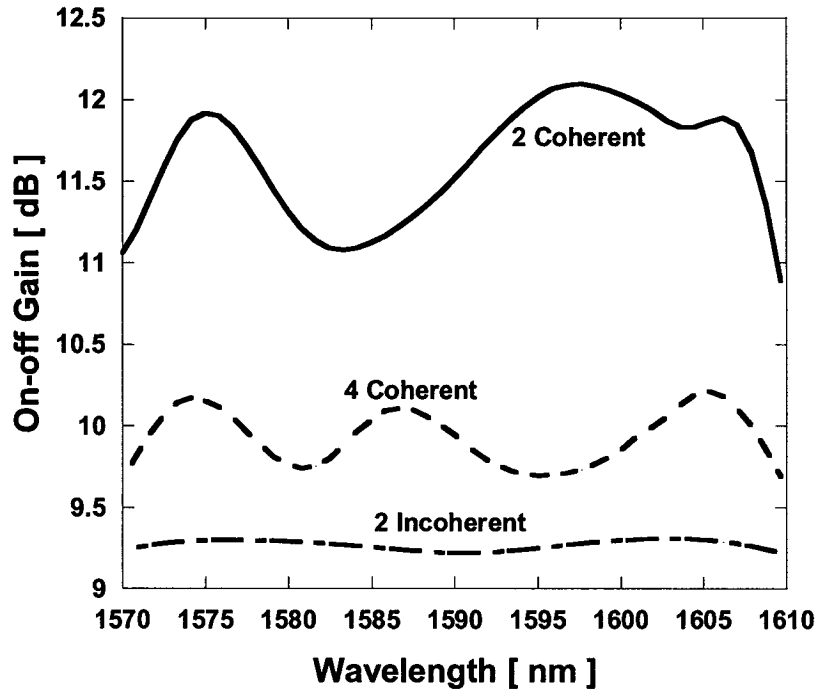

Figure 6.1.15 Gain performance for Case 8 in Section 6.1

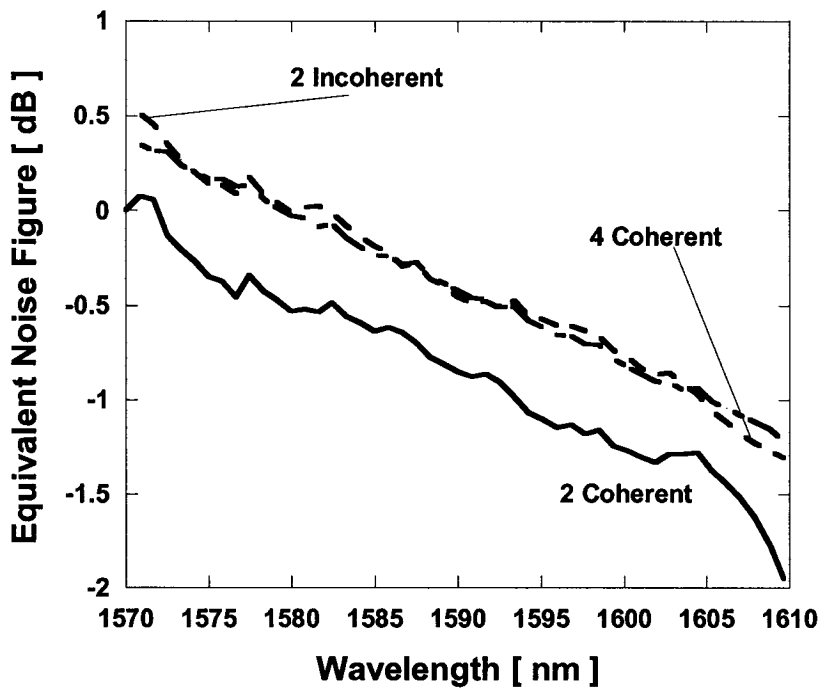

Figure 6.1.16 ENF performance for Case 8 in Section 6.1